Sulfur-Cycling in Methane-Rich Ecosystems: Uncovering Microbial Processes and Novel Niches

Thesis by
Abigail Green Saxena

In Partial Fulfillment of the Requirements for the degree
of
Doctor of Philosophy

CALIFORNIA INSTITUTE OF TECHNOLOGY
Pasadena, California
2013
(Defended 20 May 2013)

© 2013
Abigail Green Saxena
All Rights Reserved

ACKNOWLEDGEMENTS

First and foremost I would like to acknowledge my family – my parents George and Kathleen Green, my sister Katie Siddiqui-Green and her amazing daughter Elysse, and of course my fantastically incredible and endlessly entertaining husband Ankur Saxena – for all of the support they have provided me during the pursuit of my PhD. Though most of them are far, far away in Texas, their long-distance love has sustained me more thoroughly than the Trader Joe's just down the street. My sister and I grew up with a reverence for the natural world and a love of all living things thanks to our parents. I can't think of a wild animal we didn't rescue or a plant my mom can't name. Thank you for encouraging me to follow my dreams even when it terrified me, I wouldn't be here if it weren't for you.

I would like to thank the Caltech Salsa Club for providing me with the opportunity to meet my husband – he met my gaze, got my number and has yet to step on my toes. Thank you Ankur for putting up with my endless stress, diversifying my beets-and-goat-cheese-for-every-meal existence, and for making a good life greater than I could have ever imagined. You've sat through enough practice talks and beautified enough data figures to earn a second PhD. I can't thank you enough for all of the support you've given me during the last four and a half years of our life together.

And now to my advisor: Victoria Orphan. I get choked up thinking of all the ways she has contributed to or is completely responsible for the things I respect about myself as a scientist. She took me on as a naïve rotation student transitioning from macro- to microbiology, patiently helped me repair the microscope lens when I cracked my slide using the wrong objective, edited countless manuscript drafts while I awkwardly learned to use scientific language, and always asked me how I was doing before asking for a progress

report. And of course there are the life-changing adventures she sent me on – the mud volcanoes of Azerbaijan, the hyper brine pool of Mexico, a trip to the bottom of the ocean in the world famous manned submersible Alvin. I feel like the luckiest grad student on the planet and I owe it to her. The Orphan lab has always been a source of collaboration and encouragement with each member bringing their own expertise. I want to thank every member of the lab, past and present, for their contributions to my work and daily enjoyment of science.

A great man once said, *"Especially when the path gets turn-y, ignore the goal, enjoy the journey."* To the extent that I've been able to do this, graduate school has been the ride of a lifetime and I owe that to the people who have supported me through it.

ABSTRACT

Microbial sulfur cycling communities were investigated in two methane-rich ecosystems, terrestrial mud volcanoes (TMVs) and marine methane seeps, in order to investigate niches and processes that would likely be central to the functioning of these crucial ecosystems. Terrestrial mud volcanoes represent geochemically diverse habitats with varying sulfur sources and yet sulfur-cycling in these environments remains largely unexplored. Here we characterized the sulfur-metabolizing microorganisms and activity in 4 TMVs in Azerbaijan, supporting the presence of active sulfur-oxidizing and sulfate-reducing guilds in all 4 TMVs across a range of physiochemical conditions, with diversity of these guilds being unique to each TMV. We also found evidence for the anaerobic oxidation of methane coupled to sulfate reduction, a process which we explored further in the more tractable marine methane seeps. Diverse associations between methanotrophic archaea (ANME) and sulfate-reducing bacterial groups (SRB) often co-occur in marine methane seeps, however the ecophysiology of these different symbiotic associations has not been examined. Using a combination of molecular, geochemical and fluorescence *in situ* hybridization coupled to nano-scale secondary ion mass spectrometry (FISH-NanoSIMS) analyses of *in situ* seep sediments and methane-amended sediment incubations from diverse locations, we show that the unexplained diversity in SRB associated with ANME cells can be at least partially explained by preferential nitrate utilization by one particular partner, the seepDBB. This discovery reveals that nitrate is likely an important factor in community structuring and diversity in marine methane seep ecosystems. The thesis concludes with a study of the dynamics between ANME and their associated SRB partners. We inhibited sulfate reduction and followed the metabolic processes of the community as well as the effect of

ANME/SRB aggregate composition and growth on a cellular level by tracking ^{15}N substrate incorporation into biomass using FISH-NanoSIMS. We revealed that while sulfate-reducing bacteria gradually disappeared over time in incubations with an SRB inhibitor, the ANME archaea persisted in the form of ANME-only aggregates, which are capable of little to no growth when sulfate reduction is inhibited. These data suggest ANME are not able to synthesize new proteins when sulfate reduction is inhibited.

TABLE OF CONTENTS

Introduction

"If I could do it all over again, and relive my vision in the twenty-first century, I would be a microbial ecologist."

– E. O. Wilson

Introduction to Microbial Ecology

I would first like to familiarize you with the branch of environmental microbiology that encompasses my thesis, microbial ecology. Microbial ecology is the study of how microorganisms interact with their environment. Together along with the other residents of the environment, these components form an ecosystem. An ecosystem might be something as small as a termite gut or as large as a mud volcano, and it can be naturally occurring or something created/altered by humans like a sewage treatment plant or a polluted lake. Understanding the dynamics that exist between microorganisms and their environments can allow us to understand important factors affecting the ecosystem as a whole, such as why methane does not reach the atmosphere when large natural stores are slowly leaking upwards through the ocean floor. The study of microbial ecology can also uncover critical environmental factors that contribute to a microorganism's growth and proliferation. A good example of this is the understanding that microorganisms involved in bioremediation (the use of microorganisms to break down pollutants) often need a nitrogen source to effectively degrade oil spills (Röling et al., 2002, and references therein).

Microorganisms can be thought of as "ecosystem engineers" because of the central role they can play in an ecosystem. In fact, when you zoom out and view our planet as one giant ecosystem and see that microorganisms were responsible for the early oxygenation of earth (Kopp et al., 2005), you can appreciate just how powerful are these tiny members. In addition to oxygen, microorganisms are involved in the biogeochemical cycling of many chemical elements/molecules. Another example of a prominent biogeochemical cycle that is often the focus of microbial ecologists is the sulfur cycle, which contains components responsible for acid rain. Biogeochemical cycles often interact and the sulfur and carbon

cycles are prime among them – sulfate reduction, a biotic component of sulfur cycling is responsible for the conversion of up to 50% of organic matter back into CO_2 in anoxic marine sediments (Jörgensen, 1982; Canfield et al., 1993).

Overcoming Major Hurdles in Microbial Ecology

Because microbial ecology is primarily concerned with microorganisms in their native environment, it often involves working with microorganisms that are not in pure culture. "The great plate count anomaly" is a common phrase (coined by Staley and Konopka, 1985) used in microbial ecology that refers to the difference between the number of colony-forming cells versus those visible by microscopy from the same environmental sample. Often this difference is several orders of magnitude with 1% of visible cells producing colonies (Staley and Konopka, 1985; Connon and Giovannoni 2002), a testament to how many microbes are recalcitrant to culturing by common methods. Recent high-throughput cultivation techniques allow us to culture new species (Leadbetter, 2003, and references therein), however, owing to factors such as extreme environments and common symbiotic associations between different species, it is often the case that a microbial ecologist has to investigate a species or consortia without the convenience of having them in pure culture.

Molecular phylogenetic surveys are a pioneering technique in microbial ecology (Pace 1997; Woese and Fox 1977) that allow for the culture-independent characterization of microbial diversity in a sample. Briefly, this technique relies on the 16S ribosomal RNA gene, which is conserved in all bacteria and archaea, yet undergoes enough variation to allow for the detection of differences at the species level. By examining the diversity of

16S rRNA genes in an environmental sample, one can begin to understand the overall microbial diversity in an environment without needing to culture its members. A similar approach involves looking at the diversity of genes involved in a specific metabolic pathway, for example, sulfate reduction, in order to get an overview of the diversity of organisms potentially carrying out that metabolic pathway in a particular environment (Meyer and Kuever, 2007). These genes may not have the same phylogenetic resolution as 16S rRNA gene studies, but they allow one to focus on the diversity of a particular microbial guild, or functional group, in an environment.

Microbial ecologists can thus combine molecular phylogenetic surveys with a detailed study of the native environment of the microorganisms in order to guide investigations of microbial function and processes in that environment. Comparing multiple environments and their microbial communities reveals what environmental factors affect the microbial community composition and function and vice versa. Terrestrial mud volcanoes, which will be discussed in further detail below, provide an excellent opportunity for this type of comparative analysis as they represent discrete but similar environments, like mini-ecosystems, that can be compared and contrasted in order to gain an understanding of the dynamics between microbial communities and their environments. Surveying the variations in geochemistry in different mud volcanoes, reveals parameters that warrants further investigation. For example, variations in sulfate concentrations between mud volcanoes could prompt measurements of the diversity of microorganisms involved in sulfur cycling. Trends observed at this level of diversity could further lead to measurements of sulfate reduction rates from bulk samples, together creating an informative view of sulfur cycling in mud volcanoes.

The study of microbial processes, such as sulfate reduction, leads us to another major hurdle in microbial ecology: the coupling of function with phylogenetic identity. In the previous example, phylogenetic diversity of sulfur-cycling microorganisms as well as sulfate reduction rates were investigated. However, in that example there was no way of knowing which sulfate-reducing bacteria identified in the gene survey were responsible for the bulk sulfate reduction rate measurements. It could be the case that all of the bacteria from the gene survey were active, but more likely it would be the case that different ones were active or dominant under different conditions. Further, as previously described many functional gene studies do not provide phylogenetic resolution at the species or even genus level, so how do we begin to discern precisely who is doing what in an environmental sample?

There are several means of isolating individual cells from environmental samples in order to query their DNA for both 16S rRNA gene identity as well as functional genes (or even sequence the entire genome). One method developed by Ottesen and colleagues (2006), uses microfluidic PCR reactions in which individual cells are first isolated into discrete micro chambers. A dual PCR reaction is then performed in which both 16S rRNA and functional genes can be amplified and later sequenced, thus telling us the phylogenetic identity and metabolic capabilities of a single cell. Another method, developed by Pernthaler and colleagues (2008) begins with a specific fluorescence *in situ* hybridization (FISH) reaction followed by the attachment of microscopic magnetic beads to the targeted cells via antibodies, which bind the FISH fluorophores. A strong magnet can then be applied to the sample and all but the target cells washed away. Once an enrichment of target cells is thus attained, 16S rRNA and functional gene PCR amplification can be

performed on the target cells.

Stable isotope probing studies can be used to determine who is doing what in a sample. Environmental samples are incubated with a substrate of interest that has been labeled with a heavy isotope, which will be incorporated into the biomass of cells consuming the substrate. Incubations of environmental samples in small volumes (< 1 l) are often referred to as microcosms, and are often used in microbial ecology to measure microbial processes or the effects of various amendments or physiochemical perturbations on the microbial community. Once a microcosm has been incubated with a labeled substrate, for example, ^{15}N-ammonium or ^{13}C-carbon dioxide, there are two basic means for identifying which microorganisms consumed this substrate. In the first method, stable isotope probing (SIP; Radajewski et al., 2000), DNA or RNA is extracted from the microcosm and separated by density such that the DNA/RNA containing the heavier isotopes can be isolated. 16S rRNA surveys of this heavier DNA/RNA fraction can then be carried out to determine the phylogenetic identity of the organisms that consumed the labeled substrate. The second basic method involves first identifying the cells using a 16S rRNA FISH probe and then measuring the isotopes of the targeted cells to determine if the heavier isotopes have been incorporated from the labeled substrate. This method is particularly powerful as it allows microbial ecologists to couple function with identity in an environmental sample while still observing cell-cell interactions, such as symbioses, which will be explored further in the following section.

Microbial Ecology in Action: Thesis Overview

Microorganisms are a driving force behind many ecosystems that are relevant to

humans, from forests that provide oxygen, to the oceans, which absorb CO_2. Some ecosystems are particularly critical to humans simply because their balance maintains our status quo. Polar ice caps are such examples as they maintain the sea level. Though climate change has brought many such ecosystems to our attention, there are many whose balance we still take for granted. I would like to turn your attention to a very potent green house gas, methane, which is a central part of several naturally occurring ecosystems. This exists in large stores in the Earth's surface and escapes through various outlets on land and in the ocean. There are two prominent methane sources – mud volcanoes and marine methane seeps – that I focus on in my thesis. Mud volcanoes are a major source of methane flux to the atmosphere (6-9 Tg/year; Etiope and Milikov, 2004), and while the anaerobic oxidation of methane (AOM) is responsible for recycling up to 80% of the oceanic methane production (Reeburgh, 2007), an estimated 11-18 Tg are released annually (Bange et al., 1994). In order to better understand these crucial ecosystems, we set out to understand how their geochemistry interplays with their anaerobic inhabitants. Anaerobes specialize in breathing molecules other than oxygen, such as nitrate, manganese, iron and sulfate. We first chose to study anaerobic microorganisms in terrestrial mud volcanoes because they represent convenient and relatively discrete, self-contained environments whose geochemistry and microbial diversity and function could be compared to key factors in the functioning of these ecosystems.

Chapter 1 of my thesis focuses on terrestrial mud volcanoes. In October of 2008 we visited four terrestrial mud volcanoes in Azerbaijan, a region of very densely populated TMVs (Figure 1). This was a multidisciplinary group in which Hans-Martin Schultz, Jens Kallmeyer and Akper Feyzullayev measured geochemistry; Jens Kallmeyer, Patrick Sauer,

Casey Hubert and Martin Krueger measured bulk microbial processes; Martin Krueger conducted 16S rRNA qPCR analyses and I conducted 16S rRNA and functional gene analyses as well as fluorescence *in situ* hybridization. Among the many geochemical factors measured, sulfate was variable and in some habitats more than sufficient to potentially support active sulfate reducing bacteria (SRB). SRB are a ubiquitous class of microorganisms, which make a functional guild defined by the ability to respire sulfate (ie, to use sulfate as a terminal electron acceptor). This is an extremely environmentally relevant guild of microorganisms due to their role in bioremediation and oil field souring, both afforded by this guilds' ability to degrade a vast array of organic compounds. We measured active sulfate reduction whose magnitude clearly reflected the ambient sulfate concentrations. The surface connection to the deep biosphere and underlying hot fluids were an additional motivation for this study, and a surprising find was also the discovery of active thermophilic sulfate reduction, which we measured in several of the TMVs.

Measuring SR tells us what an environment's inhabitants are capable of doing, but it does not tell us about the diversity of species responsible for this process. We therefore surveyed the phylogenetic identity of genes specific to sulfur cycling in each TMV. What we found was that genes from organisms capable of sulfate reduction dominated the gene libraries from environments containing measureable levels of sulfate, whereas those with little or no sulfate were dominated by genes from organisms capable of sulfur oxidation. Among the sulfate-reducing bacterial genes we also found several interesting results. We

Figure 1. Sample collection from mud volcanoes in Azerbaijan, 2008.

were able to confirm the presence of thermophilic SRB and we found evidence for niche differentiation among two major types of SRB: those capable of degrading organic compounds completely to CO_2 and those which can only incompletely degrade carbon substrates, releasing acetate as their byproduct.

Although the nature of the samples made microscopy work difficult we were also able to identify some of the organisms detected by our gene targeted analyses, in association with anaerobic methane-oxidizing archaea (ANME). This example of a now famous symbiosis is highly suggestive of sulfate reduction coupled to methane oxidation, which we did indeed observe evidence for in subsequent microcosm activity experiments.

This symbiosis has been observed previously in terrestrial and marine mud volcanoes where the dominant form present appears to be a combination of ANME associated with SRB related to incomplete carbon-oxidizing SRB. We also observed examples of ANME with different families of bacteria and wanted to explore this phenomenon further.

In order to do this I would like to take you now to the bottom of the ocean (Figure 2) where vast stores of methane naturally exist as methane hydrates along continental margins, which slowly disassociate and seep into the overlying sediment. These are the sites from which the anaerobic oxidation of methane (AOM) was first characterized and indeed the sample type, much less viscous and often oil free sediment greatly facilitates their investigation via microscopy. This affords us a number of tools that get at one of the more crucial questions in microbial ecology, "Who is doing what?" You will notice in the prior investigation we were able to measure the activity of SRB and look at the diversity of SRB present via their genes. However with these tools it is not possible to say which SRB were responsible for which portions of the sulfate-reduction rates (SRR) we observed. The next two chapters of my thesis use a technique known as FISH-NanoSIMS (nanoscale secondary ion mass spectrometry), which allows us to measure labeled isotopes (from cells incubated with isotopically enriched substrates) inside individual cells previously identified via FISH (Orphan et al., 2001; Dekas and Orphan, 2011). Along with molecular and geochemical methods, we used FISH-NanoSIMS to explore the ANME/SRB symbiosis in marine methane seeps.

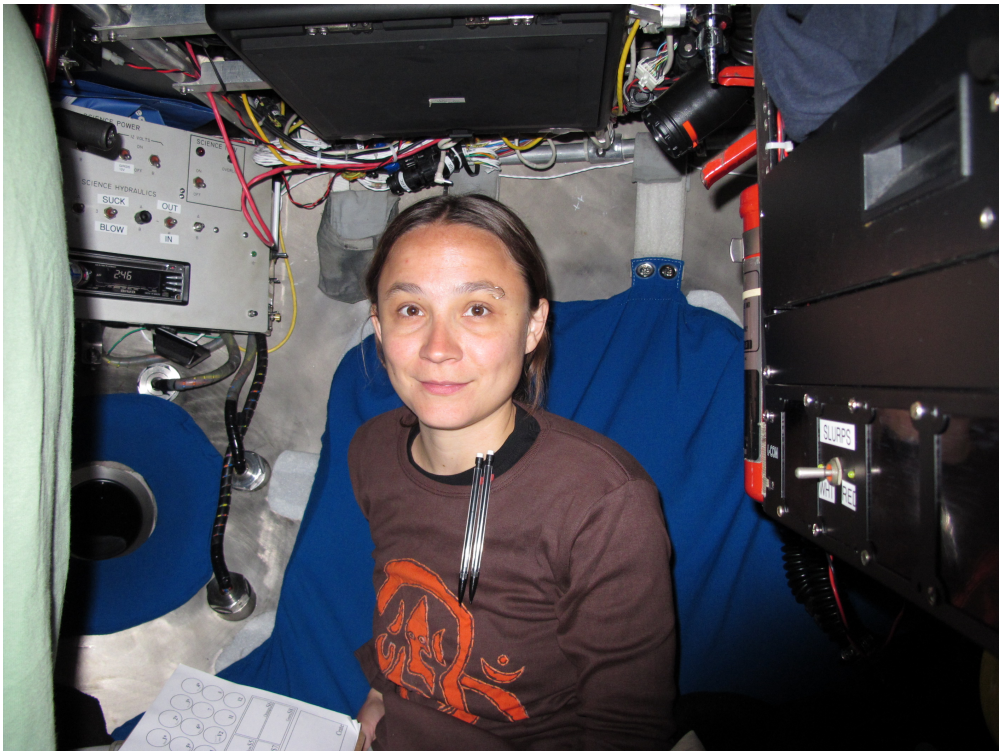

Figure 2. Sample collection from ocean floor; inside ROV Alvin, 2010.

The anaerobic oxidation of methane (AOM) is responsible for recycling up to 80% of the oceanic methane production (Reeburgh, 2007). This crucial biogeochemical process serves as a major sink for methane, a greenhouse gas with heat trapping capabilities up to 20 times stronger than CO_2 (Schiermeier, 2006). Syntrophic aggregates of ANME and SRB appear to carry out the anaerobic oxidation of methane (Orphan et al., 2001). In the following putative pathway, sulfate serves as the electron acceptor for methane (Boetius et al., 2000; Iverson and Jorgensen, 1985): $CH_4 + SO_4^{2-} \rightarrow HCO_3^- + HS^- + H_2O$. However, to date, neither ANME nor SRB involved in this reaction have been grown in pure culture, and thus the pathway for AOM, including the method for electron transfer, remains unclear (Knittel and Boetius, 2009). Indeed, Milucka and colleagues (2012) recently proposed a

new pathway in which ANME-2 is capable of both the anaerobic oxidation of methane and reduction of sulfate to disulfide (or other S0 compounds), which is then scavenged by the SRB and disproportionated to sulfide and sulfate.

First we wanted to address the importance of sulfate reduction to the ANME/SRB consortia. As sulfate-reducing bacteria were initially implicated as an agent responsible for AOM (Reeburgh, 1976), multiple studies have used sulfate reduction inhibitors such as molybdate or tungstate to validate and study dynamics of AOM (Alperin and Reeburgh, 1985; Hansen et al 1998; Iversen et al., 1987; Nauhaus et al., 2005; Orcutt et al., 2008). Due to the difficulties of getting the ANME/SRB consortia into pure culture, prior sulfate-reduction inhibition studies are based on bulk geochemical measurements in which they inhibit sulfate reduction in an entire community and measure the AOM activity rate of that community (Alperin and Reeburgh, 1985; Hansen et al. 1998; Iversen et al., 1987; Nauhaus et al., 2005; Orcutt et al., 2008). Cell specific tracking of the effects of sulfate-reducing inhibitors on ANME/SRB aggregate abundance and composition can be accomplished via FISH, which can then be coupled to NanoSIMS in order to measure growth in consortia incubated with ^{15}N-labeled ammonium (Orphan et al., 2009). FISH-nanoSIMS allows the coupling of function with identity through the measurement of ^{15}N incorporation in individual cells or aggregates whose phylogenetic identity is determined via FISH. For chapter 3 of my thesis, in order to study dynamics of AOM, we inhibited sulfate reduction and followed the metabolic processes of the microcosm community as well as the effect of aggregate composition and growth on a cellular level. We found that while bacterial cells appear to decay, ANME cells persist in the form of ANME-only aggregates, which were found to exhibit little to no growth (as measured with FISH-NanoSIMS) when sulfate

reduction is inhibited. Our data suggest the growth and metabolism of ANME is tightly linked to the bacterial partner.

Once we confirmed the importance of sulfate reduction to the growth of ANME/SRB consortia in these marine methane seeps, we began to focus (Chapter 2 of my thesis) on another critical question related to this system: why do ANME associate with multiple families of SRB in one habitat? A previous study in our lab showed that the ANME in these habitats can associate with either Desulfobacteraceae (DSS) or Desulfobulbaceae (DBB) (Pernthaler et al., 2008). Gause, one of the founders of early ecology put forth the notion that ecosystems can be defined by their niches, or habitats they provide for their inhabitants (Gause, 1934). This is true for microbial ecology as well and in fact SRB are known to divide a habitat into microniches allowing their co-existence (Dar et al., 2007). Thus the apparent functional redundancy suggested by ANME coupling with multiple SRB families in the same habitat could potentially be explained by the existence of separate niches within which each of these variants of the symbiosis thrive.

The more abundant aggregate form observed was ANME/DSS, so we decided to follow this up first by seeing how ubiquitous was the ANME/DBB symbiosis. If you look closely, it is everywhere. But importantly, it is more abundant in the shallowest parts of the examined habitats, which is not where we typically expect to see a lot of ANME/SRB thriving. Various nutrients and energy sources may be more available in these shallow horizons thus we decided to measure nitrogen species in these habitats in subsequent research cruises. In several instances we saw that nitrate peaks in the shallow depth horizons below microbial mats. Upon investigation this is where the ANME/DBB also peaked and there appeared an appaprent correlation between nitrate and relative

ANME/DBB numbers.

Incubations from methane seeps were amended with ^{15}N-nitrate and followed over time. Nitrate-amended incubations showed a higher relative number of ANME/DBB at later time point than no-nitrate incubations. In order to determine if these ANME/DBB were utilizing nitrate we used FISH-NanoSIMS to compare nitrate incorporation from ANME/DBB and ANME/DSS aggregates. We found that the ANME/DBB aggregates did indeed incorporate more nitrate than their ANME/DSS counterparts. Further, this was not true for labeled ammonium incubations, suggesting that these two types of aggregates grow at similar rates but ANME/DBB simply prefers nitrate more than do ANME/DSS aggregates. These findings are interesting as they suggest that ANME/SRB aggregate types may coexist via dividing their environment based on nitrate, with ANME/DBB using nitrate either as nutrient or energy source.

In sum these data uncover novel aspects of the sulfur-cycling microbial communities in two crucial ecosystems rich in natural methane stores. As discussed further in the conclusions section, this contribution allows for a more complete understanding of not only *in situ* communities and processes but also novel factors that may be central to the ecosystem and yet were heretofore unknown.

REFERENCES

Alperin MJ & Reeburgh WS (1985) Inhibition experiments on anaerobic methane oxidation. Applied and Environmental Microbiology 50: 940-945.

Bange HW, Bartell U, Rapsomanikis S & Andreae MO (1994) Methane in the Baltic and North Seas and a reassessment of the marine emissions of methane. Global Biogeochemical Cycles 8: 465-480.

Boetius A, Ravenschlag K, Schubert CJ, et al. (2000) A marine microbial consortium apparently mediating anaerobic oxidation of methane. Nature 407: 623-626.

Canfield DE, Jörgensen BB, Fossing H, et al. (1993) Pathways of organic carbon oxidation in three continental margin sediments. Marine Geology 113: 27-40.

Connon SA & Giovannoni SJ (2002) High-throughput methods for culturing microorganisms in very-low-nutrient media yield diverse new marine isolates. Applied and Environmental Microbiology 68: 3878-3885.

Dar S, Stams A, Kuenen J & Muyzer G (2007) Co-existence of physiologically similar sulfate-reducing bacteria in a full-scale sulfidogenic bioreactor fed with a single organic electron donor. Applied Microbiology and Biotechnology 75: 1463-1472.

Dekas AE & Orphan VJ (2011) Identification of diazotrophic microorganisms in marine sediment via fluorescence *in situ* hybridization coupled to nanoscale secondary ion mass spectrometry (FISH-NanoSIMS). Methods Enzymol 486: 281-305.

Etiope G & Milkov AV (2004) A new estimate of global methane flux from onshore and shallow submarine mud volcanoes to the atmosphere. Environmental Geology 46: 997-1002.

Gause G (1934) The struggle for existence. Williams and Wilkins, Baltimore.

Hansen LB, Finster K, Fossing H & Iversen N (1998) Anaerobic methane oxidation in sulfate depleted sediments: effects of sulfate and molybdate additions. Aquatic Microbial Ecology 14: 195-204.

Iversen N & Jörgensen B (1985) Anaerobic methane oxidation rates at the sulfate-methane transition in marine sediments from Kattegat and Skagerrak (Denmark). Limnol. Oceanogr 30: 944-955.

Iversen N, Oremland RS & Klug MJ (1987) Big Soda Lake (Nevada). 3. Pelagic methanogenesis and anaerobic methane oxidation. Limnol. Oceanogr 32: 804-808.

Jörgensen BB (1982) Mineralization of organic matter in the sea bed – the role of sulphate reduction.

Knittel K & Boetius A (2009) Anaerobic Oxidation of Methane: Progress with an unknown process. Annu. Rev. Microbiol. 63: 311-334.

Kopp RE, Kirschvink JL, Hilburn IA & Nash CZ (2005) The Paleoproterozoic snowball Earth: a climate disaster triggered by the evolution of oxygenic photosynthesis. Proceedings of the National Academy of Sciences of the United States of America 102:

11131-11136.

Leadbetter JR (2003) Cultivation of recalcitrant microbes: cells are alive, well and revealing their secrets in the 21st century laboratory. Current opinion in microbiology 6: 274-281.

Meyer B & Kuever J (2007) Molecular analysis of the diversity of sulfate-reducing and sulfur-oxidizing prokaryotes in the environment, using aprA as functional marker gene. Applied and Environmental Microbiology 73: 7664-7679.

Milucka J, Ferdelman TG, Polerecky L, et al. (2012) Zero-valent sulphur is a key intermediate in marine methane oxidation. Nature 491: 541-546.

Nauhaus K, Treude T, Boetius A & Krüger M (2005) Environmental regulation of the anaerobic oxidation of methane: a comparison of ANME-I and ANME-II communities. Environmental Microbiology 7: 98-106.

Orcutt B, Samarkin V, Boetius A & Joye S (2008) On the relationship between methane production and oxidation by anaerobic methanotrophic communities from cold seeps of the Gulf of Mexico. Environmental Microbiology 10: 1108-1117.

Orphan VJ, House CH, Hinrichs KU, McKeegan KD & DeLong EF (2001) Methane-consuming archaea revealed by directly coupled isotopic and phylogenetic analysis. Science 293: 484-487.

Orphan VJ, Turk KA, Green AM & House CH (2009) Patterns of 15N assimilation and growth of methanotrophic ANME-2 archaea and sulfate-reducing bacteria within structured syntrophic consortia revealed by FISH-SIMS. Environ Microbiol doi:10.1111/ j.1462-2920.2009.01903.x.

Ottesen EA, Hong JW, Quake SR & Leadbetter JR (2006) Microfluidic digital PCR enables multigene analysis of individual environmental bacteria. Science 314: 1464-1467.

Pace NR (1997) A Molecular View of Microbial Diversity and the Biosphere. Science 276: 734-740.

Pernthaler A, Dekas AE, Brown CT, Goffredi SK, Embaye T & Orphan VJ (2008) Diverse syntrophic partnerships from deep-sea methane vents revealed by direct cell capture and metagenomics. Proceedings of the National Academy of Sciences 105: 7052-7057.

Radajewski S, Ineson P, Parekh NR & Murrell JC (2000) Stable-isotope probing as a tool in microbial ecology. Nature 403: 646-649.

Reeburgh WS (1976) Methane consumption in Cariaco Trench waters and sediments. Earth and Planetary Science Letters 28: 337-344.

Reeburgh WS (2007) Oceanic methane biogeochemistry. Chemical Reviews 107: 486-513.

Röling WF, Milner MG, Jones DM, Lee K, Daniel F, Swannell RJ & Head IM (2002) Robust hydrocarbon degradation and dynamics of bacterial communities during nutrient-enhanced oil spill bioremediation. Applied and Environmental Microbiology 68: 5537-5548.

Schiermeier Q (2006) Methane finding baffles scientists. Nature 439: 128-128.

Staley JT & Konopka A (1985) Measurement of *in situ* activities of nonphotosynthetic microorganisms in aquatic and terrestrial habitats. Annual Reviews in Microbiology 39: 321-346.

Wilson EO (2006) *Naturalist* (Island Press).

Woese CR & Fox GE (1977) Phylogenetic structure of the prokaryotic domain: the primary kingdoms. Proceedings of the National Academy of Sciences 74: 5088-5090.

*Chapter 1**

***This chapter, written by Abigail Green Saxena, was first published in Environmental Microbiology:**

Green‐Saxena, A., Feyzullayev, A., Hubert, C. R. J., Kallmeyer, J., Krueger, M., Sauer, P., ... & Orphan, V. J. (2012). Active sulfur cycling by diverse mesophilic and thermophilic microorganisms in terrestrial mud volcanoes of Azerbaijan. *Environmental Microbiology*, *14*(12), 3271-3286.

Active sulfur cycling by diverse mesophilic and thermophilic microorganisms in terrestrial mud volcanoes of Azerbaijan

A. Green-Saxena[2], A. Feyzullayev[3], C.R.J. Hubert[4], J. Kallmeyer[5], M. Krueger[6], P. Sauer[5], H.-M. Schulz[7] and V.J. Orphan[1]

Divisions of [1]Geological and Planetary Sciences and [2]Biology, California Institute of Technology, 1200 East California Boulevard, Pasadena, CA 91125
[3]Petroleum Geology and Geochemistry Department, Geology Institute of ANAS, H. Cavid avenue 29a, Baku, AZ1143, Azerbaijan
[4]School of Civil Engineering & Geosciences, Devonshire Building, Newcastle University, Newcastle upon Tyne, NE1 7RU, United Kingdom
[5]Institute of Earth and Environmental Sciences, University of Potsdam, Haus 27, Zi. 0.34, Karl-Liebknecht-Str. 24 14476 Golm, Germany
[6]Fields of Geomicrobiology and Resource Geochemistry, Bundesanstalt fuer Geowissenschaften und Rohstoffe (BGR; Federal Institute for Geosciences and Natural Resources), Stilleweg 2, D-30655 Hannover, Germany
[7]GeoForschungsZentrum Potsdam, Section 4.3, Telegrafenberg, B 424, D-14473 Potsdam, Germany

SUMMARY

Terrestrial mud volcanoes (TMVs) represent geochemically diverse habitats with varying sulfur sources and yet sulfur cycling in these environments remains largely unexplored. Here we characterized the sulfur-metabolizing microorganisms and activity in 4 TMVs in Azerbaijan. A combination of geochemical analyses, biological rate measurements and molecular diversity surveys (targeting metabolic genes *aprA* and *dsr*A and SSU ribosomal RNA) supported the presence of active sulfur-oxidizing and sulfate-reducing guilds in all 4 TMVs across a range of physiochemical conditions, with diversity of these guilds being unique to each TMV. The TMVs varied in potential sulfate-reduction rates (SRR) by up to 4 orders of magnitude with highest SRR observed in sediments where *in situ* sulfate concentrations were highest. Maximum temperatures at which SRR were measured was 60°C in two TMVs. Corresponding with these trends in SRR, members of the potentially thermophilic, spore-forming, *Desulfotomaculum* were detected in these TMVs by targeted 16S rRNA analysis. Additional sulfate-reducing bacterial lineages included members of the Desulfobacteraceae and Desulfobulbaceae detected by *apr*A and *dsr*A analyses and likely contributing to the mesophilic SRR measured. Phylotypes affiliated with sulfide-oxidizing Gamma- and Betaproteobacteria were abundant in *apr*A libraries from low sulfate TMVs, while the highest sulfate TMV harbored 16S rRNA phylotypes associated with sulfur-oxidizing Epsilonproteobacteria. Altogether, the biogeochemical and microbiological data indicate these unique terrestrial habitats support diverse active sulfur-cycling microorganisms reflecting the in situ geochemical environment.

INTRODUCTION

Terrestrial mud volcanoes (TMVs) occur where high fluid pressure in the deep subsurface results in the transport of mud, water and gas to the surface (Feyzullalev and Movsumova, 2010; Niemann and Boetius, 2010). This process creates diverse morphological features rich in methane and other hydrocarbons (Dimitrov et al., 2002), and hosting a suite of electron acceptors including oxygen, nitrate, iron, manganese and sulfate (Planke et al., 2003; Mazzini et al., 2009; Alain et al., 2006; Chang et al., 2011). Mud volcanoes are a major source of methane flux to the atmosphere (6-9 Tg/year; Etiope and Milikov, 2004), and geochemical and microbiological studies thus far have primarily focused on microorganisms and processes involved in the oxidation of methane, including the detection of anaerobic methane-oxidizing archaea (ANME) in individual volcanoes (Niemann et al., 2006; Alain et al., 2006; Schulze-Makuch et al., 2011; Wrede et al., 2011; Yang et al., 2011; Chang et al., 2011). 16S rRNA surveys of TMVs in Romania, Taiwan and China contain a large number of putative sulfate-reducing Deltaproteobacterial phylotypes, consistent with the potential for sulfate-dependent anaerobic methane oxidation (Alain et al., 2006; Chang et al., 2011; Yang et al., 2011), however in some cases sulfate reduction rates (SRR) appear to be significantly greater than anaerobic methane oxidation rates (Alain et al., 2006).

The ecology of organisms involved in sulfur cycling remains largely unexplored in TMVs. Unlike marine MVs, very little is known about chemosynthetic communities such as sulfur-oxidizing bacterial (SOB) populations in TMVs (Niemann and Boetius, 2010) and

while sulfate-reducing bacterial (SRB) phylotypes based on 16S rRNA have been reported from individual TMVs, their diversity in these habitats has not been examined by analyzing sulfur-cycling functional genes. TMVs have the potential for supporting active sulfur cycling with typical sulfate concentrations of approximately 2 mM (Planke et al., 2003; Mazzini et al., 2009; Alain et al., 2006; Nakada et al., 2011; Yakimov et al., 2002), and these natural venting structures may also serve as a window into sulfur-cycling processes in the deep biosphere. While previous microbiological studies have characterized individual TMVs, regions hosting multiple TMVs also make it possible to focus on the same microbial guilds and processes across several sites.

Azerbaijan and its offshore expanses in the Caspian Sea represent one of the most densely populated regions of mud volcanoes and mud volcanism is one of the major factors controlling oil and gas fields in the region. Unusually high $\delta^{13}C$ values of CO_2 and bicarbonates in the TMVs are thought to result from biodegradation of oil (Feyzullayev and Movsumova, 2010), however very little is known about the microbial communities in these volcanoes. Multiple studies have characterized the complex plumbing system of the TMVs that are capable of transporting mud and fluids from origins as deep as 10 km or greater (Mazzini at al., 2008; Planke et al., 2003, and references therein), and records of eruption history as well as geochemical and isotopic compositions of emitted oil, gas, mud and water exist for several prominent TMVs in the region (Etiope et al., 2004; Feyzullayev and Movsumova, 2010; Guliyev et al., 2001; Mazzini et al., 2009; Planke et al., 2003).

Analyses of oil source-rocks ejected from mud volcanoes of Azerbaijan revealed low organic sulfur contents (less than 0.03% of the organic matter) with the majority of sulfur occurring as pyrite (Isaksen et al., 2007). Sulfate concentrations appear to vary widely with studies

reporting concentrations that are on average ~ 2 mM, but range of values from ~ 10 μM to > 30 mM (Planke et al., 2003; Mazzini et al., 2008). This diverse system of mud volcanoes provides a set of distinct habitats in which to study natural variations in the *in situ* interplay of sulfur-cycling communities and their geochemical environments. Here we conducted a comparative geomicrobiological study of 4 discrete TMVs in Azerbaijan (D: Dashgil, B: Bakhar, P: Perekyushkul and BJ: Boransyz-Julga) sourced from deep-seated fluids in order to: 1) characterize sulfur-cycling microbial communities in these unique environments, 2) place these communities in a meaningful context via geochemical and microbial rate measurement analyses and 3) examine the potential transport of thermophilic sulfur-cycling microorganisms from the deep subsurface.

RESULTS

Geochemical characterization

Inorganic and organic geochemistry of pore fluids from 4 mud volcanoes were analyzed with a particular emphasis on sulfur and carbon species (Tables 1, S4). In general, values were similar to previous reports of geochemistry from TMVs in this area (Planke et al., 2003; Mazzini et al., 2009). Sulfate contents ranged between 0.47 and 1.64 mM in D sediments except for in sample D3, which was below detection (< 0.16 mM). P surface (P1S) and deep (P1D) samples contained 0.31 and 0.80 mM sulfate, respectively. B and BJ had sulfate levels below the detection limit (< 0.16 mM). The sulfate concentrations ranged from less than 0.16 to 1.64 mM and are within the range of previously reported values from TMVs in Azerbaijan (Planke et al., 2003; Mazzini et al.,

2009) as well as those reported from TMVs in Romania (2 mM; Alaine et al., 2006), Italy (0.07 mM, Wrede et al., 2011) and China (14 mM; Yang et al., 2011). While values vary widely, none of them approach that of seawater in general (approximately 28 mM), or the Caspian Sea in particular (approximately 33 mM; Planke at al., 2003 and references therein).

Higher Cl^- values of D salse lakes/pools (312 to 464 mM) versus gryphons from D, P and BJ (56 to 68 mM) are in agreement with previously reported trends from this region, and may reflect a deep water source resulting from the dehydration of clays in the gryphons, while the salse lakes and pools may be fed by more shallow meteoric water source with higher solutes resulting from *in situ* evaporation (Mazzini et al., 2009). Higher Cl^-/Br^- ratios in salse lakes (relative to gryphons) in this region have been previously reported and may be derived from the dissolution of halite crusts which form on the outside flanks of gryphons occurring at higher elevations than salse lakes (Mazzini et al., 2009).

Reduced sulfur species associated with the solid phase materials were divided into three phases named for the compounds used to liberate them: AVS (acid-volatile sulfur; hydrogen sulfide and monosulfides): CRS (chromium-reducible sulfur, mainly pyrite): DMF (dimethylformamide-soluble fraction, mainly elemental sulfur). Values from all samples analyzed were similar, with disulfides comprising > 99% of all reduced sulfur except BJ, which contained relatively lower amounts of disulfides (96% from sample S1; 72% from S2) the difference being made up by monosulfides (Tables 1, S4).

Microbial Microcosm Measurements

Biogenic CO_2 production under aerobic conditions (heterotrophic respiration) was at least three orders of magnitude greater than CO_2 production under anaerobic conditions. In addition, anaerobic sulfide production (in the presence and absence of methane), indicative of active sulfate reduction, was also two orders greater than anaerobic CO_2 production (Table 2). Sulfide and anaerobic CO_2 production rates ranged from $1.4x10^4$ to $6.7x10^4$ and $2.7x10^2$ to $6.3x10^2$ (nmol cm^{-3} day^{-1}), respectively. Higher rates of sulfide and anaerobic CO_2 production were measured from D samples suggesting potentially higher *in situ* sulfate reduction rates in the D salse lakes (D1 and D3).

Potential sulfate-reduction rates

Sulfate reduction rates (SRR) were measured from three of the four mud volcanoes; D (deep pool sample, D2D), B (gryphon sample B1) and BJ (gryphon sample BJ1). Sediment slurries were incubated for 8 hours with sulfate radiotracer at temperatures ranging from approximately 10°C to 82°C, under three different experimental incubation conditions: following 24 hour pre-incubation, following 48 hour pre-incubation, and following 48 hour pre-incubation with VFAs. Results were highly variable with SRR spanning four orders of magnitude between sites and depending on incubation temperature, pre-incubation time, and VFA addition. Incubations with sediment from BJ, located inland from D and B (Figure 1), resulted in a temperature profile for SRR with a narrow temperature optimum around 30°C and no detectable thermophilic activity (Figure 2c). Results from D and B varied significantly in response to VFA stimulation and revealed different temperature optima for sulfate reduction despite both D and B occurring in the same hydraulic system and rock formation. Sulfate reduction maxima in the thermophilic

range were measured for B and D sediments at 54°C and 60°C, respectively, with SRR below detection at higher temperatures up to 82°C.

D samples pre-incubated for 24 and 48 hours resulted in similar temperature-activity profiles, with the highest SRR measured at 32.5°C. While sulfate reduction was not detected above 40ºC after 32 hours (i.e., 24 hour pre-incubation followed by 8 hours with radiotracer), SRR obtained for 48-56 h revealed a second peak in SRR between 50 and 70°C. This response was dramatically amplified by VFA amendment, which resulted in SRR up to 250-fold higher at these high temperatures than in the unamended samples (Figure 2a), similar to previous reports of VFA supporting high SRR in cold marine sediments incubated at these temperatures (Hubert et al. 2010). In B sediments, SRR (ranging from 0.78-3.70 nmol/cm^3/d) were much lower than those measured in D sediments (2.38-2359.88 nmol/cm^3/d) and, as observed for D, the temperature optima depended on both the pre-incubation time and the addition of VFAs. For the two unamended incubations, the temperature range for sulfate reduction was broad and showed several rate maxima between 15°C and 40°C. Notably, SRR determined after the 24- and 48 hour pre-incubations followed slightly different temperature-activity profiles, with rates measured after 24 hours being 1.5-fold higher between 25 and 32ºC than after the 48 hour treatment. VFA amendment to B samples stimulated SRR that were slightly higher than in unamended samples, with two distinct peaks at 30°C and 54°C and a third minor peak around 15°C (Figure 2b). The potential sulfate reduction rates were also low in samples from BJ, with one narrow peak at 30°C determined for all three incubation treatments. SRR in samples pre-incubated for 48 hours (3.37 nmol/cm^3/d) were approximately threefold

greater than in the 24 hour sample (1.00 nmol/cm^3/d). Unlike the samples from D and B, VFA addition to BJ samples did not result in higher SRR (2.34 nmol/cm^3/d; Figure 2c).

Determination of microbial abundance

Quantitative 16S rRNA gene analyses from D and B samples collected in 2007 suggest bacteria are an order of magnitude more abundant than archaea in D salse lakes (D1 and D3), while the two Domains appear equally abundant in the small salse lake sample from B (Table S3). The depth from which the sample was taken did not appear to influence these trends. Across all samples, bacterial 16S rRNA gene copies range from approximately $1x10^7$ to $1x10^9$ copies/g, and archaeal 16S rRNA gene copies range from $1x10^7$ to $1x10^8$ copies/g.

Molecular characterization of sulfur-cycling bacteria

Samples for phylogenetic analysis were selected based on sulfate-reduction rate data and *in situ* sulfate concentrations. Here we targeted the *apr*A gene (adenosine-5-phosphosulfate [APS] reductase) encoding the enzyme required for dissimilatory sulfate-reduction and used in many sulfur-oxidation pathways (Meyer and Kuever, 2007a). Two *apr*A clone libraries were constructed from samples of the same Dashgil pool; one from the surface (D2S) and one collected approximately 4 meters below the surface (D2D). Three clone libraries were constructed from gryphon samples. The B (B1) and BJ (BJ1) samples were collected at the surface of the gryphon, and the P (P1D) sample was recovered from approximately 2 meters below the surface.

The *aprA* gene sequences recovered from 4 of the 5 mud volcano samples contained representatives from several groups within the Gamma, Beta, and Deltaproteobacteria representing multiple sulfate-reducing and sulfur-oxidizing bacterial clades. The exception to this was BJ, where 96% of the recovered *apr*A sequences were affiliated with sulfide-oxidizing Betaproteobacterial members related to *Thiobacillus* (Figure 3a). Gammaproteobacterial clones from the *apr*A lineages I and II (as defined in Meyer and Kuever; 2007b) were present in all but the BJ sample, with lineage I representing the majority of these clones. Gammaproteobacterial *apr*A lineage I sequences from B, P and both D samples formed two distinct clusters each of which grouped with distinct *apr*A sequences from two *Thioalkalivibrio* strains (Figure 3a). Sequences within lineage I also included representatives grouping within the Chromatiaceae (D2S) and environmental sequences reported from the ground waters of an evaporative, calcareous, salt lake. Putative sulfide-oxidizing Gammaproteobacterial *apr*A lineage II clones from B, P and both D samples also formed two distinct clusters, one affiliated with environmental clones from sulfate-reducing bioreactors treating mine drainage (Hiibel et al., 2008); the other grouping with members of *Thiodicton* sp., within the Chromatiaceae. Only one sequence, retrieved from BJ, appears loosely affiliated with an uncultured Alphaproteobacteria (Figure 3a).

All sulfate-reducing bacterial sequences from *apr*A libraries grouped with mesophilic Deltaproteobacteria, with the exception of a clone recovered from D2D, which grouped within the gram-posistive *Desulfotomaculum* subcluster 1b, which includes thermophilic sulfate reducers (Meyer and Kuever, 2007c). The majority of sequences within the Desulfobacteraceae were from D surface and deep samples (D2D and D2S), several of

which formed a distinct cluster distantly associated with *Desulfosarcina variabilis*. Clones from P, B and D surface samples made up the majority of Desulfobulbaceae sequences, mainly grouping into 3 clusters with either no described relative or a distant association with *Desulfurivibrio alkaliphilus* (Figure 3b).

The ratio of *apr*A clones recovered from sulfur-oxidizing versus sulfate-reducing bacteria (SOB:SRB) varied between samples, with SOB clones dominant in BJ (98% SOB) and B (68% SOB). The SOB populations in these samples were distinct, B contained *apr*A clones within the Gammaproteobacteria (43% *apr*A lineage I, 25% lineage II) while BJ contained 96% Betaproteobacterial (*apr*A lineage II) clones and a single clone putatively from the Alphaproteobacteria. B also contained clones (30% of library) from the Deltaproteobacterial family Desulfobulbaceae while BJ did not contain SRB-affiliated *apr*A sequences.

P and D surface and deep samples were dominated by *apr*A clones affiliated with SRB lineages. The D deep sample (D2D) was almost entirely dominated by Desulfobacteraceae (83%), with only a single clone each from Desulfobulbaceae and Desulfotomaculum (Figure 3b). Similar to D2D, the P sample was collected several meters below the gryphon surface, but had an SRB profile more similar to the D2S surface sample. The majority (56%) of P clones grouped within the Desulfobulbaceae with 4% affiliated with Desulfobacteraceae. The D surface sample also contained a number of *apr*A sequences from the Desulfobulbaceae and Desulfobacteraceae family (63% and 18%, respectively). Additionally, there appeared to be a trend between libraries dominated by SRB sequences and the occurrence of Gammaproteobacterial lineage I clones comprising the dominant SOB group.

As an independent check of the *apr*A results, a single *dsr*A library was constructed from D2D. Similar to the *apr*A library from the same sample, the recovered *dsr*A sequences were dominated (84%) by Desulfobacteraceae, with one Desulfobulbaceae clone and 9 clones with no closely described relatives (Table S2). A phylogenetic analysis using known reference sequences placed several of these unidentified clones within a cluster of *Desulfotomaculum* sequences (data not shown).

Molecular characterization of 16S rRNA bacterial diversity

A bacterial 16S rRNA survey was completed from the D2D pool sample. Of the recovered diversity, 59% of the clones were Epsilonproteobacteria, followed by Chloroflexi (19%), Deltaproteobacteria (9%), and a low number of sequences associated with the Firmicutes (5%) and Bacteroidetes (3%). Epsilonproteobacterial sequences were highly similar (96-99% max identity) to environmental clones from the facultatively anaerobic SOB *Sulfurovum* sp. and all Chloroflexi clones were highly similar (96%) to environmental clones from landfill leachate pond sediments (Liu et al., 2011). Among the Deltaproteobacteria, clones were similar to environmental sequences from wetlands (3 clones, 94% max identity) and a river (2 clones, 99%), as well as strains isolated from oil reservoirs (2 clones, 95%; Table S2). Firmicutes and Bacteroidetes clones were similar to environmental sequences from a soda lake (4 clones, 93%) and river (2 clones, 98%) respectively. To further assess the occurrence and distribution of putative thermophilic SRB contributing to the observed 60°C SRR, we used 16S rRNA primers targeting the genus *Desulfotomaculum* (Stubner and Meuser, 2000), since this genus was detected in both *dsrA* and *aprA* gene libraries. This 16S rRNA gene-based approach independently

confirmed the presence of *Desulfotomaculum* sequences in Dd and B samples.

DISCUSSION

Here we characterize the geochemistry and sulfur-cycling communities of four terrestrial mud volcanoes in Azerbaijan: D (Dashgil) and B (Bakhar), located near the Caspian Sea, and two inland TMVs, P (Perekyushkul) and BJ (Boransyz-Julga), located on the foothills of the Great Caucasses (Figure 1). Molecular and geochemical data support the presence of active sulfur-oxidizing and sulfate-reducing guilds across a range of physiochemical conditions. While both guilds were present in all four TMVs, the diversity within each guild was unique for each mud volcano suggesting a complex interplay of ecological and environmental factors influence the structure of sulfur-metabolizing communities. Molecular data revealed SOB were present in mud volcanoes with low and high sulfate levels and co-occurred with an active SRB population. *Apr*A phylotypes affiliated with SOB revealed putative chemosynthetic metabolisms including sequences clustering with obligate aerobes and facultative anaerobes collectively capable of coupling the oxidation of a variety of sulfur species to the respiration of both oxygen and nitrate. SRB community analyses together with SRR measurements support a predominance of Desulfobulbaceae members and active sulfate reduction across a range of temperatures with potential rates reflecting ambient sulfate levels. Thermophilic sulfate reduction was also detected in these approximately 20^{o}C mud volcanoes and together with molecular detection of putatively thermophilic Desulfotomaculum spp., supports the hypothesis that mud volcanoes transporter themophilic microorganisms from deep warm habitats up to the cooler surface

where they have been previously discovered as endospores (Hubert et al., 2009).

Microbial Ecology of the Azerbaijan Mud Volcanoes

The investigated mud volcanoes support microbial assemblages similar in abundance to other TMVs with bacterial abundance being greater than or equal to that of archaea (Table S3), depending on site and depth examined (Alain et al., 2006; Chang et al., 2011; Schulze-Makuch et al., 2011). Molecular analyses and rate measurements presented here indicate that bacterial diversity is moderate and dominated by meso- and thermophilic sulfur-cycling microorganisms.

Geochemical data suggest the large salse lakes and smaller pools, both of which continuously emit gas and water but very little sediment, have a shallower fluid source than gryphons (conical-shaped mounds emitting viscous mud, gas and water). These data are similar to prior studies from this region (Etiope et al., 2004; Mazzini et al., 2009), and may also explain differences observed in sulfate-reducing bacterial phylotypes retrieved from these distinct habitats. *In situ* sulfate concentrations were highly variable and did not appear to be correlated with specific habitats (salse vs. gryphon) or proximity to the Caspian Sea, and may therefore result from deep sources. Measurements of abundance and composition of reduced sulfur species (Tables 1, S4) are consistent with published studies from this region, revealing sulfur to be primarily in the form of disulfides such as pyrite (Isaksen et al., 2007). Monosulfides and elemental sulfur may therefore have a short residence time in these systems due to rapid sulfur cycling. Rock-Eval pyrolysis revealed higher concentrations of free hydrocarbons in sulfate-depleted volcanoes (B and BJ) suggesting

more labile carbon may be available to microbes in these sites, perhaps resulting from a scarcity of heterotrophic SRB.

Relevant microbial processes affecting carbon cycling that were not directly measured here include methanogenesis and methanotrophy. Studies of TMVs have reported evidence of anaerobic methane-oxidizing ANME archaea by CARD-FISH, molecular, and rate analyses (Alain et al., 2006; Schulze-Makuch et al., 2011; Wrede et al., 2011; Yang et al., 2011; Chang et al., 2011). In the present study, CARD-FISH analyses also revealed the occurrence of ANME/SRB aggregates (Figure S2), and sulfide production was observed in anaerobic microcosms incubated with methane (Table 2).

Sulfur Cycling

Microbial rate measurements and molecular analyses were used to further examine sulfur cycling in these dynamic environments. Unlike marine MVs, very little is known about chemosynthetic communities such as sulfur-oxidizing bacterial (SOB) populations in TMVs (Niemann and Boetius, 2010), though these communities can be a significant source of primary production (Levin et al., 2002). *Apr*A phylotypes associated with putative SOB were recovered from all samples and were similar in three out of the four TMVs. Phylogenetic analyses reveal that phylotypes from B, D and P cluster together to the exclusion of reference sequences from cultured species (Figure 3a). The majority of these sequences have as their closest relative *Thioalkalivibrio* spp., an aerobic Gammaproteobacterial genus isolated from soda lakes (Sorokin 2001). The occurrence of these potential alkalophilic SOB phylotypes in P is also consistent with the recovery of SRB phylotypes from the same clone library (48/93 total clones), which fell within a

cluster of sequences most closely related to *Desulfurivibrio alkaliphilus* (Figure 3b). The pH values of all investigated TMVs were approximately 8.0; with waters of P (and BJ) with a total mineralization in the range of 1.6 to 2.6 g/l, defined as highly alkaline, hydrocarbonate-sodium type water compared to D (and B) which show total mineralization in the range of 2.5 to 8.2 g/l (data not shown). BJ, while sharing some physical and geochemical features with other TMVs, had distinct *apr*A phylotypes, most of which (96%) grouped closely together in one cluster of Betaproteobacteria including sequences from *Thiobacillus denitrificans*, a facultative anaerobe capable of respiring nitrate and oxygen. 16S rDNA phylotypes from D also provided evidence for the presence of SOB with Epsilonproteobacteria comprising a significant proportion of recovered sequences. As both putative aerobic and nitrate-respiring SOB phylotypes were recovered, these data suggest the sulfur-oxidizing guild may be common to TMVs in the region with the environment dictating the dominant SOB lineage (Table S2). Total nitrogen and $\boldsymbol{\delta}^{15}$N were measured with similar values across all TMVs. Although the composition of nitrogen species was not measured here nitrate versus oxygen availability could be a driver of dominant SOB lineages. Future studies focusing on nitrogen cycling in TMVs may reveal SOB as an important microbial component.

SRB communities can be broadly categorized into two groups based on their carbon oxidation pathways; complete oxidizers are capable of complete mineralization of organic substrates to CO_2, while incomplete oxidizers excrete acetate as a final byproduct (Canfield, 2005). There exists a taxonomic relationship between carbon oxidation pathway and many genera or even families of SRB; most members of the *Desulfobacteraceae* family are complete oxidizers while most members of the *Desulfobulbaceae* are not (Kuever at al., 2005).

CARD-FISH analyses revealed the occurrence of *Desulfobacteraceae* (Figure S2) and Desulfobulbaceae (data not shown) cells. Of the SRB phylotypes retrieved from the investigated mud volcanoes, putative incomplete carbon-oxidizing genera within the *Desulfobulbaceae* family were dominant at all sites except the deep Dd sample, which is dominated by *Desulfobacteraceae* (Figure 3b). All clone libraries originated from gryphon mud volcanoes, except for the D libraries, which were associated with a mud volcano pool. While gryphons contain viscous mud that may be more susceptible to mixing by rising gas bubbles throughout the depth column, pools contain water with comparatively minor amounts of fine sediment overlying a more discrete benthic layer. Interestingly, the diversity recovered from D, sampled at the surface (Ds) and at the bottom sediment (Dd) showed a dominance of complete carbon oxidizers in the underlying sediment layer but not in the surface sample. *DsrA* gene surveys from deep Dd also confirmed a significant fraction of recovered sequences were associated with complete carbon-oxidizing Desulfobacteraceae (Table S2). The P gryphon was also sampled at depth (2 m) however here showed a dominance of putative incomplete carbon-oxidizing Desulfobulbaceae. Cultured representative of incomplete oxidizing SRB are known to have comparatively faster growth rates, and outcompete complete oxidizing SRB in enrichments with substrates like lactate and thus may have a selective advantage in habitats where organic matter input is variable (Canfield, 2005). It is possible that gryphons and the shallow surfaces of salse lake waters are more dynamic environments giving incomplete carbon-oxidizers an advantage.

Microbial rate measurements were performed in order to assay carbon utilization and

temperature optimum among active SRB communities. Previous studies have confirmed an approximate 2:1 stoichiometry of CO_2 produced per sulfate consumed in habitats where sulfate reduction represents the primary means of carbon mineralization (Thamdrup and Canfield, 1996; Vandieken et al., 2006). In the present study CO_2 and sulfide production rates based on microcosm experiments revealed anaerobic CO_2 production was several orders of magnitude less than sulfate consumption (Table 2), consistent with a significant fraction of sulfate reduction carried out by incomplete carbon-oxidizing SRB. In most TMVs sampled, the addition of volatile fatty acids (VFAs) did not substantially stimulate SRRs suggesting these samples were not limited by bioavailable carbon and consistent with Rock Eval analyses (Figure 2). The exception was the deep Dd sample in which VFA addition caused a several orders of magnitude increase in SRR. Notably, *apr*A phylotypes recovered from this sample were uniquely related to putative autotrophic genera suggesting a potential adaptation to carbon limitation.

Evidence of Deep Biosphere Activity

Terrestrial mud volcanoes have been proposed to serve as conduits that connect Earth's surface environments with the underlying deep biosphere whereby the same processes that trigger mud volcanism also lead to a transport of materials from great depths (Hubert et al., 2009; Niemann and Boetius, 2010). While ambient surface mud temperatures of approximately 20 ^{o}C were measured in the current study (Table 1), conduits of $>$ 10 km have been modeled from Azeri mud volcanoes (Planke et al., 2003) suggesting a potential for the transport of organisms from deeper warmer underlying strata. Maximum SRR in the thermophilic range were observed from 20 ^{o}C mud collected at B and D, exhibiting

temperature optima (55 °C and 60°C, respectively) within the activity range of thermophilic SRB belonging to the genus *Desulfotomaculum*. SRR at these high temperatures were stimulated by the addition of VFAs, which members of this genus are known to use as electron donors (Widdel, 2006). Targeted 16S rRNA primers specific for the genus *Desulfotomaculum*, which was detected in both *dsrA* and *aprA* gene libraries, independently confirmed the presence of *Desulfotomaculum* sequences in those samples exhibiting sulfate reduction at high temperatures.

Desulfotomaculum have been detected in several deep subsurface habitats such as 5 km deep faults and 3.2 km gold mine boreholes (Baker et al., 2003; Moser et al., 2005) and mud volcanoes were hypothesized as a mechanism of transport of thermophilic SRB of the genus *Desulfotomaculum* from deep warm habitats to the arctic seabed (Hubert et al., 2009). This idea is strongly supported by our observation of high SRR in mud volcano samples originally at 20°C *in situ* that are heated to 50-70°C, and by the detection of putatively thermophilic *Desulfotomaculum* spp. in the same samples. Based on our *in situ* temperature measurements (Tables 1, S4), and the reported geothermal gradient in the South Caspian Basin (Planke et al., 2003; and references therein) temperatures of 50 to 65°C (optimal SRR as shown in figure 2 and consistent with the thermal range of several *Desulfotomaculum*; Widdel, 2006) exist at approximately 2 to 3 km below the surface. Consistent with a lack of SR detection above 60°C, we saw no molecular evidence of hyperthermophilic sulfate reducers, either archaea or bacteria.

CONCLUSIONS

Mud volcanism in Azerbaijan is one of the controlling factors for the vast oil and gas fields in this area; thus elucidating microbial processes in this region is important as these processes can play an important role in the degradation of hydrocarbon inside the reservoirs. The ability to analyse the geochemistry and microbial diversity and processes of distinct TMVs afforded by their high density in this region gives new insights into the interplay between S-cycling microorganisms and their environment. Sulfur cycling in TMVs has been largely unexplored and here we provide a comparative view of the microbial communities and processes involved in sulfur cycling in multiple TMVs of Azerbaijan. Sulfate-reducing and sulfur-oxidizing bacterial guilds were present in all TMVs but differed at the genus level between individual mud volcanoes. Detection of thermophilic SRB in 20°C habitats suggest that these TMVs, with conduits extending 10 km or more into deep thermic sediment, may actively transport microorganisms adapted to the deep biosphere.

EXPERIMENTAL PROCEDURES

Site Descriptions

Four mud volcanoes in the South Caspian Basin of eastern Azerbaijan were investigated: Dashgil (D), Bakhar (B), Perekyushkul (P) and Boransyz-Julga (BJ). Samples were taken from the following TMV features (described in Mazzini et al., 2009): gryphons (conical-shaped features less than 3 m in height which continuously emit gas, water, oil and viscous mud from their craters), pools (small round features with a diameter

up to 2 m, which continuously release water and gas with a minor amount of fine sediment) and salse lakes (lake-like features up to 30 m in diameter and 10 m deep, which vigorously vent large quantities of gas and water with only a limited amount of mud).

Despite regional and geological differences there is evidence that all four investigated mud volcanoes are sourced from the Maikop Series (Berner et al., 2009), which is Oligocene-Low Miocene in age and rich in organic carbon. Sediments of the Maikop Series are unconsolidated due to rapid burial and overpressure. Overpressuring is enhanced by biogenic and thermogenic gas generation, and results in upward migration at tectonically weak zones or due to earthquakes. Although all four mud volcanoes likely share this common source, D and B are located near the Caspian seaside lying on young Quaternary sediments while BJ and P are situated on the SE foothill of Great Caucasus and lie on comparatively older Oligocene-Miocene deposits (Figure 1).

D was photographed in 1997 by Hovland and colleagues, and together with B and P can be found in published maps of the South Caspian Basin along with background geochemical data (Etiope et al., 2004; Feyzullayev and Movsumova, 2010; Guliyev at al., 2001; Planke et al., 2003; Mazzini et al., 2009). D has more than 60 gryphons and salses, and has erupted at least 6 times since 1882; B has around 30 gryphons and salses, has erupted 11 times since 1853, the last recorded eruption occurred in 1992 (Etiope et al., 2004 and references therein). B is considered to have higher eruptive potential (Etiope et al., 2004), but both D and B have high seep activity (Planke et al., 2003). To our knowledge, there are no prior studies of BJ. Both P and BJ are visible from public satellite imaging (see Tables 1, S4 for GPS coordinates) and appeared to be dominated by uplifted clusters of gryphons during the October 2008 trip (Figure S1). Several of the gryphons in P

and BJ had white crust on the dry outer flanks. In BJ, dead arthropods (mainly beetles) were observed floating on the surface along the sides of several gryphons, along with a visually identified microbial mat. While mud volcanoes are considered dormant in the interval between eruptions (Mazzini et al., 2009), all four TMVs investigated exhibited active seepage of gas and mud.

Sampling

Samples were collected in 2007 from two D salse lakes (D1 and D3 in 2008 data) and one small salse lake within a satellite vent of B (see Planke et al., 2003 and Mazzini et al., 2009 for location of satellite relative to main vent). During a second collection trip in October 2008 samples were collected from D, the same B satellite vent, BJ, and P. Unless stated otherwise, all samples were collected directly into sterile 50 ml falcon tubes. Due to the morphological diversity of D and abundance of published background data, multiple features were sampled within this volcano. Sample D1 was taken from a large, actively bubbling salse lake (referred to as "Salse A" in Planke et al., 2003 and Mazzini et al., 2009). These samples were taken from the surface of the lake approximately 1 m from the shore using an extendable pole. Ds and Dd were taken from the surface and depths, respectively, of a small pool approximately 3 m from D1 (see Figure S1 for photograph). Deeper sample Dd was collected from approximately 4 m below the surface of the salse using a 65 cm drop core. Mud for microbial analyses was sampled from the center portion of the core. D3 samples were taken from a smaller salse lake ("Salse B" in Planke et al., 2003 and Mazzini et al., 2009) with visibly clearer water than that of D1. Samples were scooped from the bottom of this salse using a large ladle attached to the end of an

extendable pole. D4 samples were collected directly into a falcon tube from the thick bubbling surface of a gryphon. B samples were also taken directly from the surface of an actively bubbling gryphon at a site known as the Bakhar satellite vent. At the BJ site, surface material from a viscous gryphon was sampled (BJ) along with sediments from the bottom of a less viscous gryphon (BJ2). Ps and P were taken from the surface and depths, respectively, of a gryphon in P. Deeper sample P was taken from the bottom of a 65 cm drop core extended approximately 2 m below the surface.

Field conditions required that all samples be kept at ambient temperature until the end of each sampling day (approximately 5 hours) when they were processed and stored at the Geology Institute of ANAS (The Azerbaijan National Academy of Sciences) research lab in Baku prior to their shipment to either GFZ, Potsdam, Germany or CIT, USA.

Geochemical Analyses

Air-dried mud material was investigated by all methods further mentioned except for organic-petrographical analyses, for which the mud was freeze-dried. For determination of organic acids the freshly collected mud samples were immediately amended with 5% (v/v) of 10N NaOH to stop microbial activity. Water samples were collected by removal of the supernatant after centrifugation, followed by filtration. The samples for turnover measurements were immediately transferred into glass flasks, filled without headspace and once back in Baku lab, stored at 4°C. Organic geochemical parameters were determined on samples that were collected in pre-cleaned Teflon cups and stored in liquid nitrogen within a few hours after sampling.

Determination of anions

All water extracts were analyzed in replicate by ion chromatography with conductivity detection (ICS 3000, Dionex Corp.). For chromatographic separation of the anions the analytical column AS 11 HC (Dionex Corp.) was used at a temperature of 35 °C. The sample was eluted by KOH solution of varying concentration over time. The initial KOH concentration was 0.5 mM, maintained for 8 min. After 10 min, 15 mM KOH solution was reached and kept constant for 10 min. After 30 min analysis time, 60 mM KOH concentration was reached, followed by a rapid increase to 100 mM after 32 min. At 32 min analysis time, KOH concentration was again at the initial level of 0.5 mM and kept there for an additional 15 min to equilibrate the system. For quantification of organic acids (formate, acetate) and inorganic anions (F-, Cl-, Br-, SO_4^{2-}) standards containing all of the investigated compounds were measured in different concentrations every day. Standard deviation of sample and standard quantification is below 10 %.

Determination of Reduced Sulfur Species/Fractionated distillation

Solid reduced sulfur species were quantified separately based on the extraction scheme of (Zhabina and Volkov, 1978) with some modifications for the separation of elemental sulfur. The sample is placed into a cold distillation apparatus (Kallmeyer et al., 2004). In a first step 8 ml of 6 M hydrochloric acid is used to liberate the acid-volatile sulfur (AVS) fraction, comprising hydrogen sulfide and monosulfides. In the second step 16 ml of a 1 M chromous chloride ($CrCl_2$) solution is added to the sample to liberate the chromium-reducible sulfur (CRS) fraction, comprising mainly pyrite and other disulfides.

In the third step 20 ml N,N-dimethylformamide is added to the sample to obtain the elemental sulfur fraction (ES).

A constant flow of nitrogen is used to strip the liberated hydrogen sulfide gas from the sample and quantitatively collect it in a trap filled with 7 ml of 5% (w/v) zinc acetate solution. For each fraction a fresh trap is used; the reagents are simply added to the existing slurry. Each distillation step takes two hours to ensure sufficient time for the reaction.

The zinc acetate from the traps interferes with the spectrophotometric sulfide quantification (Cline, 1969), therefore the precipitated zinc sulfide is separated by centrifugation, the clear supernatant carefully decanted off and the pellet resuspended in demineralised water for analysis.

Potential Sulfate Reduction Rates (SRR)

The samples used for quantification of potential SRR were collected during October 2008 from three different mud volcanoes: at Dd from a depth of approximately four meters, at B and BJ from the surface of an actively mud-emitting pool. For sulfate reduction rate quantification the mud samples were diluted with anaerobic saline solution (for composition see Table S1) in a 1:1 ratio (w/v) in a 500 ml Duran flask. The flask was pre-flushed with gas (N_2/CO_2 80/20) for 5 minutes before quickly scooping in the mud, followed by flushing for another 5 minutes before screwing on the cap. After determination of the exact volume of mud by weighing, anaerobic saline solution was added to the flask and the slurry stirred for one hour. Aliquots of 3 ml were dispensed anaerobically into 30 autoclaved 16 ml screw cap culture tubes using a syringe and a needle. A mixture of 6 volatile fatty acids (VFA; acetate, butyrate, lactate, propionate, pyruvate, succinate) and

ethanol, each with a final concentration of 1 mM were added to the remaining slurry. From this VFA-slurry again 3 ml each were dispensed into each of 15 anoxic autoclaved screw cap culture tubes. Because of the storage in the cold room the samples were preincubated at their respective incubation temperature for 24 or 48 hours and labeled "24" and "48" accordingly. The VFA-amended samples were preincubated for 48 hours and labeled "48-VFA".

In order to avoid any sulfate limitation and thereby causing potential biases when comparing the microbial activity between the different sites, all samples were incubated with the same final sulfate concentration of 20 mM. A thermal gradient block (TGB) was used for experiments requiring different incubation temperatures (eg, Elsgaard et al., 1994; Sagemann et al., 1998). One end of the block was heated to 95°C while the other was cooled to 5°C resulting in a temperature gradient from 82.6 to 10.8°C. The linearity of the thermal gradient was checked after one day of equilibration with a digital thermometer. The positions of the culture tubes in the TGB were chosen to achieve a resolution of 5°C. All experiments were done in duplicates.

After 24 or 48 hours of preincubation, approximately 1 MBq (15 µl) of radioactive $^{35}SO_4^{2-}$ tracer was added to each sample with a syringe. A carrier-free tracer radiotracer stock solution was diluted with a saline solution containing the same major salts as the anoxic saline solution that was used to prepare the slurry. Incubation with the tracer lasted 8 hours and was terminated by adding 3 ml of 20% (w/v) zinc acetate (ZnAc) solution and immediate vortexing (Sagemann et al., 1998). The ZnAc-fixed slurry was poured into a 50 ml centrifuge tube. Remaining sediment was washed out of the tube with twice 3 ml 20% ZnAc. The sediment-ZnAc slurry was then centrifuged (5 min, 4500 g) and the supernatant

carefully decanted off. A small amount of supernatant was kept for quantification of the total radioactivity. The pellet was used for sulfate reduction rate measurements. The samples were processed according to the cold chromium distillation protocol of Kallmeyer et al. (2004). In short, the pellet was washed out of the tube with 20 ml dimethylformamide (DMF) into a three-neck round-bottom flask, then 8 ml HCl and 16 ml $CrCl_2$ solution was added. The liberated H_2S was flushed with N_2 into a 5% ZnAc trap. The radioactive sulfide was quantified using a Packard 2900 TR Tri-Carb scintillation counter. The sulfate reduction rate (SRR) was determined according to (Jørgensen, 1978). Control samples that were first fixed in ZnAC prior to radiotracer addition were processed together with the regular samples to quantify the background and to calculate the minimum detection limit.

Microcosms to Test Sulfide and CO_2 production

Mud and water samples were collected in 2007 from the D and B mud volcanoes. Experiments were carried out in glass tubes (20 ml) sealed with butyl-rubber stoppers and screw caps. Sediment samples (from 2007 trip) were mixed 1:1 with artificial mineral medium (after Widdel & Bak 1992; similar in composition to medium used for potential sulfate reduction rate measurements) to obtain homogenous slurries. Subsequently, 9 ml of medium were added to 3 ml of sediment slurry. All manipulations were performed under an atmosphere of nitrogen in an anoxic glove box. The headspace of the incubation tubes consisted either of methane (100%), air (100%) or of N_2/CO_2 (90/10 [v/v]; with CO_2 levels similarly unlimited as with gas composition used for potential sulfate reduction rate measurements). CO_2 was determined in all incubations using a GC 14B gas chromatograph

(Shimadzu) as described in Nauhaus *et al.* (2002). Sulfide was determined in anaerobic incubations using the formation of copper sulfide (Cord-Ruwisch, 1985).

Gene quantification by qPCR

Mud and water samples were collected in 2007 from D (salse lakes D1 and D3 in 2008 data) and B (small salse within same B satellite visited in 2008) mud volcanoes. DNA extraction was carried out using a Fast DNA for Soil Kit (Fast DNA Spin Kit for soil, BIO 101, MP Biomedicals, Germany). To block sedimentary nucleic acid binding capacities, 10 µl of a 1% polyadenylic acid solution were added in the initial step (Webster, 2003). Directly before PCR, 125 µl of 0.3% bovine serum albumine (BSA) in ultra-pure water were added as blocking agent to the Taqman master mix (Applied Biosystems, Germany) or the SYBR green® master mix (Eurogenetec, Germany). A real-time PCR instrument (ABI Prism 7000, Applied Biosystems) was employed to determine the 16S rRNA gene copy numbers of *Archaea* (Takai, 2000) and *Bacteria* (Nadkarni, 2002).

Molecular biological determination of sulfur-cycling bacteria

DNA Extraction

Mud samples collected from D, B, BJ and P during October 2008 for molecular analyses were stored at approximately ¯20°C before and after room temperature shipment. DNA extractions were conducted using the MoBio Ultraclean soil kit following a previously published protocol (Orphan et al., 2001). Due to inconsistencies in mud viscosity, the following starting material was used from each sample: Ds, 500 µl; Dd 0.5 gm weight wet; B1, 250 µl; BJ, 0.5 gm weight wet; P, 50 µl.

PCR Amplification and Cloning

Unless otherwise noted, amplification reactions followed published PCR mixtures and conditions (Harrison et al., 2009) with 0.5µl of Hotmaster Taq polymerase (Eppendorf AG, Hamburg, Germany). Bacterial 16S rRNA genes were amplified from Dashgil (D2D) using bacterium specific forward primer BAC-27F and universal reverse primer U-1492R (Lane, 1991). Thermocycling conditions included an initial 94°C denaturating step for 2 minutes followed by 30 cycles of 94°C for 1 minute, 54°C for 1 minute and 72°C for 1 minute, and then a final 72°C elongation step for 6 minutes. The products of 2 reactions were pooled and cleaned using a Multiscreen HTS plate (Millipore). The resulting purified 16S rRNA gene amplicons were ligated into pGEM-T Easy vector and used to transform JM109 chemically competent cells (Promega, Stoughton, WI). Genus-specific 16S rRNA primers DEM116F and DEM1164R were used to check for presence of *Desulfotomaculum* (Stubner and Meuser, 2000). Thermocycling conditions included an initial 94°C denaturation step for 1 minute followed by 40 cycles of 94°C for 45 seconds, 57.5°C for 45 seconds and 72°C for 1 minute, and then a final 72°C elongation step for 6 minutes.

An equimolar mix of forward primers DSR1F, DSR1Fa, DSR1Fb, DSR1Fc, and DSR1Fd and reverse primers DSR4R, DSR4Ra, DSR4Rb, DSR4Rc, DSR4Rd, and DSR4Re (Zverlov et al., 2005) was used to amplify the 1.9 kB *dsr*AB fragment from Dashgil (D2D). The 1.9 kb PCR product was excised from a 1% agarose gel and purified using a Quiaquick Gel Extraction kit (Qiagen Corp., Valencia, CA). Resulting DsrAB amplicons were ligated into pGEM-T Easy vector and used to transform JM109 chemically competent cells (Promega, Stoughton, WI).

The primer set AprA-1-FW/AprA-5-RV was used to amplify the approximately 0.4 kb fragment of the *aprA* gene (Meyer and Kuever, 2007a) from 2 µl of Dd and BJ and 1 µl of Ds, B and P DNA extractions. Thermocycling conditions included an initial 94°C denaturation step for 3 minutes followed by 40 cycles of 94°C for 30 seconds, 54°C for 55 seconds and 72°C for 1 minute, and then a final 72°C elongation step for 6 minutes. The products (1 reaction each from Dd, Ds, B and P templates, and 2 pooled reactions from the BJ template) were cleaned using a Multiscreen HTS plate (Millipore). The resulting purified *apr*A gene amplicons were ligated into pGEM-T Easy (D2D and S1; Promega) or pCR 4.0 TOPO TA (Ds, B and P; Invitrogen Corp., Carlsbad, CA) vectors and used to transform JM109 (Dd and BJ; Promega, Stoughton, WI) or One-Shot TOP10 (Ds, B and P; Invitrogen Corp., Carlsbad, CA) chemically competent cells according to the manufacturer's instructions.

Sequencing and Phylogenetic Analysis

HaeIII restriction fragment length polymorphism (RFLP) analysis was performed on products amplified with the standard primer set M13F/M13R (Pernthaler et al., 2008; Harrison et al., 2009; New England Biolabs, Ipswich, MA) from all 16S rDNA, *dsr*A and *apr*A clones. One RFLP pattern from Ds had representative clones from two distinct phylogenetic groups; all clones from with this pattern were further digested with PstI (New England Biolabs, Ipswich, MA) and the pattern divided accordingly. From the Dashgil_D2D samples, 62 *dsr*A clones were screened (11 unique RFLP patterns), and 74 bacterial 16S rDNA clones were screened (11 unique RFLP patterns). The following number of *apr*A clones were retrieved (with number of unique RFLP patterns in parenthesis) from each

TMV: Ds: 89 (16), Dd: 47 (9), B: 69 (14), BJ: 76 (6), P: 93 (21). Representative clones with unique restriction patterns were cleaned using Multiscreen HTS plates (Millipore) and sequenced unidirectionally either in house with a CEQ 8800 capillary sequencer according to the DTCS protocol (Beckman Coulter, Fullerton, CA), or at the ASGPB DNA Sequencing Facility of the University of Hawai'i at Manoa. All sequences were manually edited using Sequencher 4.5 software (Gene Codes, Ann Arbor, MI) and closest relatives in the GenBank database were identified using BLASTN (Altschul et al., 1997). All *apr*A sequences (131 translated amino acid characters each) were manually aligned using the ARB software package (version 7.12.07org, ARB_EDIT4; Ludwig et al., 2004) into an alignment of full-length *apr*A SRP and SOB reference strains and closest relatives recovered from the public databases. The aligned sequences were then added to the existing full length *apr*A tree using the quick add maximum parsimony method with a filter to mask regions outside of the 131 amino acid characters. Genbank accession numbers for *apr*A, *dsr*A and 16S rRNA sequences are JX908299-JX908360 and JX889577-JX889588.

ACKNOWLEDGEMENTS

We would like to acknowledge Dr. Chingiz Aliyev and Rauf Bagirli for assistance during field trip and laboratory investigations in Baku; Daniela Zoch and Holger Probst for technical work at BGR, and Andrea Vieth-Hillebrandt and Kristin Günther for water analysis at Helmholtz Centre Potsdam GFZ. Funding for this work was provided by a DOE Career grant (to VJO), a NSF GRFP (to AG-S) and through the Forschungsverbund GeoEnergie of the German Ministry for Education and Research (BMBF, to JK and PS).

REFERENCES

Alain, K., Holler, T., Musat, F., Elvert, M., Treude, T., and Kruger, M. (2006). Microbiological investigation of methane- and hydrocarbon-discharging mud volcanoes in the Carpathian Mountains, Romania. *Environmental Microbiology* 8**,** 574-590.

Altschul, S.F., Madden, T.L., Schäffer, A.A., Zhang, J., Zhang, Z., Miller, W., and Lipman, D.J. (1997). Gapped BLAST and PSI-BLAST: a new generation of protein database search programs. *Nucleic Acids Research* 25**,** 3389-3402.

Baker, B.J., Moser, D.P., Macgregor, B.J., Fishbain, S., Wagner, M., Fry, N.K., Jackson, B., Speolstra, N., Loos, S., Takai, K., Lollar, B.S., Fredrickson, J., Balkwill, D., Onstott, T.C., Wimpee, C.F., and Stahl, D.A. (2003). Related assemblages of sulphate-reducing bacteria associated with ultradeep gold mines of South Africa and deep basalt aquifers of Washington State. *Environmental Microbiology* 5**,** 267-277.

Beller, H.R., Chain, P.S.G., Letain, T.E., Chakicherla, A., Larimer, F.W., Richardson, P.M., Coleman, M.A., Wood, A.P., and Kelly, D.P. (2006). The Genome Sequence of the Obligately Chemolithoautotrophic, Facultatively Anaerobic Bacterium Thiobacillus denitrificans. *J. Bacteriol.* 188**,** 1473-1488.

Berner, U., Scheeder, G., Kus, J., Movsumova, U. (2009). "Mud Volcanoes of Azerbaijan – Windows to the Subsurface", in: *AAPG.* (Denver).

Canfield, D.E., Kristensen, E. And Thamdrup, B., (2005). *Aquatic Geomicrobiology*. San Diego: Elsevier.

Chang, Y.-H., Cheng, T.-W., Lai, W.-J., Tsai, W.-Y., Sun, C.-H., Lin, L.-H., and Wang, P.-L. (2012). Microbial methane cycling in a terrestrial mud volcano in eastern Taiwan. *Environmental Microbiology***,** n/a-n/a.

Cline, J.D. (1969). Spectrophotometric Determination of Hydrogen Sulfide in Natural Waters. *Limnology and Oceanography* 14**,** 454-458.

Cord-Ruwisch, R. (1985). A quick method for the determination of dissolved and precipitated sulfides in cultures of sulfate-reducing bacteria. *Journal of Microbiological Methods* 4**,** 33-36.

Dimitrov, L.I. (2002). Mud volcanoes--the most important pathway for degassing deeply buried sediments. *Earth-Science Reviews* 59**,** 49-76.

Elsgaard, L., Isaksen, M.F., Jørgensen, B.B., Alayse, A.-M., and Jannasch, H.W. (1994).

Microbial sulfate reduction in deep-sea sediments at the Guaymas Basin hydrothermal vent area: Influence of temperature and substrates. *Geochimica et Cosmochimica Acta* 58**,** 3335-3343.

Etiope, G., Feyzullayev, A., Baciu, C.L., and Milkov, A.V. (2004). Methane emission from mud volcanoes in eastern Azerbaijan. *Geology* 32**,** 465-468.

Etiope, G., and Milkov, A.V. (2004). A new estimate of global methane flux from onshore and shallow submarine mud volcanoes to the atmosphere. *Environmental Geology* 46**,** 997-1002.

Feyzullayev, A., and Movsumova, U. (2010). The nature of the isotopically heavy carbon of carbon dioxide and bicarbonates in the waters of mud volcanoes in Azerbaijan. *Geochemistry International* 48**,** 517-522.

Guliyev, I.S., Feyzulayev, A.A., and Huseynov, D.A. (2001). Isotope geochemistry of oils from fields and mud volcanoes in the South Caspian Basin, Azerbaijan. *Petroleum Geoscience* 7**,** 201-209.

Harrison, B.K., Zhang, H., Berelson, W., and Orphan, V.J. (2009). Variations in Archaeal and Bacterial Diversity Associated with the Sulfate-Methane Transition Zone in Continental Margin Sediments (Santa Barbara Basin, California). *Appl. Environ. Microbiol.* 75**,** 1487-1499.

Hiibel, S.R., Pereyra, L.P., Inman, L.Y., Tischer, A., Reisman, D.J., Reardon, K.F., and Pruden, A. (2008). Microbial community analysis of two field-scale sulfate-reducing bioreactors treating mine drainage. *Environmental Microbiology* 10**,** 2087-2097.

Hubert, C., Loy, A., Nickel, M., Arnosti, C., Baranyi, C., Brüchert, V., Ferdelman, T., Finster, K., Christensen, F.M., Rosa De Rezende, J., Vandieken, V., and Jørgensen, B.B. (2009). A Constant Flux of Diverse Thermophilic Bacteria into the Cold Arctic Seabed. *Science* 325**,** 1541-1544.

Hubert C, Arnosti C, Brüchert V, Loy A, Vandieken V, Jørgensen BB. (2010) Thermophilic anaerobes in Arctic marine sediments induced to mineralize complex organic matter at high temperature. *Environmental Microbiology* 12: 1089-1104.

Isaksen, G.H., Aliyev, A., Barboza, S.A., Plus, D., Guliyev, I.S., (2007). "Regional evaluation of source rock in Azerbaijan from the geochemistry of organic-rich rocks in mud-volcano ejecta. ," in *Oil and Gas of the Greater Caspian Area* ed. P.O. Yilmaz, Isaksen, G.H.: AAPG Studies in Geology), 51-64.

Jørgensen, B.B. (1978). A comparison of methods for the quantification of bacterial sulfate reduction in coastal marine sediments. *Geomicrobiology Journal* 1**,** 11-27.

Kallmeyer, J., and Boetius, A. (2004). Effects of Temperature and Pressure on Sulfate Reduction and Anaerobic Oxidation of Methane in Hydrothermal Sediments of Guaymas Basin. *Applied and Environmental Microbiology* 70**,** 1231-1233.

Kelly, D.P., and Wood, A.P. (2000). Confirmation of Thiobacillus denitrificans as a species of the genus Thiobacillus, in the beta-subclass of the Proteobacteria, with strain NCIMB 9548 as the type strain. *International Journal of Systematic and Evolutionary Microbiology* 50**,** 547-550.

Kuever, J., Rainey, F., and Widdel, F. (2005). "Genus I. *Desulfobulbus* Widdel 1981, 382VP (Effective publication: Widdel 1980, 374) in *Bergey's Manual® of Systematic Bacteriology,* eds. D.J. Brenner, N.R. Krieg, G.M. Garrity, J.T. Staley, D.R. Boone, P. Vos, M. Goodfellow, F.A. Rainey & K.-H. Schleifer. Springer US), 988-992.

Liu, J., Wu, W., Chen, C., Sun, F., and Chen, Y. (2011). Prokaryotic diversity, composition structure, and phylogenetic analysis of microbial communities in leachate sediment ecosystems. *Applied Microbiology and Biotechnology* 91**,** 1659-1675.

Levin, L.A. and Michener, R.H. (2002). Isotopic Evidence for Chemosynthesis-Based Nutrition of Macrobenthos: The Lightness of being at Pacific Methane Seeps. *Limnology and Oceanography* 47 (5), 1336-1345.

Lösekann, T., Knittel, K., Nadalig, T., Fuchs, B., Niemann, H., Boetius, A., and Amann, R. (2007). Diversity and Abundance of Aerobic and Anaerobic Methane Oxidizers at the Haakon Mosby Mud Volcano, Barents Sea. *Applied and Environmental Microbiology* 73**,** 3348-3362.

Ludwig, W., Strunk, O., Westram, R., Richter, L., Meier, H., Yadhukumar, Buchner, A., Lai, T., Steppi, S., Jobb, G., Förster, W., Brettske, I., Gerber, S., Ginhart, A.W., Gross, O., Grumann, S., Hermann, S., Jost, R., König, A., Liss, T., Lüßmann, R., May, M., Nonhoff, B., Reichel, B., Strehlow, R., Stamatakis, A., Stuckmann, N., Vilbig, A., Lenke, M., Ludwig, T., Bode, A., and Schleifer, K.-H. (2004). ARB: a software environment for sequence data. *Nucleic Acids Research* 32**,** 1363-1371.

Mazzini, A., Svensen, H., Planke, S., Guliyev, I., Akhmanov, G.G., Fallik, T., and Banks, D. (2009). When mud volcanoes sleep: Insight from seep geochemistry at the Dashgil mud volcano, Azerbaijan. *Marine and Petroleum Geology* 26**,** 1704-1715.

Meyer, B., and Kuever, J. (2007a). Phylogeny of the alpha and beta subunits of the dissimilatory adenosine-5'-phosphosulfate (APS) reductase from sulfate-reducing prokaryotes - origin and evolution of the dissimilatory sulfate-reduction pathway. *Microbiology-Sgm* 153**,** 2026-2044.

Meyer, B., and Kuever, J. (2007b). Molecular analysis of the distribution and phylogeny of dissimilatory adenosine-5'-phosphosulfate reductase-encoding genes (aprBA) among

sulfuroxidizing prokaryotes. *Microbiology-SGM* 153**,** 3478-3498.

Meyer, B., and Kuever, J. (2007c). Molecular analysis of the diversity of sulfate-reducing and sulfur-oxidizing prokaryotes in the environment, using aprA as functional marker gene. *Applied and Environmental Microbiology* 73**,** 7664-7679.

Moser, D.P., Gihring, T.M., Brockman, F.J., Fredrickson, J.K., Balkwill, D.L., Dollhopf, M.E., Lollar, B.S., Pratt, L.M., Boice, E., Southam, G., Wanger, G., Baker, B.J., Pfiffner, S.M., Lin, L.-H., and Onstott, T.C. (2005). Desulfotomaculum and Methanobacterium spp. Dominate a 4- to 5-Kilometer-Deep Fault. *Applied and Environmental Microbiology* 71**,** 8773-8783.

Nadkarni, M.A., Martin, F.E., Jacques, N.A., and Hunter, N. (2002). Determination of bacterial load by real-time PCR using a broad-range (universal) probe and primers set. *Microbiology* 148**,** 257-266.

Nakada, R., Takahashi, Y., Tsunogai, U., Zheng, G.D., Shimizu, H., and Hattori, K.H. (2011). A geochemical study on mud volcanoes in the Junggar Basin, China. *Applied Geochemistry* 26**,** 1065-1076.

Nauhaus, K., Boetius, A., Krüger, M., and Widdel, F. (2002). In vitro demonstration of anaerobic oxidation of methane coupled to sulphate reduction in sediment from a marine gas hydrate area. *Environmental Microbiology* 4**,** 296-305.

Niemann, H., and Boetius, A. (2010). "Mud Volcanoes Handbook of Hydrocarbon and Lipid Microbiology," ed. K.N. Timmis. Springer Berlin Heidelberg), 205-214.

Niemann, H., Duarte, J., Hensen, C., Omoregie, E., Magalhães, V.H., Elvert, M., Pinheiro, L.M., Kopf, A., and Boetius, A. (2006). Microbial methane turnover at mud volcanoes of the Gulf of Cadiz. *Geochimica et Cosmochimica Acta* 70**,** 5336-5355.

Orphan, V.J., Hinrichs, K.U., Ussler, W., Paull, C.K., Taylor, L.T., Sylva, S.P., Hayes, J.M., and Delong, E.F. (2001). Comparative analysis of methane-oxidizing archaea and sulfate-reducing bacteria in anoxic marine sediments. *Applied and Environmental Microbiology* 67**,** 1922-1934.

Pernthaler, A., Dekas, A.E., Brown, C.T., Goffredi, S.K., Embaye, T., and Orphan, V.J. (2008). Diverse syntrophic partnerships from deep-sea methane vents revealed by direct cell capture and metagenomics. *Proc Natl Acad Sci U S A* 105**,** 7052-7057.

Planke, S., Svensen, H., Hovland, M., Banks, D.A., and Jamtveit, B. (2003). Mud and fluid migration in active mud volcanoes in Azerbaijan. *Geo-Marine Letters* 23**,** 258-268.

Sagemann, J., Jørgensen, B.B., and Greeff, O. (1998). Temperature dependence and rates of sulfate reduction in cold sediments of Svalbard, Arctic Ocean. *Geomicrobiology Journal*

15**,** 85-100.

Sass, H., Cypionka, H., and Babenzien, H.-D. (1997). Vertical distribution of sulfate-reducing bacteria at the oxic-anoxic interface in sediments of the oligotrophic Lake Stechlin. *FEMS Microbiology Ecology* 22**,** 245-255.

Schulze-Makuch, D., Haque, S., Antonio, M.R.D., Ali, D., Hosein, R., Song, Y.C., Yang, J.S., Zaikova, E., Beckles, D.M., Guinan, E., Lehto, H.J., and Hallam, S.J. (2011). Microbial Life in a Liquid Asphalt Desert. *Astrobiology* 11**,** 241-258.

Stubner, S., and Meuser, K. (2000). Detection of Desulfotomaculum in an Italian rice paddy soil by 16S ribosomal nucleic acid analyses. *FEMS Microbiology Ecology* 34**,** 73-80.

Takai, K., and Horikoshi, K. (2000). Rapid Detection and Quantification of Members of the Archaeal Community by Quantitative PCR Using Fluorogenic Probes. *Applied and Environmental Microbiology* 66**,** 5066-5072.

Thamdrup, B., and Canfield, D.E. (1996). Pathways of Carbon Oxidation in Continental Margin Sediments off Central Chile. *Limnology and Oceanography* 41**,** 1629-1650.

Vandieken, V., Knoblauch, C., and Jørgensen, B.B. (2006). Desulfotomaculum arcticum sp. nov., a novel spore-forming, moderately thermophilic, sulfate-reducing bacterium isolated from a permanently cold fjord sediment of Svalbard. *International Journal of Systematic and Evolutionary Microbiology* 56**,** 687-690.

Webster, G., Newberry, C.J., Fry, J.C., and Weightman, A.J. (2003). Assessment of bacterial community structure in the deep sub-seafloor biosphere by 16S rDNA-based techniques: a cautionary tale. *Journal of Microbiological Methods* 55**,** 155-164.

Widdel, F., Bak, F. (1992). "Gram-negative mesophilic sulfate-reducing bacteria.," in *The prokaryotes,* ed. A. Balows, Truper, H. G., Dworkin, M., Harder, W., Schleifer, K-H. (New York, New York: Springer-Verlag), 3352-3378.

Wrede, C., Brady, S., Rockstroh, S., Dreier, A., Kokoschka, S., Heinzelmann, S.M., Heller, C., Reitner, J., Taviani, M., Daniel, R., and Hoppert, M. (2011). Aerobic and anaerobic methane oxidation in terrestrial mud volcanoes in the Northern Apennines. *Sedimentary Geology*.

Yakimov, M.M., Giuliano, L., Crisafi, E., Chernikova, T.N., Timmis, K.N., and Golyshin, P.N. (2002). Microbial community of a saline mud volcano at San Biagio-Belpasso, Mt. Etna (Italy). *Environmental Microbiology* 4**,** 249-256.

Yamamoto, M., and Takai, K. (2011). Sulfur metabolisms in epsilon- and gamma-Proteobacteria in deep-sea hydrothermal fields. *Frontiers in Microbiology* 2.

Yang, H.-M., Lou, K., Sun, J., Zhang, T., and Ma, X.-L. (2011). Prokaryotic diversity of an active mud volcano in the Usu City of Xinjiang, China. *Journal of Basic Microbiology***,** n/a-n/a.

Zhabina, N.N., And Volkov, I.I. (1978). "A method of determination of various sulfur compounds in sea sediments and rocks," in *Environmental biogeochemistry and geomicrobiology,* ed. W.E. Krumbein. Ann Arbor Sci.), 735-745.

Zverlov, V., Klein, M., Lucker, S., Friedrich, M.W., Kellermann, J., Stahl, D.A., Loy, A., and Wagner, M. (2005). Lateral Gene Transfer of Dissimilatory (Bi)Sulfite Reductase Revisited. *J. Bacteriol.* 187**,** 2203-2208.

Figures and Tables

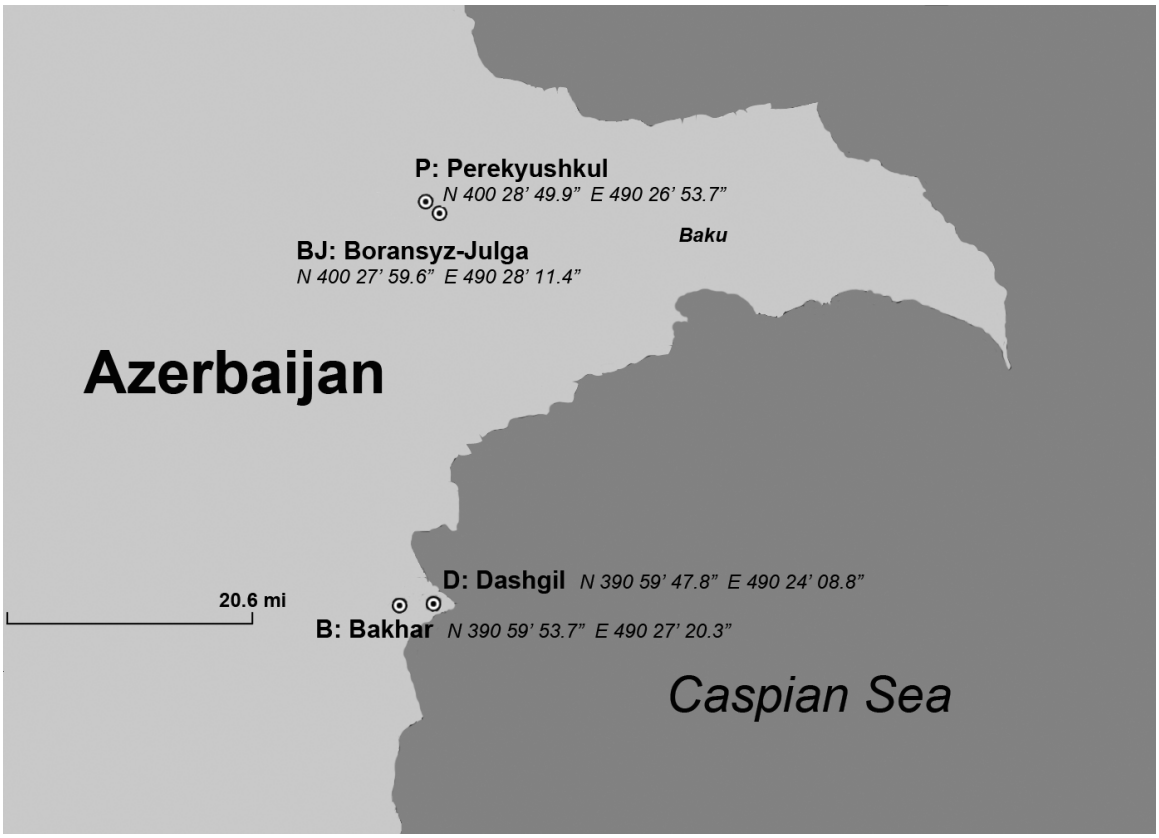

Figure 1. Location of terrestrial mud volcanoes in Azerbaijan sampled in 2007 and 2008

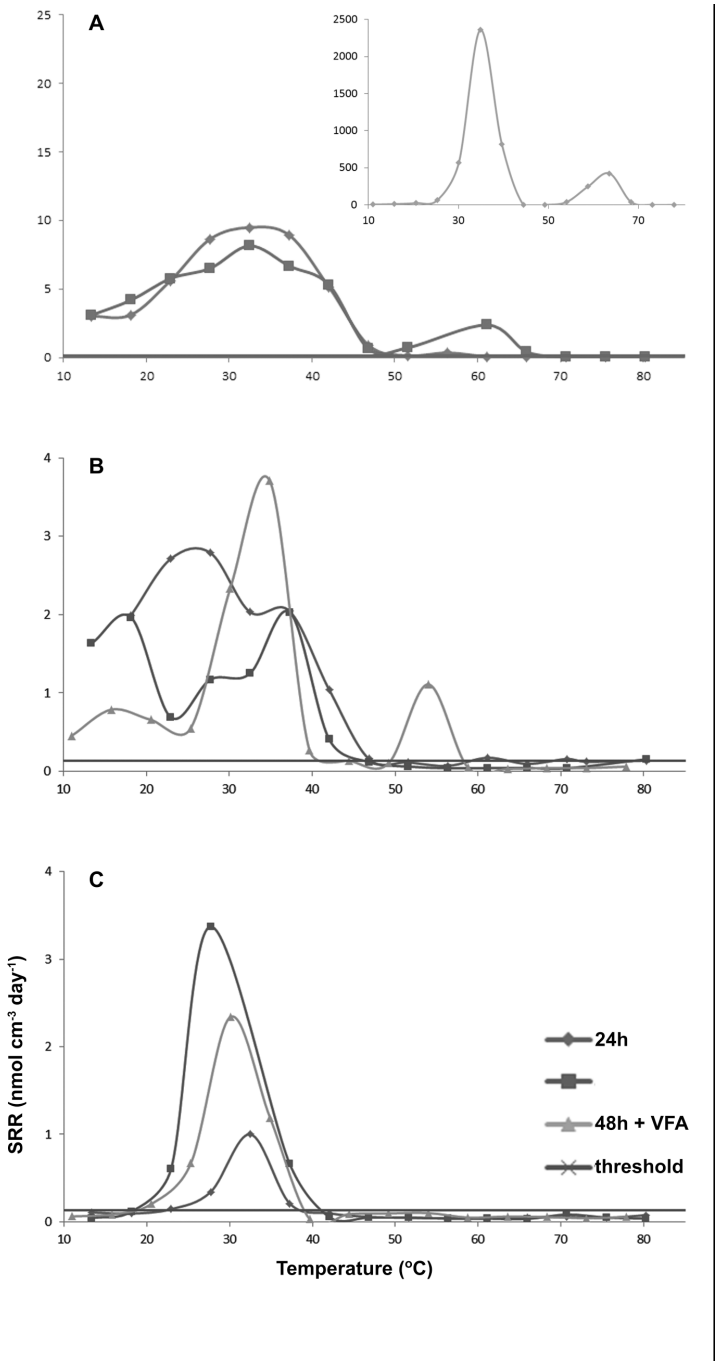

Figure 2. Potential sulfate reduction rates for A) Dashgil (Dd), B) Bakhar (gryphon sample B) and C) Boransyz-Julga (gryphon sample BJ). Rate measurements were taken on a thermal gradient block ranging from approx. 10°C to 82°C, with 3 incubation treatments: 24-hour preincubation, 48 hour preincubation, and 48 hour preincubation with volatile fatty

acids (VFAs). The dashed line indicates the minimum detection limit was 0.12 nmol/cm^3/d, which is the average of all blank measurements plus 3 times the standard deviation.

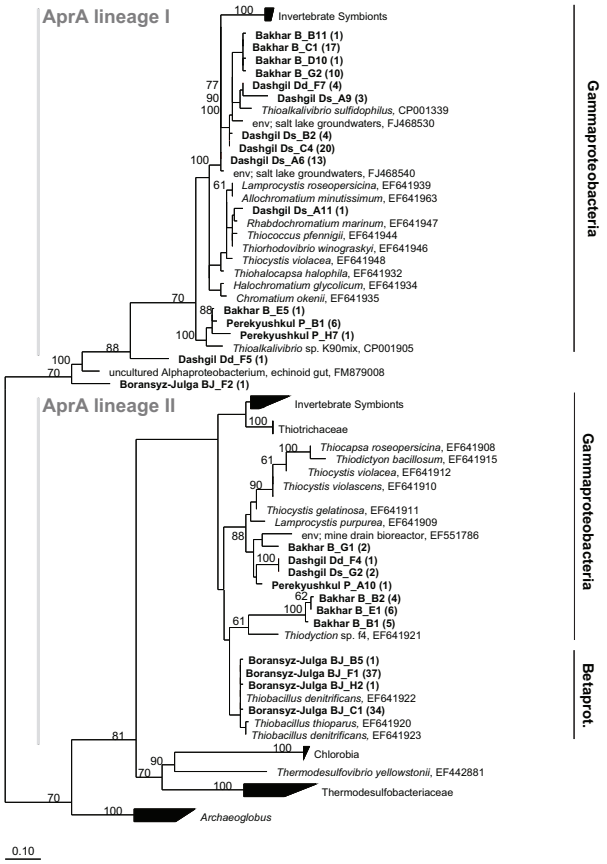

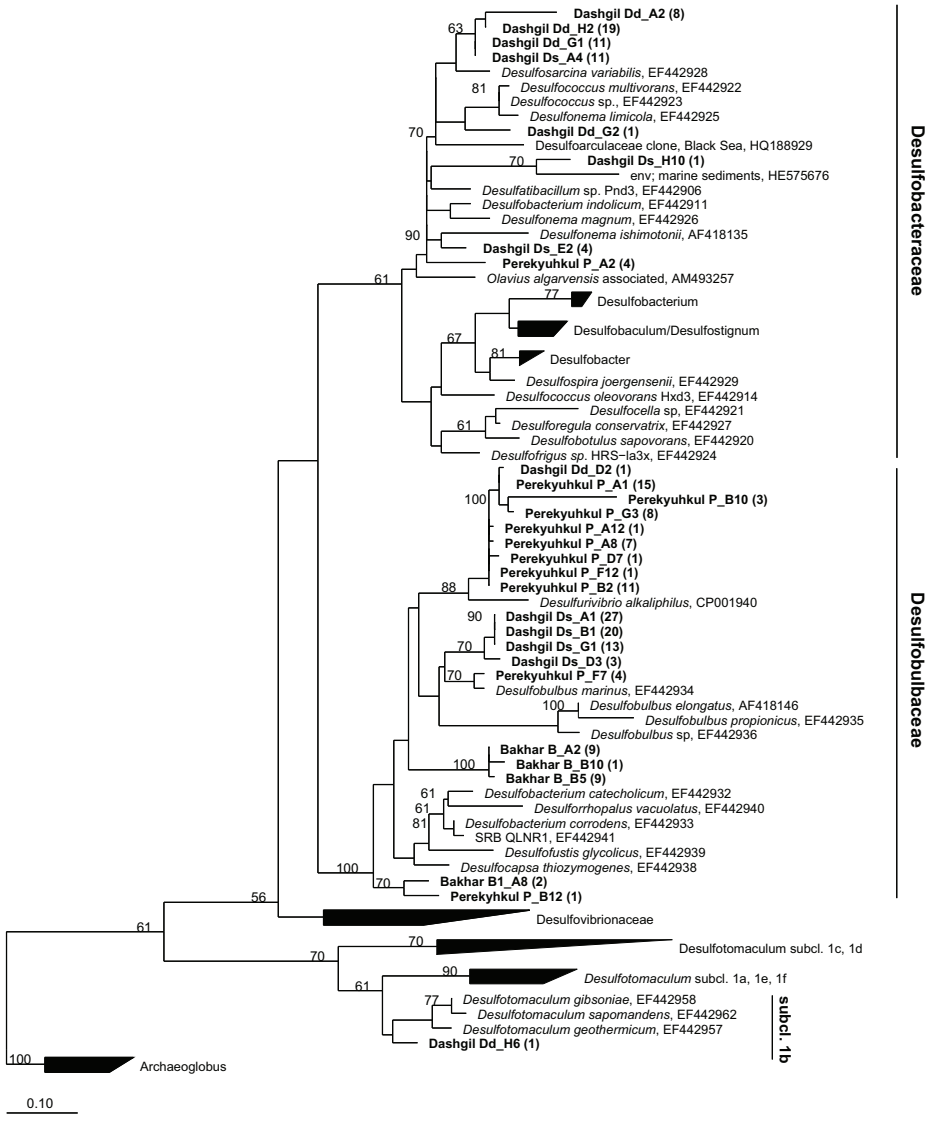

Figure 3. Phylogenetic relationships of A) putative sulfur-oxidizing bacterial and B) putative sulfate-reducing bacterial *apr*A sequences retrieved from Dashgil (Dd, Ds; 89 and 47 clones, respectively), Bakhar (B; 69 clones), Boransyz-Julga (BJ; 76 clones) and Perekyushkul (P; 93 clones) mud volcanoes sampled in 2008 and inferred via maximum parsimony using the ARB software package. The number of clones represented by each

OTU sequence in the tree is listed in parenthesis after the name. The scale bar corresponds to 10% estimated sequence divergence.

Table 1. Geochemical and biological characteristics of four terrestrial mud volcanoes of Azerbaijan sampled in October 2008. ***n/a = not available; SRR = Sulfate Reduction Rate***

Mud Volcano	**D: Dashgil**		**B: Bakhar**	**P: Perekyushkul**	**BJ: Boransyz-Julga**
Geographic Setting	*Proximal to Caspian Sea* Quaternary Sediments		*Proximal to Caspian Sea* Quaternary Sediments	*Foothills of Great Caucasus* Oligocene-Lower Miocene Deposits	*Foothills of Great Caucasus* Oligocene-Lower Miocene Deposits
Coordinates	N 39º 59' 47.8" E 49º 24' 08.8"		N 39º 59' 53.7" E 49º 27' 20,3"	N 40º 28' 49.9" E 49º 26' 53.7"	N 40º 27' 59.6" E 49º 28' 11.4"
Sample Name and Feature	**Ds: Pool (surface)**	**Dd: Pool (deep)**	**B: Gryphon**	**P: Gryphon (deep)**	**BJ: Gryphon**
Temperature, °C (measurement depth, m)	17.2 (0.2)	20.6 (1.0), 20.8 (1.25)	19.6 (0.2), 20.7 (3.5)	17.6 (2.5)	18.5 (0.2), 18.3 (1.5)
POREWATER GEOCHEMISTRY					
Sulfate (mM)	1.65	1.22	< 0.16	0.80	< 0.16
Cl/Br (mass ratio)	220	219	189	>197.95	206
Acetate (mM)	0.018	0.029	0.027	0.049	n/a
Formate (mM)	0.018	0.024	0.030	0.047	n/a
REDUCED SULFUR SPECIES					
(AVS:CRS:DMF)	n/a	n/a	n/a	0.23: 99.72: 0.05	3.85: 96.13: 0.02
MICROBIOLOGICAL ANALYSES					
Desulfotomaculum detection (16S)	n/a	+	+	-	-
Dominant Guild (*aprA* clone library)	SRB	SRB	SOB	SRB	SOB
SRR Preincubation conditions:					
24 hr: temp. opt., °C (SRR, nmol/cm³/d)	n/a	32 (9.5)	25 (2.8), 39 (2.0)	n/a	31 (1.0)
48 hr: temp. opt., °C (SRR, nmol/cm³/d)	n/a	32 (8.2), 61 (2.4)	18 (2.0), 39 (2.0)	n/a	29 (3.4)
48 hr + VFA: temp. opt., °C (SRR, nmol/cm³/d)	n/a	35 (2359.9), 63 (424.5)	15 (0.8), 34 (3.7), 54 (1.1)	n/a	30 (2.3)

Table 2. CO_2 and H_2S production (nmol cm^{-3} day^{-1}) from microcosms inoculated with D (Dashgil) and B (Bakhar) sample slurries collected in 2007. ***n/a = not available***

Sample, depth collected	CO_2 under air	CO_2 under N_2/CO_2	H_2S under N_2/CO_2	H_2S under CH_4
Dashgil (D1) big salse lake, 5.8m	8.20E+05 +/- 1.10E+05	4.30E+02 +/- 7.90E+01	2.90E+04 +/- 8.00E+03	5.60.E+04 +/- 4.00E+03
Dashgil (D1) big salse lake, 0.5m	6.40E+05 +/- 8.20E+04	4.80E+02 +/- 9.30E+01	1.40E+04 +/- 3.00E+03	3.90.E+04 +/- 1.00E+04
Dashgil (D3) small salse lake, 6.5m	1.07E+06 +/- 2.20E+05	6.30E+02 +/- 1.10E+02		
Dashgil (D3) small salse lake, 0.2m	8.60E+05 +/- 1.40E+05	5.80E+02 +/- 8.30E+01	3.00E+04 +/- 2.00E+03	6.70.E+04 +/- 1.00E+04
Bakhar small salse lake, 4.2m	4.90E+05 +/- 2.30E+04	3.10E+02 +/- 2.00E+01	1.40E+04 +/- 3.00E+03	3.80.E+04 +/- 4.00E+03
Bakhar small salse lake, 0.2m	4.70E+05 +/- 5.60E+04	2.70E+02 +/- 4.10E+01	1.60E+04 +/- 1.00E+04	3.10.E+04 +/- 8.00E+03

SUPPLEMENTAL ONLINE MATERIAL

RESULTS

Geochemical characterization

The organic matter (OM) of all samples appears to be a mixture of marine and terrestrial material, sourced from sediments with a thermal maturity of around 0.5 % vitrinite reflectance. The total organic carbon (TOC) composition within the 4 mud volcanoes ranged between 0.58 and 1.5% with $d^{13}C$ values between -25.2‰ down to -26.7‰. With the exception of the salse lake at D (D3), $d^{13}Corg$ for the coastal mud volcanoes (D and B) were approximately 1‰ heavier (avg. -25.2‰) compared with the inland sites (P and BJ (avg. -26.5‰; Tables 1, S4). Thermal maturity for the majority of samples had a T_{max} around 420 to 430°C, with the exception of B, which showed slightly lower T_{max} values (392ºC; Tables 1, S4). B samples also exhibited strong degradation of metabolizable OM, with a loss of n-alkanes and occurrence of an unresolved complex

mixture (UCM). These samples were also characterized by lower contents of TOC (< 0.7 % TOC) in comparison with the other volcano samples (1.2 to 1.3 % TOC on average), and an obvious type II signal in the Rock Eval programs. Based on the thermal maturity, the organic material of the B volcano may have originated from a shallower source relative to the other three volcanoes in this study. Rock Eval programs exhibited relatively higher S1 signals in B and BJ samples indicating free bitumen in the rock matrix (Tables S4, S5). Organic acids in the pore fluids (formate and acetate) were detected in all but D (D1) and ranged between 14 to 49 μM. The carbonate fraction of the muds in the BJ and P volcanoes were characterized by heavy $\delta^{13}C$ (1.4 to 3.0‰) and $\delta^{18}O$ (-2.4 to -2.9‰) values relative to carbonates from D and B ($\delta^{13}C$: 0.28 to -2.4‰ and $\delta^{18}O$: -2.5 to -4.3‰).

Indirect evidence of methanogenesis was found in stable isotope analyses from inland mud volcanoes, P and B, with enriched $\delta^{13}C$ values of carbonate suggestive of carbonate precipitation under methanogenic conditions (Feyzullayev and Movsumova, 2010).

***In situ* detection of archaeal sulfate-reducing consortia by epifluorescent microscopy**

Due to high viscosity/hydrocarbon content of the mud samples, CARD-FISH hybridization reactions were only successful with some of the samples. In the D1 sample, cell aggregations consisting of ANME-2 archaea and SRB associated with the Desulfosarcina/Desulfococcus group (Figure S2) and members of the Desulfobulbaceae (data not shown) were detected. These aggregates were also detected in shallow Ds and BJ2 samples, and single cells staining only with DAPI were visible in all samples (data not shown). Aggregates ranged in diameter from 3 μm to 8 μm with three distinct

morphologies similar to those previously observed in cold seeps: ANME core with SRB shell, adjoined clumps or a heterogeneous mixture of both (eg, Orphan et al., 2002).

EXPERIMENTAL PROCEDURES

Geochemical Analyses

Analysis of the stable isotope composition

Total organic carbon (TOC) and $\delta^{13}C_{org}$ as well as total nitrogen (TN), $\delta^{15}N$ and total carbon (TC) were determined using an elemental analyzer (NC2500 Carlo Erba) coupled with a ConFlowIII interface on a DELTAplusXL mass spectrometer (ThermoFischer Scientific) at the Deutsches GeoForschungsZentrum in Potsdam, Germany. The isotopic composition is given in delta notation relative to a standard: d (‰) = $[(R_{sample} - R_{standard})/R_{standard})] \times 1000$. The isotopic ratio (R) and standard for carbon is $^{13}C/^{12}C$ and VPDB (Vienna PeeDee Belemnite), respectively, and for nitrogen is $^{15}N/^{14}N$ and air.

The TOC contents and $\delta^{13}C_{org}$ values were determined on decalcified samples. Around 3 mg of sample material were weighed into Ag-capsules, dropped with 20% HCl, heated for 3 h at 75°C, and finally wrapped into the Ag-capsules and measured as described above. The calibration was performed using elemental (Urea) and certified isotope standards (USGS24, CH-7) and proofed with an internal soil reference sample (Boden3). The reproducibility for replicate analyses is 0.2% for TOC and 0.2‰ for $\delta^{13}C_{org}$.

For total carbon, nitrogen and $\delta^{15}N$ determination, around 20 mg of sample material was loaded in tin capsules and combusted in the elemental analyzer. Total carbon and

nitrogen content were calibrated against Acetanilide whereas for the nitrogen isotopic composition two ammonium sulfate standards (eg, IAEA N-1 and N-2) were used. Replicate determinations show a standard deviation less than 0.2% for C and N and 0.2‰ for $\delta^{15}N$.

The stable isotope compositions of carbonates ($\delta^{13}C$ and $\delta^{18}O$) were determined in continuous flow mode using a Finningan GasBenchII with carbonate option coupled to a DELTA^{plus}XL mass spectrometer. From each sample, about ~ 250 mg were loaded into 10 ml Labco Exetainer vials. After automatically flushing with He, the carbonate samples were reacted in phosphoric acid (100 %) at 75°C for 60 min, following the analytical procedure described in Spötl and Vennemann (2003). The $\delta^{18}O$ values refer to Vienna-Standard Mean Ocean Water (SMOW), and the $\delta^{13}C$ values to the Cretaceous Pee Dee Belemnite (PDB). The isotope compositions were given relative to the VPDB standard in the conventional delta notation, and were calibrated against two international reference standards (NBS 19 and NBS18). The standard deviation for reference analyses was 0.06% for $\delta^{13}C$ and 0.08‰ for $\delta^{18}O$.

Rock Eval pyrolysis

Powdered samples were analyzed for organic carbon content (TOC, after acidification of samples to remove carbonate) using a Leco CS-244 analyzer. Pyrolysis measurements were performed using a Rock-Eval 6 instrument, using the following temperature profile: Start at 300 °C (3 min isothermally), then heated for 25 °C/min up to 650 °C (0 min.). Jet-Rock 1 was run as standard and checked against the acceptable range given in NIGOGA (Norwegian Industry Guide to Organic Geochemical Analyses).

Catalyzed reporter deposition fluorescence *in situ* hybridization (CARD-FISH)

Mud samples collected during October 2008 for *in situ* analyses were fixed in 2% formaldehyde for approximately 1.5 hours at room temperature, washed twice with phosphate-buffered saline (PBS; Pernthaler et al., 2008), once with 1:1 PBS: ethanol, resuspended in 100% ethanol and stored at approximately -20°C before and after room temperature shipment. For CARD-FISH analyses, 50 µl mud collected from D1 was brought to 1.5 ml in a TE (10 mM Tris-HCl and 1 mM EDTA (pH 9.0)), 0.01 M pyrophosphate solution, heated in a histological microwave oven (Microwave Research and Applications) for 3 minutes at 60°C, cooled to room temperature and incubated in 0.1% hydrogen peroxide for 10 minutes. The solution was then sonicated on ice for two 5 second bursts with a Vibra Cell sonicating wand (Sonics and Materials, Danbury, CT) at an amplitude setting of 30 and overlaid on a Percoll density gradient (Orphan et al., 2002). Resulting filters were permeabilized in sequential HCl, SDS and lysozyme solutions as described by Pernthaler et al. (2004). Horseradish peroxidase-labeled probes (Biomers) targeting *Desulfobacteraceae* (DSS_658, 50% formamide hybridization buffer; Manz et al., 1998) and anaerobic methane-oxidizing archaeal clade ANME-2 (Eel_MS_932, 45% formamide hybridization buffer; Boetius et al., 2000) were then used in a dual-hybridization CARD-FISH reaction (Pernthaler et al., 2008). The first hybridization reaction took place in a histological microwave oven (Microwave Research and Applications) for 30 minutes at 46°C, followed by an amplification reaction using fluorescein-labeled tyramides. The second hybridization reaction was carried out in a

hybridization oven for 2.5 hours at 46°C followed by an amplification reaction using Alexa Fluor 546-labeled tyramides. Micrograph images were taken with a Deltavision RT microscope system (Applied Precision; Pernthaler et al., 2008).

SUPPLEMENTAL REFERENCES

Boetius, A., Ravenschlag, K., Schubert, C.J., Rickert, D., Widdel, F., Gieseke, A., Amann, R., Jørgensen, B.B., Witte, U., Pfannkuche, O. (2000). A marine microbial consortium apparently mediating anaerobic oxidation of methane. *Nature* 407(6804): 623-626.

Feyzullayev, A., and Movsumova, U. (2010). The nature of the isotopically heavy carbon of carbon dioxide and bicarbonates in the waters of mud volcanoes in Azerbaijan. *Geochemistry International* 48**,** 517-522.

Manz, W., Eisenbrecher, M., Neu, T.R., and Szewzyk, U. (1998). Abundance and spatial organization of Gram-negative sulfate-reducing bacteria in activated sludge investigated by *in situ* probing with specific 16S rRNA targeted oligonucleotides. *FEMS Microbiology Ecology* 25**,** 43-61.

Orphan, V.J., House, C.H., Hinrichs, K.-U., Mckeegan, K.D., and Delong, E.F. (2002). Multiple archaeal groups mediate methane oxidation in anoxic cold seep sediments. *Proceedings of the National Academy of Sciences* 99**,** 7663-7668.

Pernthaler, A., and Amann, R. (2004). Simultaneous Fluorescence *In situ* Hybridization of mRNA and rRNA in Environmental Bacteria. *Applied and Environmental Microbiology* 70**,** 5426-5433.

Pernthaler, A., Dekas, A.E., Brown, C.T., Goffredi, S.K., Embaye, T., and Orphan, V.J. (2008). Diverse syntrophic partnerships from deep-sea methane vents revealed by direct cell capture and metagenomics. *Proc Natl Acad Sci U S A* 105**,** 7052-7057.

Figures and Tables

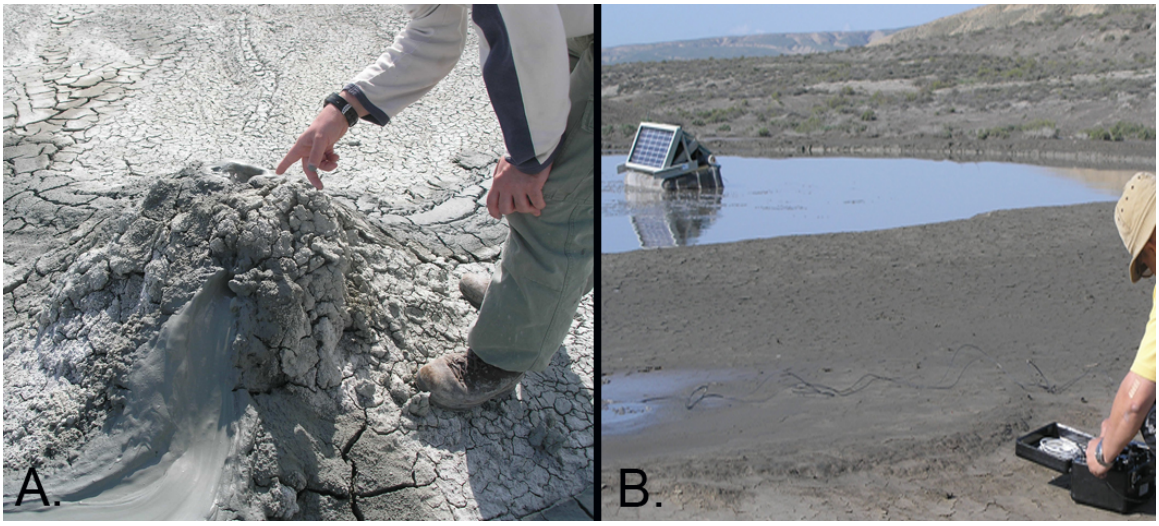

Figure S1. Photographs taken in October 2008 of A) Boransyz-Julga gryphon and B) Dashgil salse lake.

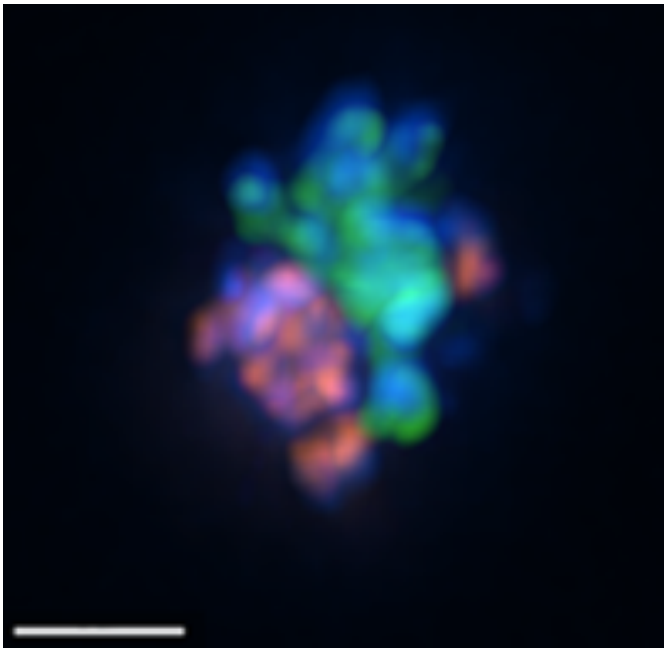

Figure S2. Putative methane-oxidizing aggregates from Dashgil (D1) mud samples identified by CARD-FISH after hybridization with oligonucleotide probes specific to anaerobic methane-oxidizing archaea ANME-2 (EelMsMX_932; red), and *Desulfosarcina-Desulfococcus* members (DSS_658; green). The general DNA stain DAPI is shown in blue. Scale bar = 2 µm.

Table S1. Composition of the synthetic saline solution; the solutions were added after the anoxic cooling post autoclaving

	14 g NaCl, 2.1 g $MgCl_2*6H_2O$, 0.105 g $CaCl_2*2H_2O$, 2.8 g Na_2SO_4, 0.175 g NH_4Cl, 0.14 g KH_2PO_4, 0.2 g KCl per Liter
Add after anoxic cooling past autoclaving:	
1 ml trace elements mixture	50 ml H_2O + 2.1 g $FeSO_4*7H_2O$ + 13 ml HCl (25%), 30 mg H_3BO_3, 100 mg $MnCl_2*4H_2O$, 190 mg $CoCl_2*6H_2O$, 24 mg $NiCl_2*6H_2O$, 2 mg $CuCl_2*2H_2O$, 144 mg $ZnSO_4*7H_2O$, 36 mg $Na_2MoO_4*2H_2O$ per Liter,autoclaved
2 ml SeW-solution	200 mg NaOH, 6 mg $Na_2SeO_3*5H_2O$, 8 mg $Na_2WO_4*2H_2O$ per Liter, autoclaved
60 ml 1 M $NaHCO_3$-solution	84 g $NaHCO_3$ per Liter, anoxic, autoclaved
2 ml 7-vitamin mixture	100 ml H_2O + 4 mg 4-amino benzoic acid, 1 mg D(+)-biotin, 10 mg nicotinic acid, 5 mg Ca-D(+)-pantothenat, 15 mg pyridoxine hydrochloride, 10 mg thiamine chloride hydrochloride, filtered sterile
2 ml B_{12}-solution	5 mg cyan cobalamine in 100 ml H_2O, filtered sterile

Table S2. Closest relatives of phylotypes retrieved from A.) 16S rRNA and B.) *dsrA* gene clone libraries of Dashgil sample (deep pool Add). *env.* = *environmental sequence*

A.

Classification	clone (frequency)	Accession	Description	Similarity
Bacteroidetes	D12 (2)	JF806919	env., river	98%
Chloroflexi	A10 (6)	HQ183882	env., landfill leachate pond sediment	98%
Chloroflexi	B6 (4)	HQ397021	env., landfill leachate pond sediment	97%
Chloroflexi	C8 (30	HQ689286	env., landfill leachate pond sediment	96%
Chloroflexi	G4 (1)	HQ183892	env., landfill leachate pond sediment	99%
Delta-proteobacteria	B4 (3)	FJ517079	env., wetlands	94%
Delta-proteobacteria	F1 (2)	JF806819	env., river	99%
Delta-proteobacteria	H2 (1)	NR_044429	*Geoalkalibacter subterraneus* strain Red1	99%
Delta-proteobacteria	G5 (1)	AF177428	env., oil reservoir	95%
Epsilon-proteobacteria	A1 (39)	JF806914	Uncultured *Sulfurovum* sp.	96%
Epsilon-proteobacteria	G1 (5)	JF806947	Uncultured *Sulfurovum* sp.	99%
Firmicutes	C12 (4)	GQ848205	env., soda lake	93%

B.

Classification	clone (frequency)	Accession	Description	Similarity
Desulfobacteraceae	B2 (29)	EU496887	env., methane-seep sediment	82%
Desulfobacteraceae	A3 (15)	AF482455	*Desulfobacterium anilini*	79%
Desulfobacteraceae	D5 (4)	AY626030	*Desulfonema ishimotonii* strain DSM 9680	76%
Desulfobacteraceae	E2 (1)	AY626031	*Desulfonema limicola* strain DSM 2076	75%
Desulfobulbaceae	G4 (1)	CP001940	*Desulfurivibrio alkaliphilus* AHT2	80%
	F7 (3)	AB124917	Uncultured sulfate-reducing bacterium, hydrothermal vent	87%
	H2 (5)	FJ748851	Uncultured sulfate-reducing bacterium, estuarine sediment	82%
	H7 (3)	JF950248	Uncultured bacterium, anoxic fjord sediments	77%
	H4 (1)	FJ748848	Uncultured sulfate-reducing bacterium, estuarine sediment	77%

Table S3. Archaeal and Bacterial 16S rRNA gene abundance from D (Dashgil) and B (Bakhar) samples collected in 2007.

Sample, depth collected	Total Archaea			Total Bacteria		
Dashgil (D1) big salse lake, 5.8m	2.99E+07	+/-	1.81E+07	2.23E+08	+/-	1.83E+07
Dashgil (D1) big salse lake, 0.5m	7.62E+07	+/-	5.12E+07	3.77E+08	+/-	3.14E+07
Dashgil (D3) small salse lake, 6.5m	8.80E+08	+/-	8.74E+07	1.29E+09	+/-	4.78E+08
Dashgil (D3) small salse lake, 0.2m	1.97E+08	+/-	7.65E+07	1.09E+09	+/-	1.53E+08
Bakhar small salse lake, 4.2m	1.30E+07	+/-	6.06E+06	1.02E+07	+/-	1.26E+07
Bakhar small salse lake, 0.2m	2.11E+07	+/-	2.66E+06	3.43E+07	+/-	2.02E+07

Table S4. Geochemical characteristics of terrestrial mud volcanoes of Azerbaijan sampled in October 2008.
n/a = not available

Mud Volcano	**D: Dashgil**			**P: Perekyushkul**	**BJ: Boransyz-Julga**
Geographic Setting	*Proximal to Caspian Sea* Quaternary Sediments			*Foothills of Great Caucasus* Oligocene-Lower Miocene Deposits	*Foothills of Great Caucasus* Oligocene-Lower Miocene Deposits
Coordinates	N 39º 59' 47.8" E 49º 24' 08.8"			N 40º 28' 49.9" E 49º 26' 53.7"	N 40º 27' 59.6" E 49º 28' 11.4"
Sample Name and Feature	**D1: Salse Lake**	**D3: Salse Lake**	**D4: Gryphon**	**Ps: Gryphon (surface)**	**BJ2: Gryphon**
Temperature, °C (measurement depth, m)	19 (0.2), 18.7 (5.5)	n/a	n/a	16.3 (0.2)	n/a
POREWATER GEOCHEMISTRY					
Fluoride (mM)	0.18	0.14	n/a	n/a	< 0.05
Sulfate (mM)	0.75	< 0.16	0.47	0.32	< 0.16
Chloride (mM)	378	464	209	68	64
Bromide (mM)	0.82	0.97	0.54	0.16	0.16
Cl/Br (mass ratio)	205	213	173	183	177
Acetate (mM)	< 0.010	0.020	n/a	n/a	0.016
Formate (mM)	< 0.013	0.027	n/a	n/a	0.034
STABLE ISOTOPE COMPOSITION					
$\delta^{15}N$ ‰	2.2	2.5	2.0	2.7	3.0
N_{total} wt. %	0.09	0.09	0.10	0.11	0.09
C_{total} wt. %	2.55	2.74	2.67	2.41	1.77
TOC wt. %	1.05	0.78	0.95	1.29	0.71
$\delta^{13}C_{org}$ ‰	-25.1	-26.4	-24.9	-26.6	-26.3
$CaCO_3$ calc %	12.5	16.3	14.4	9.3	8.8
$\delta^{13}C_{carb}$ ‰	0.42	-0.59	-1.04	2.71	4.83
$\delta^{18}O_{carb}$ ‰	-3.47	-2.50	-4.03	-2.41	-1.23
ORGANIC ANALYSIS					
S1, S2, S3 (mg/g)	0.42, 2.22, 1.01	0.13, 1.46, 1.21	0.33, 2.62, 0.71	0.48, 4.87, 1.26	0.24, 2.16, 1.51
Tmax (°C)	431	431	433	431	428
Hydrogen Index HI (mg HC/gTOC)	193	150	224	316	214
Oxygen Index OI (mg CO_2/g TOC)	88	124	61	82	150
TOC (%)	1.15	0.97	1.17	1.54	1.01
REDUCED SULFUR SPECIES (AVS:CRS:DME)	n/a	0.01: 99.91: 0.08	0.00: 99.95: 0.05	n/a	27.68: 72.30: 0.02

Table S5. Geochemical characteristics of four terrestrial mud volcanoes of Azerbaijan sampled in October 2008. n/a = not available

Mud Volcano	D: Dashgil		B: Bakhar	P: Perekyushkul	BJ: Boransyz-Julga
Geographic Setting	*Proximal to Caspian Sea* Quaternary Sediments		*Proximal to Caspian Sea* Quaternary Sediments	*Foothills of Great Caucasus* Oligocene-Lower Miocene Deposits	*Foothills of Great Caucasus* Oligocene-Lower Miocene Deposits
Coordinates	N 39º 59' 47.8" E 49º 24' 08.8"		N 39º 59' 53.7" E 49º 27' 20,3"	N 40º 28' 49.9" E 49º 26' 53.7"	N 40º 27' 59.6" E 49º 28' 11.4"
Sample Name and Feature	**Ds: Pool (surface)**	**Dd: Pool (deep)**	**B: Gryphon**	**P: Gryphon (deep)**	**BJ: Gryphon**
Temperature, °C (measurement depth, m)	17.2 (0.2)	20.6 (1.0), 20.8 (1.25)	19.6 (0.2), 20.7 (3.5)	17.6 (2.5)	18.5 (0.2), 18.3 (1.5)
POREWATER GEOCHEMISTRY					
Fluoride (mM)	0.03	< 0.05	< 0.05	0.06	n/a
Chloride (mM)	312	321	255	56	60
Bromide (mM)	0.63	0.65	0.60	< 0.13	0.13
STABLE ISOTOPE COMPOSITION					
$d^{15}N$ ‰	2.0	2.4	2.6	2.7	3.0
N_{total} wt. %	0.10	0.07	0.05	0.10	0.09
C_{total} wt. %	2.93	2.33	2.88	2.56	2.12
TOC wt. %	1.50	0.70	0.58	1.26	1.24
$d^{13}C_{org}$ ‰	-25.6	-25.3	-25.1	-26.6	-26.7
$CaCO_3$ calc %	11.9	13.6	19.2	10.8	7.3
$d^{13}C_{carb}$ ‰	0.20	n/a	-0.28	3.02	1.41
$d^{18}O_{carb}$ ‰	-4.02	n/a	-4.33	-2.46	-2.91
ORGANIC ANALYSIS					
Tmax (°C)	423	432	392	432	425
TOC (%)	1.63	0.83	0.72	1.58	1.46

*Chapter 2**

***This chapter, written by Abigail Green Saxena, is currently in review.**

Nitrate-based niche differentiation by distinct sulfate-reducing bacteria involved in the anaerobic oxidation of methane

A. Green-Saxena[1], A. E. Dekas[2,4], N. F. Dalleska[3] and V.J. Orphan[2]

Divisions of [1]Biology and [2]Geological and Planetary Sciences, and [3]Global Environmental Center, California Institute of Technology, 1200 East California Boulevard, Pasadena, CA 91125
[4]Chemical Sciences Division, Lawrence Livermore National Laboratory, P.O. Box 808, L-231, Livermore CA 94551-9900

ABSTRACT

Diverse associations between methanotrophic archaea (ANME) and sulfate-reducing bacterial groups (SRB) often co-occur in marine methane seeps, however the ecophysiology of these different symbiotic associations has not been examined. Here we applied a combination of molecular, geochemical and FISH-NanoSIMS analyses of *in situ* seep sediments and methane-amended sediment incubations from diverse locations (Eel River Basin, Hydrate Ridge and Costa Rican Margin seeps) to investigate the distribution and physiology of a newly identified subgroup of the *Desulfobulbaceae* (seepDBB) found in consortia with ANME-2c archaea, and compared these to the more commonly observed associations between the same ANME partner and the *Desulfobacteraceae* (DSS). Fluorescence *in situ* hybridization (FISH) analyses revealed structured aggregates of seepDBB cells in association with ANME-2 from both environmental samples and laboratory incubations that are distinct in structure relative to co-occurring ANME/*Desulfobacteraceae* consortia (ANME/DSS). ANME/seepDBB aggregates were most abundant in shallow sediment depths below sulfide-oxidizing microbial mats. Depth profiles of ANME/seepDBB aggregate abundance (relative to ANME/DSS aggregate abundance) revealed a positive correlation with elevated porewater nitrate in all seep sites examined. This relationship with nitrate was experimentally confirmed using sediment microcosms, in which the abundance of ANME/seepDBB was greater with the addition of nitrate relative to the unamended control. Additionally, FISH coupled to nanoscale secondary ion mass spectrometry (FISH-NanoSIMS) revealed significantly higher ^{15}N-

nitrate incorporation levels in individual aggregates of ANME/seepDBB relative to ANME/DSS aggregates from the same incubation. These combined results suggest that nitrate is a geochemical effector of ANME/seepDBB aggregate distribution, and may provide a unique niche for these consortia through the utilization of a greater range of nitrogen substrates than the ANME/DSS.

KEY WORDS: niche differentiation, nitrate assimilation, *Desulfobulbaceae*, methane seep, symbiosis

INTRODUCTION

In the decades following the initial implication of sulfate-reducing bacteria in the anaerobic oxidation of methane (AOM; Reeburgh, 1976) significant advances have been made towards understanding the symbiosis responsible for this process. While the availability of the primary respiratory substrates, methane and sulfate, have been shown key to the functioning of this symbiosis (Nauhaus et al., 2005), studies have revealed an unexpected diversity in both the archaeal and bacterial partners capable of AOM (Orphan et al. 2002; Knittel et al. 2005 and 2003; Knittel and Boetius, 2009; Niemann et al., 2006; Pernthaler et al., 2008; Kleindienst et al., 2012; Holler et al 2011).

The archaeal groups ANME-1, -2 and -3 have been found to co-occur at many methane seep sites, but within these sites, specific groups or subgroups often dominate in specific seep habitats (chemosynthetic clam beds or microbial mats) or sediment depth horizons (Nauhaus et al., 2005; Knittel et al., 2005; Krüger et al., 2008; Lloyd et al., 2010; Rossell et al., 2011). Geochemical characterizations of the underlying seep sediment have revealed these distinct chemosynthetic communities are also defined by distinct methane,

sulfate and sulfide gradients (Orphan et al., 2004; Sahling et al., 2002; Torres et al., 2002; Boetius and Suess, 2004). However, the relevant factors selecting for dominant ANME subgroups and their symbiotic sulfate-reducing bacterial partners in these niches have yet to be defined.

The 16S rRNA gene diversity found within and between ANME groups is mirrored by that of their sulfate-reducing bacterial partners (Knittel et al, 2003 and 2005; Schreiber et al, 2010). While seepSRB1a members of the *Desulfobacteraceae* family are the dominant partner of ANME-2 (Schreiber et al., 2010), ANME-3 associates primarily with members of the *Desulfobulbaceae* family (Losekann et al., 2007). However, there appears to be flexibility in partner selection; aggregates of ANME-3 and seepSRB1 cells have been reported (Schreiber et al., 2010), novel ANME-1 consortia have been shown to associate with deltaproteobacteria from the HotSeep-1 cluster (Holler et al., 2011) and ANME-2c (an ANME-2 subgroup) cells were also found in association with those of seepSRB2 (Kleindienst et al., 2012), *Desulfobulbaceae* and other bacteria (Pernthaler et al., 2008). Interestingly, in both of the latter cases these alternative aggregate forms were found coexisting with the dominant consortia type (ANME/DSS), suggesting the different SRB partners may occupy distinct niches.

Cultured members of the *Desulfobacteraceae* and *Desulfobulbaceae* families differ in several key metabolic pathways; *Desulfobulbaceae* contain species capable of sulfur disproportionation as well as using nitrate, metal oxides and sulfur as alternate terminal electron acceptors (Kuever et al., 2005b). While the majority of *Desulfobacteraceae* are capable of complete carbon oxidation, most, if not all, *Desulfobulbaceae* are not (Kuever et al., 2005a and b). Major differences such as these suggest uncultured syntrophic SRB

lineages belonging to these families may also have different ecophysiologies. Although very little is known about which factors lead to differences in syntrophic SRB distribution, it is possible that these same factors are important to the symbiosis as a whole, presenting a unique opportunity to uncover additional environmental regulators of AOM via single cell comparative physiology and distribution of two very distinct syntrophic SRB.

FISH-NanoSIMS (nanoscale secondary ion mass spectrometry) analyses of sediments incubated with stable isotope-labeled substrates allows the simultaneous detection of phylogenetic identity and metabolic activity at single cell resolution. This provides a unique opportunity to investigate potential ecophysiological differences between ANME/DSS and ANME/seepDBB aggregates. Due to the broad substrate range of *Desulfobulbaceae* we used FISH-NanoSIMS to investigate the potential role of nitrogen substrates in defining unique niches for ANME/seepDBB, focusing on nitrate as it is known to be dynamic in methane seep sediments (Bowles and Joye, 2010). Using a combination of molecular, *in situ*, and NanoSIMS analyses of environmental and incubation samples from diverse methane seeps (Eel River Basin, Hydrate Ridge and Costa Rican Margin) we investigated the role of nitrate in ANME/seepDBB (versus ANME/DSS) aggregate distribution and metabolism.

METHODS

Site Selection, Sampling and Processing:

Detailed information for all samples used in this study can also be found in Table S1.

Eel River Basin (AT 15-11) October 2006

Samples from the Northern Ridge of Eel River Basin (40°N 48.6 124°W 36.6; 520 m

water depth), an active methane seep off the coast of Northern California (described in Orphan et al., 2004), were collected by manned submersible Alvin in October of 2006 using push cores. Four, 30 cm long push cores were collected during dive AD4256 along a transect which spanned two habitats defined by distinct chemosynthetic communities residing at the sediment surface in a 'bulls-eye' pattern (governed by sulfide concentration gradients). Microbial mats were present in the center (PC29:mat), surrounded by clam beds (PC17:clam1 and PC23:clam2), which decrease in abundance towards the outer rim of the 'bulls-eye' which has lower methane flux and a low concentration of sulfide (PC20:low methane). Two additional cores, AD4254 PC11 and AD4254 PC14 were collected from a clam bed (40°N 47.2 124°W 35.7) and microbial mat (40°N 47.2 124°W 35.7), respectively, for incubation experiments. Cores were processed shipboard (as described in Pernthaler et al., 2008).

Costa Rica Margin (AT 15-44) February 2009, Hydrate Ridge (AT 15-68) August 2010, Hydrate Ridge (AT 18-10) September 2011

Push core samples were also collected in February 2009 from active methane seeps in the Costa Rica Margin (Mau et al., 2006; Sahling et al., 2008) and Hydrate Ridge (Boetius and Seuss 2004) off the coast of Oregon using manned submersible Alvin and remotely operated vehicle Jason (AT 18-10 only). These push cores were collected through three microbial mats (AD4633 PC2: Hydrate Ridge Mat 1: SE Knoll, 44°N 26.99 125°W 01.69, 625 m water depth, AD4635 PC18: Hydrate Ridge Mat 2: Hydrate Ridge South, 44°N 34.09 125°W 9.14, 775 m water depth; and AD4636 PC19: Hydrate Ridge Mat 3: Hydrate Ridge South, 44°N 34.09 125°W 9.14, 772 m water depth) from Hydrate Ridge and two

microbial mats (AD4510: Jaco Summit, 9°N 10.29 84°W 47.92, 745 m water depth; PC6: Costa Rica Mat 1 and PC1: Costa Rica Mat 2) from Costa Rica Margin. Samples for DNA extractions were also collected from Hydrate Ridge AT 15-68 (AD4629 PC9:Hydrate Ridge South, 44°N 34.1 125°W 9.1, 772 m) and AT18-10 (J2 593 E3 PC47: Hydrate Ridge North, 44°N 40.0 125°W 6.0, 600 m water depth 0-9 cm horizon below microbial mat). All cores for this study were processed shipboard (as described in Pernthaler et al., 2008).

Microcosm experiments

The microcosm experiments used in this study have been previously described by Dekas et al. (2009). Briefly, sediments from Eel River Basin clam bed core AD4254 PC11 (top 12 cm) and microbial mat core AD4254 PC14 (top 15 cm) were mixed approximately 1:1 with filtered seawater sparged with argon. The sediment slurries were amended to 0 or 2 mM ^{15}N-nitrate (PC-11) or 2 mM ^{15}N-ammonium (PC-14) and incubated anaerobically with a headspace of methane (overpressed to 30 PSI) in glass bottles with butyl stoppers at 4-8 ºC. Sediment samples were taken anaerobically via syringe at 3 (nitrate incubations) and 6 months (ammonium incubations). Sediment samples were fixed in 4% formaldehyde for one hour, washed with PBS, then PBS and EtOH (1:1), and then resuspended in EtOH, and stored at -20 C.

DNA Extraction and Clone Library Analysis

DNA was extracted from methane seep sediment collected from Costa Rica (AT15-44 AD4510 PC6: 0-1 cm below a microbial mat), Hydrate Ridge (AT 15-68 AD4629 PC9:Hydrate Ridge South, 44°N 34.1 125°W 9.1, 772 m water depth, 0-3 cm below a

microbial mat; sediment incubated with an initial 500 μm nitrate under 30 psi methane and sampled after 4 months), and from magneto-FISH-captured aggregates (see below for details on magneto-FISH) from Eel River Basin (AT15-11 AD4256 PC29: 3-6 cm horizon below microbial mat) and Hydrate Ridge (AT18-10 J2 593 E3 PC47: Hydrate Ridge North, 44°N 40.0 125°W 6.0, 600 m water depth 0-9 cm horizon below microbial mat) using probes seepDBB653 and ANME_2c_760 (Knittel et al., 2005), respectively. Sediment extractions were conducted using the MoBio Ultraclean soil kit following a previously published protocol (Orphan et al., 2001). DNA extraction from magneto-FISH-captured aggregates was conducted as described in Pernthaler et al. (2008). Following extraction, magneto-FISH DNAs from Eel River Basin were amplified using Multiple Displacement Amplification (MDA performed using REPLI-g Mini Kit from Qiagen, Valencia, CA) prior to PCR amplification.

Bacterial 16S rRNA genes were amplified from Hydrate Ridge, Eel River Basin and Costa Rica Margin samples using bacteria specific forward primer BAC-27F and universal reverse primer U-1492R (Lane, 1991). Thermocycling conditions consisted of an initial 94°C denaturing step for 3 minutes followed by 30 cycles of 94°C for 45 seconds, 54°C for 45 seconds and 72°C for 1 minute 20 seconds, and then a final 72°C elongation step for 7 minutes. Amplification reactions followed published PCR mixtures and conditions (Harrison et al., 2009) with 0.5μl of Hotmaster Taq polymerase (Eppendorf AG, Hamburg, Germany).

Sequencing and Phylogenetic Analysis

The amplified 16S rRNA gene products were cleaned using a Multiscreen HTS

plate (Millipore). The purified amplicons were ligated into pCR 4.0 TOPO TA (Invitrogen Corp., Carlsbad, CA) vectors and used to transform One-Shot TOP10 (Invitrogen Corp., Carlsbad, CA) chemically competent cells according to the manufacturer's instructions. A minimum of 10 clones were cleaned using Multiscreen HTS plates (Millipore, Billerica, MA) and sequenced either in house with a CEQ 8800 capillary sequencer according to the DTCS protocol (Beckman Coulter, Fullerton, CA), at the ASGPB DNA Sequencing Facility of the University of Hawai'i at Manoa or at the Laragen sequencing facility (www.laragen.com).

Sequences were manually edited using Sequencher 4.5 software (Gene Codes, Ann Arbor, MI) and aligned using SILVA online aligner (SINA; http://www.arb-silva.de/aligner) followed by the ARB software package (version 7.12.07org, ARB_EDIT4; Ludwig et al., 2004) into the Silva 108 full-length 16S rRNA gene alignment (http://www.arb-silva.de/). A distance tree of all previously published 16S rRNA genes used for this study, inferred by Neighbor-joining with the Jukes and Cantor model, was used to estimate distances using the ARB database SSURef-108-SILVA-NR (www.arb-silva.de) and the provided bacterial filter. Bootstrap values were obtained in PAUP* 4.0b10 by Neighbor-joining with 1000 bootstraps. Sequences *Acidobacterium capsulatum* (CP0001472), *Terriglobus roseus* (DQ660892), *Acanthopleuribacter pedis* (AB303221) and *Geothrix fermentans* (AB303221) served as outgroups to root the tree. Sequences from this study were added to the existing full-length 16S rRNA tree using the quick add maximum parsimony method. Genbank accession numbers are (KC598077-KC598083).

Probe Design:

An alignment of pure culture and putative *Desulfobulbaceae* 16S rRNA gene sequences retrieved from Eel River Basin by Pernthaler and colleagues (2008) was used to design oligonucleotide probe seepDBB653 (CTTTCCCCTCCGATACTCA). This 19 bp probe contains one mismatch, at position 660, to sequences retrieved in this earlier study that makes the probe less homologous to *Desulfobacteraceae* and more homologous to pure culture *Desulfobulbaceae* reference sequences.

Clone-FISH (Schramm et al., 2002; Wagner et al., 2003) was performed to test seepDBB653 and determine the optimal formamide concentration. Single-use BL21 (DE3) LysS cells (Promega, Madison, WI) were transformed with a Topo TA PCR4.0 vector (Invitrogen, Grand Island, NY) containing a 16S rRNA insert of the original seepDBB sequences extracted from Eel River Basin methane seep by Pernthaler and colleagues (EU622294; Pernthaler et al., 2008). CARD-FISH reactions were performed on resulting cells using a range of formamide concentrations from 10% to 60%. The optimal formamide concentration was 15% to 25%. Subsequent CARD-FISH reactions on environmental samples using probe seepDBB653 yielded an optimal signal at 15% formamide. Likely due to the low formamide concentration, seepDBB653 has a faint cross hybridization with DSS cells, which is clearly discerned from the true signal when dual hybridizations of seepDBB653 and DSS658 probes are conducted. The specificity of seepDBB653 was further tested via a magneto-FISH reaction targeting seepDBB-containing aggregates; all examined bacterial 16S rRNA gene sequences (n = 9 randomly sequenced clones) were within the seepDBB group initially recovered by Pernthaler et al (2008).

Catalyzed Reporter Deposition Fluorescence *in situ* Hybridization (CARD-FISH):

Sediment samples were fixed in 2% formaldehyde for approximately 1.5 hours at room temperature, washed twice with phosphate-buffered saline (PBS; Pernthaler et al., 2008), once with 1:1 PBS: ethanol, resuspended in 100% ethanol and stored at -20°C. For CARD-FISH analyses, 40-75 µl fixed sediment collected from each depth horizon was brought to 1.5 ml in a TE (10 mM Tris-HCl and 1 mM EDTA (pH 9.0)), 0.01 M pyrophosphate solution, heated in a histological microwave oven (Microwave Research and Applications, Carol Stream, IL) for 3 minutes at 60°C, cooled to room temperature and incubated in 0.1% hydrogen peroxide for 10 minutes. The solution was then sonicated on ice for two 5 second bursts with a Vibra Cell sonicating wand (Sonics and Materials, Danbury, CT) at an amplitude setting of 3.0 and overlaid on a Percoll density gradient (Orphan et al., 2002) prior to filtration onto a 3.0 µm pore filter (Millipore, Billerica, MA). Resulting filters were permeabilized in sequential HCl, SDS and lysozyme solutions as described by Pernthaler et al. (2004). Horseradish peroxidase-labeled probes (Biomers, Ulm, Germany) targeting seep *Desulfobulbaceae* (seepDBB653, 15% formamide; this study) and either *Desulfobacteraceae* (DSS_658, targets *Desulfosarcina* spp./*Desulfococcus* spp./*Desulfofrigus* spp. and *Desulfofaba* spp; Manz et al., 1998) or anaerobic methane-oxidizing archaeal clade ANME-2 (Eel_MS_932; Boetius et al., 2000) were then used in a dual-hybridization CARD-FISH reaction (Pernthaler et al., 2008). The first hybridization reaction was conducted in a histological microwave oven for 30 minutes at 46°C, followed by an amplification reaction using fluorescein-labeled tyramides. The second hybridization reaction was carried out in a hybridization oven for 2.5 hours at 46°C followed by an amplification reaction using Alexa Fluor 546-labeled tyramides. Samples were then counter

stained with 4',6' -diamidino-2-phenylindole (DAPI). Micrograph images were taken with a Deltavision RT microscope system (Applied Precision, Issaquah, WA).

Magneto-FISH:

Magneto-FISH was performed on 75 µl of fixed sediment, with probes Eel_MS_932 (Boetius et al., 2000) and seepDBB653, as described in (Pernthaler et al., 2008) with the following modifications. During the amplification reactions, 0.1% blocking reagent was used instead of BSA. Following the CARD-FISH reaction, monoclonal mouse anti-fluorescein-antibodies (Molecular Probes) were applied directly to the sediment (approximately 1 µg/10^6 cells), incubated for 10 minutes on ice, and washed via two centrifugation steps at 300 x g for 8 minutes with re-suspension in PBS (containing 0.1% BSA; pH 7.4) in 1.5 ml tubes. Sediment was then incubated with pan-mouse paramagnetic beads (5 µm diameter; approximately 25 µl/10^7 cells) (Dynal, AS, Norway) at 4°C, rotating, for one hour. Tubes of sediment were then washed 15 times by placing near a magnet (Dynal MPC-E) for 2 minutes, removing supernatant and re-suspending in PBS (containing 0.1% BSA; pH 7.4), with a final re-suspension in TE prior to DNA extraction.

Morphological Data:

Morphological data were collected from ANME/seepDBB aggregates (using probes seepDBB653 probe and Eel_MS_932) in sediment samples from four push cores collected along a transect within an Eel River Basin methane seep. A total of 86 positively hybridized aggregates were imaged and characterized as one of the following morphotypes: shell, partial shell, clumped or mixed (Figure S2).

Morphological data were also collected from ANME/seepDBB and ANME/DSS aggregates (using probes seepDBB653 probe and DSS_658, respectively) in Eel River Basin sediment incubated with 2 mM ^{15}N-nitrate or ^{15}N-ammonium and sampled at 4 or 6 months, respectively. A total of 84 aggregates were imaged, characterized as one of the four morphotypes (shell, partial shell, clumped or mixed).

Aggregate counts:

Nitrate depth profiles (details below) were used to select low (< 50 μM nitrate) and high (> 50 μM nitrate) nitrate cores to examine via CARD-FISH. Depth profiles of relative DAPI/seepDBB (versus DAPI/DSS) aggregate abundance were generated from these push cores, which were collected through three microbial mats (AD4633 PC2: Hydrate Ridge Mat 1, AD4635 PC18: Hydrate Ridge Mat 2 and AD4636 PC19: Hydrate Ridge Mat 3) from Hydrate Ridge and two microbial mats (AD4510 PC6: Costa Rica Mat 1 and AD4510 PC1: Costa Rica Mat 2) from Costa Rica Margin. Samples for aggregate counts were obtained from 1 cm (Hydrate Ridge Mat 2 and Costa Rica Mat 1) or 3 cm (Hydrate Ridge Mats 1 and 3 and Costa Rica Mat 2) core slices and hybridized with probes seepDBB653 and DSS_658. DAPI/seepDBB and DAPI/DSS aggregates were counted from a total of 50 aggregate-containing fields per sample. Relative numbers of DAPI/seepDBB aggregates are expressed as percent DAPI/seepDBB of total DAPI/SRB aggregates.

Samples for Eel River Basin aggregate counts were obtained from 3 cm core slices and hybridized with probes seepDBB653 and Eel_MS_932. A total of 100 ANME-containing aggregates were counted per sample. Relative numbers of ANME/seepDBB aggregates are expressed as percent ANME/seepDBB of total ANME-containing

aggregates. Total aggregate counts were also done via epifluorescent microscopy after staining the sediment with DAPI. Briefly, 0.1 to 0.5 µl of fixed and washed sample, diluted in PBS, was filtered onto 0.22 µm pore filters (Millipore, Billerica, MA) and enumerated according to Turley (1993).

Samples for incubation aggregate counts came from a previously described push core collected through a clam bed in Eel River Basin (PC11) and incubated with and with out 2 mM nitrate under a methane headspace as described in Deskas et al., (2009). After performing a Percoll density separation as describe above, samples were hybridized with probes seepDBB653 and DSS_658 (Manz et al., 1998). DAPI/seepDBB and DAPI/DSS aggregates were counted from a total of fifty aggregate-containing fields per sample. Due to sample limitation, counts were made from 3 replicate methane-only incubations and from 3 filter wedges from one nitrate-amended incubation. Relative numbers of DAPI/seepDBB aggregates are expressed as percent DAPI/seepDBB of total DAPI/SRB aggregates.

Geochemical:

Geochemical depth profiles (at 3 cm resolution) of methane, sulfate and sulfide concentrations were generated from push cores collected at Eel River Basin. Methane and sulfate were measured via ion and gas chromatography as described by Orphan and colleagues (2004). Sulfide was measured using the Cline Assay (Cline, 1969) as described by Dekas and colleagues (2009).

Nitrate and nitrate concentrations for Costa Rica Margin samples were analyzed with an

Antek chemiluminescence detector at the University of Georgia, Athens, and reported in (Dekas et al., submitted).

Nitrate concentrations for Hydrate Ridge samples were measured as follows. Pushcore pore-water squeezed from sediments immediately after collection was filtered via a 0.2 μm filter and frozen at -20˚C until analysis. Parallel ion chromatography systems operated simultaneously (Dionex DX-500, Environmental Analysis Center, Caltech) were used to measure ammonium, nitrate, nitrite and sulfate in the porewater samples. A single autosampler loaded both systems' sample loops serially. The 10 μl sample loop on the anion IC system was loaded first, followed by a 5 μl sample loop on the cation IC system. Temperatures of the columns and detectors were not controlled. Measurements of cationic species is not presented in this work so is not discussed further.

Nitrite, nitrate and sulfate were resolved from other anionic components in the sample using a Dionex AS-19 separator (4x250 mm) column protected by an AG-19 guard (*4x50 mm). A hydroxide gradient was produced using a potassium hydroxide eluent generator cartridge and pumped at 1 mL per minute. The gradient began with a 10 mM hold for 5 minutes, increased linearly to 48.5 mM at 27 minutes and finally to 50 mM at 41 minutes. 10 minutes were allowed between analyses to return the column to initial conditions. Nitrite and nitrate were determined for UV absorption at 214 nm using a Dionex AD25 Absorbance detector downstream from the conductivity detection system. Suppressed conductivity detection using a Dionex ASRS-300 4 mm suppressor operated in eluent recycle mode with an applied current of 100 mA was applied to detect all other anions, including redundant measurement of nitrite and nitrate. A carbonate removal

device (Dionex CRD 200 4 mm) was installed between the suppressor eluent out and the conductivity detector eluent in ports.

Standard curves were generated for each species. For nitrate, nitrite, and sulfate, standard measurements were fitted to a linear curve. Standard ranges were 10 μM to 2 mM (nitrate, nitrite) and 500 μM to 32 mM (sulfate). Standard deviation of repeated injections of a standard (250 μM nitrate and nitrite, 8000 μM sulfate) throughout the analysis were 4.2 μM (nitrate), 5.8 μM (nitrate) and 113 μM (sulfate).

Fluorescence *in situ* Hybridization Nanoscale Secondary Ion Mass Spectrometry (FISH-NanoSIMS):

Thirteen ANME/SRB aggregates (7 ANME/seepDBB and 6 ANME/DSS) were examined from an ammonium-amended incubation (approximately 2 mM ^{15}N-ammonium, sampled at 6 months) inoculated with methane seep sediment slurries from a push core collected through a microbial mat in Eel River Basin (PC-14; Dekas et al, 2009). Fourteen ANME/SRB aggregates (6 ANME/seepDBB and 8 ANME/DSS) were examined from a nitrate-amended incubation (2 mM ^{15}N-nitrate, sampled at 3 months) inoculated with methane seep sediment slurries from a push core collected through a clam bed in Eel River Basin (PC-11; Dekas et al., 2009).

All samples were deposited onto 1” diameter round microprobe slide (Lakeside city, IL) and hybridized with HRP-labeled probes seepDBB653 and DSS_658; DAPI/seepDBB and DAPI/DSS aggregates were then mapped for nanoSIMS analysis (Orphan et al., 2002; Dekas and Orphan, 2011). Clostridia spores (with known δ^{13}C and δ^{15}N) were spotted onto a blank section of the glass and used as standards during the analysis. Samples were then

gold-coated and analyzed using a CAMECA NanoSIMS 50L housed at Caltech, using a mass resolving power approximately 5,000. A primary Cs^+ ion beam (4.3 to 22 pA) was used to raster over target cells, with a raster size ranging from 8 to 25 μm. Secondary ion images were collected at 256 x 256 pixel resolution with a dwell time of 14,000 ct/pixel over a period of 4 to 20 hours, resulting in 7 to 97 cycles, depending on target size. This range of ion beam current was used to maximize counts with no offset in ^{15}N observed in standards run before and after the analysis. Clostridia spores were measured periodically as a standard to ensure there were no matrix effects throughout the analysis in isotope mode using the same range in ion beam current. Several masses were collected in parallel including: $^{12}C^{14}N^-$, and $^{12}C^{15}N^-$ using electron multiplier detectors. Resulting ion images were processed using the L'Image software (developed by L. Nittler, Carnegie Institution of Washington, Washington D.C.). The reported isotope ratio for each aggregate was extracted from the image by identifying a region of interest – the aggregate – within each image. The aggregate edge was automatically defined in L'image by setting a lower threshold of 35% of the maximum value of $^{12}C^{15}N/^{12}C^{14}N$ counts within a given cycle. The ratio from the cycle with the highest $^{12}C^{15}N/^{12}C^{14}N$ was then collected from each aggregate. The $^{12}C^{15}N/^{12}C^{14}N$ ratio is hereafter referred to as the $^{15}N/^{14}N$ ratio.

RESULTS

Phylogenetic characterization of *Desulfobulbaceae* from multiple seeps

Bacterial 16S rRNA gene sequences distantly related to cultured *Desulfobulbaceae* sequences were recovered from methane seep sediment collected from Costa Rica and Hydrate Ridge. These sequences formed a well-supported clade putatively within the

Desulfobulbaceae family, along with seepDBB sequences previously retrieved from magneto-FISH enriched ANME-2c aggregates from Eel River Basin (Pernthaler et al., 2008), and distinct from the ANME-3 partners and previously described seepSRB3 and seepSRB4 clades (Knittel et al., 2005); (Figure 1). Initial Eel River Basin sequence data from this clade were used to design an oligonucleotide probe for CARD-FISH analyses of ANME/seepDBB consortia in situ.

Aggregate characterization

Environmental data

A total of 86 positively hybridized ANME/seepDBB aggregates from Eel River Basin samples were characterized by aggregate morphology, with the majority of *Desulfobulbaceae* aggregates consisting of partial shell (37%) followed by whole shells and clumped aggregates (24% and 27%, respectively); mixed aggregates represented 12% (Figure 2b, S3). The majority (75%) of examined aggregates were 2-6 μm in diameter, with smaller percentages forming aggregates greater than 6 μm.

Incubation data

Similar to the *in situ* observations, the dominant ANME/seepDBB morphology in the nitrate incubation was also partial shell (69%), followed by mixed (19%) and clumped aggregates (13%; Figure 2a). The ANME/seepDBB aggregates in the ammonium incubation were dominated by clumped morphology (44%), followed by partial shell (34%), whole shell (16%) then mixed (19%; Figure 2a). The average ANME/seepDBB aggregate diameter was 6.6 μm in the nitrate incubation and 4.5 μm in the ammonium

incubation.

The dominant ANME/DSS morphology in the nitrate incubation was whole shell (50%), followed by equal proportions of mixed and partial shells (25%), with no clumped aggregates detected (Figure 2c). The ammonium incubation in contrast, was dominated by mixed ANME/DSS morphology (45%), followed by clumped (35%), partial shell (15%) and whole shell (5%).

Geochemistry and ANME/seepDBB distribution in diverse methane seep environments

Eel River Basin (AT 15-11)

The seepDBB653 probe along with Eel_MS_932 (targeting ANME cells, Boetius et al., 2000) was initially used to calculate abundance of aggregates associated with the three main seep habitats (clam, mat, low-methane flux periphery) and with increasing sediment depth. Four cores were selected along a transect (*mat, clam1, clam2* and *low methane*) containing one central mat, two flanking clam beds and the surrounding sediment.

The relative ANME/seepDBB aggregate abundance decreased with depth in 3 of 4 cores (mat, clam2 and low-methane flux site; Figure S1). The geochemical profiles of clam1 indicate relatively low levels of sulfate depletion compared to clam2 and mat, perhaps resulting from lower methane flux along the periphery of the clam bed. The apparent correlation between relative ANME/seepDBB aggregate abundance and depth seen in mat, clam2 and low methane did not appear to be related to sulfate, sulfide or methane concentrations.

Costa Rican Margin (AT 15-44) and Hydrate Ridge (AT 15-68)

Porewater nitrate concentration profiles were used to select cores containing greater than 50 μM nitrate for further analysis. Nitrate profiles from Costa Rica Margin cores are previously described in Dekas et al. (in review). Cores collected through microbial mats had the highest levels of porewater nitrate of the habitats examined, with the greatest concentrations associated with sediments just below microbial mats, similar to previous reports (Bowles and Joye, 2010). The cores examined in this study contained nitrate ranging from 97 to 1227 μM in the shallowest depth horizon (0-3 cmbsf in Hydrate Ridge Mat1, 0-1 cmbsf in Costa Rica Mat and Hydrate Ridge Mat2) that decreased below the detection limit in the deeper depth horizons (> 7 cmbsf; Figure 3). Depth profiles of relative DAPI/seepDBB (versus DAPI/DSS) aggregate abundance positively correlated with those of nitrate in the resulting cores in both Hydrate Ridge and the Costa Rican Margin (n = 3 cores). Low-nitrate (< 50 μM nitrate) cores were also examined (n = 2 cores), revealing consistently low (DAPI/seepDBB aggregates < 10% of total aggregates) relative DAPI/seepDBB (versus DAPI/DSS) aggregate abundance.

Microcosm Analyses via FISH-NanoSIMS

CARD-FISH analyses using probes seepDBB653 and DSS658 were employed on previously prepared methane-amended incubations of seep sediment from the Eel River Basin supplemented with 2 mM nitrate, 2 mM ammonium or no amendment (Dekas et al. 2009). The relative abundance of ANME/seepDBB aggregates (represented as a fraction of total DAPI/SRB aggregates) at 3 months was greater in the nitrate-amended incubation (0.146; Std Err Mean = 0.027) than a non-amended control (0.087; Std Err Mean = 0.010).

A total of fourteen ANME/SRB aggregates (6 ANME/seepDBB and 8 ANME/DSS) were examined via FISH-NanoSIMS from the same nitrate-amended microcosm at 3 months. Significantly higher maximum ^{15}N incorporation levels were observed in ANME/seepDBB (versus ANME/DSS) aggregates where $^{15}N/^{14}N$ ratios ranged from 0.07 to 0.19 in ANME/seepDBB aggregates and from 0.01 to 0.09 in ANME/DSS aggregates (Figure 4; nonparametric Wilcoxon Pval = 0.024). Overall levels of ^{15}N enrichment were likely lower in nitrate-amended (relative to ammonium-amended) incubations due to differences in sediment source, sampling times and ability of microorganisms to assimilate the two nitrogen sources, as previously observed in Dekas et al. (2009). Isotope imaging showed that several of the aggregates (n = 6) from the ^{15}N-nitrate-amended incubation exhibited highest ^{15}N enrichment in the region corresponding to SRB cells (Figure 5).

To compare relative uptake of ^{15}N-ammonium, a total of thirteen ANME/SRB aggregates (7 ANME/seepDBB and 6 ANME/DSS) were examined via FISH-NanoSIMS from the ammonium-amended microcosm (sampled at 6 months). There was no significant difference in maximum ^{15}N incorporation levels between ANME/seepDBB and ANME/DSS aggregates (Figure 4; nonparametric Wilcoxon Pval = 0.175). $^{15}N/^{14}N$ ratios for ranged from 0.81 to 1.39 in ANME/seepDBB aggregates and from 0.60 to 2.07 in ANME/DSS aggregates. At 6 months the level of ^{15}N enrichment in ammonium-amended incubations was too high ($^{15}N/^{14}N$ ratios ranged from 0.60 to 2.07) to distinguish higher incorporation levels in SRB regions versus ANME regions of the aggregate.

DISCUSSION

Molecular tools such as 16S rRNA gene surveys have advanced environmental microbiology towards an understanding of the diversity of communities residing in an ecosystem (Lane, 1991; Pace et al., 1985). This has afforded knowledge of community composition and relative abundance of phylotypes that has become increasingly more accurate as our sequence technologies progress towards the ability to deeply sample the 16S rRNA diversity in an environment (Prosser et al., 2012). This increasing level of detail in our knowledge of community diversity opens up more questions, such as how microorganisms in such a complex community not only relate to each other but also to the environment they inhabit. Stable isotope probing allows the simultaneous detection of identity and metabolic capability (Dumont and Murrell, 2005). Using methods affording a finer scale of spatial resolution, such as FISH-SIMS, HISH-SIMS, and microfluidic digital PCR (Orphan et al., 2001; Musat et al., 2008; Ottesen et al., 2006), we can begin to tease out the function of specific members of a community, and particularly with isotopic approaches, we can understand metabolic processes connecting these organisms to one another and their environment.

Characterization of seepDBB partner

Compared to the ANME, very little is known about the potential physiologies or habitat preferences of the various groups of SRB involved in AOM (Knittel and Boetius, 2009). Though a recent study reports seepSRB1a members of the *Desulfobacteraceae* family are the dominant partner of ANME-2 (Schreiber et al., 2010), other SRB and unknown bacterial partners have been documented for ANME-2 (Orphan et al., 2002; Knittel et al., 2005; Kleindienst et al., 2012; Pernthaler et al., 2008; Schreiber et al., 2010). Using an

immuno-magnetic cell capture technique (magneto-FISH) to enrich for ANME-2c aggregates, Pernthaler and colleagues (2008) reported the detection of ANME/*Desulfobulbaceae* co-existing with ANME/DSS aggregates and phylogenetically distinct from the *Desulfobulbaceae* group previously described in association with ANME-3 (Niemann et al., 2006; Losekann et al., 2007; Figure 1). Here we studied the distribution and ecophysiology of co-occurring SRB/ANME consortia, as well as expanded the known distribution of ANME-associated *Desulfobulbaceae* (seepDBB) cells.

SeepDBB was first described from a single sample collected from a seep site at Eel River Basin (Pernthaler et al., 2008); in the present study CARD-FISH analyses were used to better characterize the depth and habitat distribution of the ANME/seepDBB consortia. We examined push cores from a transect spanning three habitats (a sulfur-oxidizing microbial mat, a Calyptogena clam bed and the peripheral sediments with lower methane flux) within this methane seep. Incubations of Eel River Basin sediment amended with either 2 mM nitrate or ammonium were also examined. The majority of ANME/seepDBB aggregates from both environmental and incubation data sets were 2-7 μm in diameter and had either a partial shell or clumped morphology (Figure 2a and 2b). Interestingly, while these morphotypes were also observed in ANME/DSS aggregates, the dominant morphology was either whole shell or mixed (Figure 2c), suggesting different dynamics may exist between the partners comprising ANME/seepDBB versus ANME/DSS consortia.

Percoll density gradients were used in this study to concentrate aggregates from fixed sediments prior to CARD-FISH analyses and are likely necessary for ANME/seepDBB detection in many methane seep habitats due to their lower abundance, which may explain the lack of their detection in previous studies (eg, Schreiber et al., 2010). When the relative

number of the ANME/seepDBB aggregates are low, fluorescence *in situ* hybridization in sediment samples often requires significant dilution to avoid masking of cells by particles. Use of these density based or magnetic enrichment methods (magneto-FISH; Pernthaler et al., 2008) enable the processing of a greater amount of sediment, increasing the potential for detecting rarer phylotypes.

While ANME/seepDBB aggregates were found in all Eel River Basin habitats examined, as well as below microbial mat habitats in HR and CR methane seeps, they were always found as a lower proportion of total ANME/SRB aggregates relative to ANME/DSS (Figures S1 and 3). Despite the relative difference in abundance, the consistent coexistence of two types of ANME/SRB aggregates could result from niche partitioning, which has been demonstrated in cultured species of SRB within the same class (Dar et al., 2007). ANME-associated DSS and seepDBB belong to distinct families (*Desulfobacteraceae* and *Desulbulbaceae*, respectively) whose cultured representatives differ in several key metabolic pathways (Kuever et al., 2005a and b). With the possible exception of *Desulfofustis*, no genera in the *Desulfobulbaceae* family are capable of completely oxidizing carbon substrates, whereas most genera of *Desulfobacteraceae* family can (Kuever et al., 2005a and b). The *Desulfobulbaceae* are also distinct for harboring species capable of sulfur disproportionation as well as respiring metal oxides, nitrate and sulfur as alternate terminal electron acceptors (Kuever et al., 2005b). Indeed, Milucka and colleagues (2012) recently proposed ANME-2 to be capable of both the anaerobic oxidation of methane and reduction of sulfate to disulfide (or other S^0 compounds), which is scavenged by the DSS and disproportionated to sulfide and sulfate. In this model, multiple SRB can serve as disulfide scavengers, including *Desulfobulbaceae*, but it remains

unclear why multiple syntrophic SRB lineages co-exist. Major differences between cultured members of the *Desulfobacteraceae* and *Desulfobulbaceae* families suggest these syntrophic SRB lineages may also have distinct ecophysiologies, which we first explored by comparing their distribution in diverse methane seeps to the geochemical gradients in these habitats.

Geochemical profiles and ANME/seepDBB distribution in diverse methane seep environments

Investigated cores from Eel River Basin were collected along a transect spanning multiple seep habitats (Figure S1). ANME/seepDBB aggregates were typically most abundant in the shallower depth horizons of the Eel River Basin transect, with the greatest relative proportions documented below a sulfur-oxidizing microbial mat (Figure S1). Available depth profiles of methane, sulfate and sulfide did not appear to explain this distribution. A review of published 16S rRNA and FISH-based studies reporting the presence of *Desulfobulbaceae* in methane seep sediment also revealed an increase in seepDBB-affiliated cells and sequences in shallow horizons beneath sulfur-oxidizing microbial mats (Orphan et al,. 2001; Knittel et al., 2003; Niemann et al., 2006; Losekann et al., 2007, Pernthaler et al., 2008). While geochemical porewater profiles for methane, sulfate and sulfide in the 0 – 10 cm sediment horizons are highly variable between methane seep sites (Knittel and Boetius, 2009; Lloyd et al., 2010; Bowles et al., 2011; Niemann et al., 2006; Valentine and Reeburgh, 2000; Linke et al., 2005), nitrate levels from methane seeps are typically highest just below microbial mats (Linke et al., 2005; Bowles et al., 2010; Priesler et al., 2007; Lichtschlag et al., 2010). Given the documented nitrate usage by

cultured members of the *Desulfobulbaceae* and their high relative abundance in near seafloor sediments beneath microbial mats, we hypothesized nitrate to be one potential geochemical effector of ANME/seepDBB aggregate distribution, and focused subsequent studies on sediment cores varying in nitrate concentration.

Environmental trends in seepDBB abundance from Costa Rican margin and Hydrate Ridge methane seep sites suggested a potential relationship with nitrate. Highest proportions of ANME/seepDBB (> 35% of all ANME/SRB aggregates) were seen in the shallow horizons of the Costa Rica Margin core where two peaks of increased ANME/seepDBB aggregates were observed at different depths. Interestingly this was the only core that had two peaks of increased nitrate concentrations, which roughly correspond to the increase in ANME/seepDBB aggregates (Figure 3d). To understand the relationship between seepDBB cells and nitrate, we next studied the effects of nitrate-amendment on the anabolic activity of ANME/seepDBB and ANME/DSS aggregates in microcosms of methane seep sediment.

Nitrate utilization by ANME/seepDBB aggregates

Methane seep sediment previously collected from Eel River Basin and amended with 2 mM ^{15}N-labeled nitrate or ammonium (under methane headspace; Dekas et al., 2009) was used in the current study for CARD-FISH and NanoSIMS analyses. Active sulfide production was previously measured from both incubations (Dekas et al., 2009). After three months the relative abundance of ANME/seepDBB (represented as a percent of total DAPI/SRB aggregates) was greater in the nitrate-amended incubation 0.146) than the non-amended control (0.087). The reported doubling time of ANME/SRB aggregates has

been estimated between 3 to 7 months (Orphan et al., 2009; Nauhaus et al., 2007), and the increase in seepDBB documented here may result both from the growth/division of new ANME/SRB aggregates as well as from an increase in the size of smaller aggregates less than < 3 μm in diameter into sizes large enough to be retained on the 3 μm pore size filter used for density gradient separation prior to CARD-FISH (ANME/seepDBB from this incubation had an average diameter of 6.6 μm).

Higher maximum ^{15}N incorporation levels were observed in ANME/seepDBB aggregates versus ANME/DSS aggregates from the ^{15}N-nitrate incubation (Figure 4a), while there was no significant difference in maximum ^{15}N incorporation levels between ANME/seepDBB and ANME/DSS aggregates from the ^{15}N-ammonium incubation (Figure 4b). These data suggest similar assimilation rates for ANME/seepDBB and ANME/DSS in the presence of ammonium, and control for the possible artifact of overall higher growth rates in ANME/seepDBB (versus ANME/DSS) aggregates leading to increased incorporation of any labeled nutrient. Previous FISH-SIMS studies using ^{15}N-labeled ammonium- and N_2-amended sediment incubations showed the greatest ^{15}N assimilation by the ANME archaea (Orphan et al., 2009; Dekas et al., 2009). In contrast, several ANME/SRB aggregates analyzed from the labeled nitrate incubation showed clear ^{15}N enrichment in the region associated with SRB cells (Figure 5), suggesting that the SRB partner may be responsible for the majority of the nitrogen incorporation from nitrate in these aggregates.

Although ANME/seepDBB aggregates were consistently less abundant than ANME/DSS, their role in nitrate processing may afford them a more prominent role in marine methane seep ecosystems than their numbers suggest. Keystone species are not necessarily the most

abundant members of the community, for example, FISH-NanoSIMS analysis by Musat and colleagues showed that *Chromatium okenii*, representing approximately 0.3% of total microbial cell numbers, was responsible for over 40% of total ammonium uptake and 70% of total carbon fixation in oligotrophic, meromictic Lake Cadagno (Musat et al., 2008). While our results indicate that ANME/seepDBB aggregates have a greater capability (or preference) than ANME/DSS for using nitrate, it is currently unclear if ANME/seepDBB aggregates are using nitrate for anabolism, respiratory energy, or both. Studies of nitrate-reducing SRB in pure culture have documented the dissimilatory reduction of nitrate to ammonium (DNRA), which can then be incorporated into biomass (Rabus et al., 2006). Thus both dissimilatory and assimilatory pathways for nitrate reduction in these SRB could lead to incorporation of nitrogen sourced from the ^{15}N nitrate into biomass.

The co-existence of physiologically related species may be explained by niche partitioning (Gause, 1934). Complex environments, such as those encountered in seep sediments, are defined by steep chemical gradients, which can lead to distinct microniches, and, in turn, can result in diversification of species harbored in these habitats (Gray et al., 1999; Torsvik et al., 2002). The observed preference for nitrate by ANME/seepDBB versus ANME/DSS aggregates may be one such mechanism by which two apparently functionally redundant consortia can coexist via partitioning the environment into niches defined by nitrogen source.

CONCLUSIONS

Very little is known about factors influencing the distribution and fitness of distinct sulfate-reducing bacteria partnered with methanotrophic ANME archaea. Poorly

constrained ecological and physico-chemical factors are almost certainly important to the AOM symbiosis as a whole, and present a unique opportunity to uncover additional environmental regulators of sulfate-dependent methane oxidation. Most studies to date have focused on the dynamics of carbon and sulfur metabolism by the AOM symbiosis. Here we demonstrate a role for nitrate as a geochemical effector influencing the distribution of *Desulfobulbaceae*-ANME consortia within methane seeps. While bulk geochemical and molecular analyses provide information on community level diversity and activity, complementary single cell techniques, like the FISH-NanoSIMS method used in this study, provide direct information on the metabolic function of phylogenetically identified microorganisms *in situ* and allow for the assessment of ecophysiological differences among co-existing microbial species.

ACKNOWLEDGEMENTS

We would like to acknowledge Grayson Chadwick for his help with image analysis, Elizabeth Trembath-Reichert for contributing clone sequences, Ankur Saxena for figure design, Yunbin Guan for his assistance with NanoSIMS, Tsege Embaye for methane and sulfate measurements from AT 15-11 and the science party of cruises AT 15–11, AT 15-44, AT 15-68 and AT 18-10 and pilots of the D.S.R.V. Alvin and R.O.V. Jason for their assistance with various aspects of this work. Funding for this work was provided by the Department of Energy Division of Biological Research (DE-SC0004949; to V.J.O.), and a National Science Foundation Graduate Research Fellowship (to A.G.-S.). Samples were collected with funding from the National Science Foundation (BIO-OCE #0825791; to V.J.O.).

REFERENCES

Boetius A, Ravenschlag K, Schubert CJ, Rickert D, Widdel F, Gieseke A, et al. (2000) A marine microbial consortium apparently mediating anaerobic oxidation of methane. Nature 407: 623-626.

Boetius A & Suess E. (2004) Hydrate Ridge: a natural laboratory for the study of microbial life fueled by methane from near-surface gas hydrates. Chemical Geology 205: 291-310.

Bowles M & Joye S. (2010) High rates of denitrification and nitrate removal in cold seep sediments. The ISME journal 5: 565-567.

Bowles MW, Samarkin VA, Bowles KM & Joye SB. (2011) Weak coupling between sulfate reduction and the anaerobic oxidation of methane in methane-rich seafloor sediments during ex situ incubation. Geochimica et Cosmochimica Acta 75: 500-519.

Cline JD. (1969) Spectrophotometric determination of hydrogen sulfide in natural waters. Limnology and Oceanography 454-458.

Dar S, Stams A, Kuenen J & Muyzer G. (2007) Co-existence of physiologically similar sulfate-reducing bacteria in a full-scale sulfidogenic bioreactor fed with a single organic electron donor. Applied Microbiology and Biotechnology 75: 1463-1472.

Dekas AD, Poretsky RS & Orphan VJ. (2009) Deep-sea archaea fix and share nitrogen in methane-consuming microbial consortia. Science 326: 422-426.

Dekas AE & Orphan VJ. (2011) Identification of diazotrophic microorganisms in marine sediment via fluorescence *in situ* hybridization coupled to nanoscale secondary ion mass spectrometry (FISH-NanoSIMS). Methods Enzymol 486: 281-305.

Dekas, AE, Chadwick, GL, Bowles, MW, Joye, SB and Orphan, VJ. (in review) Spatial distribution of nitrogen fixation in methane seep sediment and the role of the ANME Archaea.

Dumont, MG, & Murrell, JC. (2005). Stable isotope probing—linking microbial identity to function. Nature Reviews Microbiology, 3(6), 499-504.

Gause G. (1934) The struggle for existence. Williams and Wilkins, Baltimore.

Gray N, Howarth R, Rowan A, Pickup R, Jones JG & Head I. (1999) Natural communities of Achromatium oxaliferum comprise genetically, morphologically, and ecologically distinct subpopulations. Applied and Environmental Microbiology 65: 5089-5099.

Harrison BK, Zhang H, Berelson W & Orphan VJ. (2009) Variations in archaeal and bacterial diversity associated with the sulfate-methane transition zone in continental margin sediments (Santa Barbara Basin, California). Applied and Environmental Microbiology 75: 1487-1499.

Holler T, Widdel F, Knittel K, Amann R, Kellermann MY, Hinrichs K-W, et al. (2011) Thermophilic anaerobic oxidation of methane by marine microbial consortia. The ISME journal 5: 1946-1956.

Kleindienst S, Ramette A, Amann R & Knittel K. (2012) Distribution and *in situ* abundance of sulfate‚Äêreducing bacteria in diverse marine hydrocarbon seep sediments. Environmental Microbiology.

Knittel K & Boetius A. (2009) Anaerobic Oxidation of Methane: Progress with an unknown process. Annu. Rev. Microbiol. 63: 311-334.

Knittel K, Boetius A, Lemke A, Eilers H, Lochte K, Pfannkuche O, et al. (2003) Activity, Distribution, and Diversity of Sulfate Reducers and Other Bacteria in Sediments above Gas Hydrate (Cascadia Margin, Oregon). Geomicrobiology Journal 20: 269 - 294.

Knittel K, Losekann T, Boetius A, Kort R & Amann R. (2005) Diversity and distribution of methanotrophic archaea at cold seeps. Applied and Environmental Microbiology 71: 467-479.

Krüger M, Blumenberg M, Kasten S, Wieland A, Känel L, Klock J-H, et al. (2008) A novel, multi-layered methanotrophic microbial mat system growing on the sediment of the Black Sea. Environmental Microbiology 10: 1934-1947.

Kuever J, Rainey F & Widdel F. (2005a) Family I. Desulfobacteraceae fam. nov. Bergey's Manual® of Systematic Bacteriology. (Brenner DJ, Krieg NR, Garrity GM, et al., eds.), pp. 960-962. Springer US.

Kuever J, Rainey F & Widdel F. (2005b) Family II. Desulfobulbaceae fam. nov. Bergey's Manual® of Systematic Bacteriology. (Brenner DJ, Krieg NR, Garrity GM, et al., eds.), pp. 988-992. Springer US.

Lane D. (1991) 16S/23S rRNA sequencing. Nucleic acid techniques in bacterial systematics.

Lichtschlag A, Felden J, Brüchert V, Boetius A & De Beer D. (2010) Geochemical processes and chemosynthetic primary production in different thiotrophic mats of the Håkon Mosby Mud Volcano (Barents Sea). Limnology and Oceanography 55.

Linke P, Wallmann K, Suess E, Hensen C & Rehder G. (2005) *In situ* benthic fluxes from an intermittently active mud volcano at the Costa Rica convergent margin. Earth and Planetary Science Letters 235: 79-95.

Lloyd KG, Albert DB, Biddle JF, Chanton JP, Pizarro O & Teske A. (2010) Spatial Structure and Activity of Sedimentary Microbial Communities Underlying a Beggiatoa spp. Mat in a Gulf of Mexico Hydrocarbon Seep. PLoS ONE 5: e8738.

Losekann T, Knittel K, Nadalig T, Fuchs B, Niemann H, Boetius A & Amann R. (2007) Diversity and abundance of aerobic and anaerobic methane oxidizers at the Haakon Mosby mud volcano, Barents Sea. Applied and Environmental Microbiology 73: 3348-3362.

Ludwig W, Strunk O, Westram R, Richter L, Meier H, Buchner A, et al. (2004). ARB: a software environment for sequence data. Nucleic acids research, 32(4), 1363-1371.

Manz W, Eisenbrecher M, Neu TR & Szewzyk U. (1998) Abundance and spatial organization of Gram-negative sulfate-reducing bacteria in activated sludge investigated by *in situ* probing with specific 16S rRNA targeted oligonucleotides. Fems Microbiology Ecology 25: 43-61.

Mau S, Sahling H, Rehder G, Suess E, Linke P & Soeding E. (2006) Estimates of methane output from mud extrusions at the erosive convergent margin off Costa Rica. Marine Geology 225: 129-144.

Milucka J, Ferdelman TG, Polerecky L, Franzke D, Wegener G, Schmid M, et al. (2012) Zero-valent sulphur is a key intermediate in marine methane oxidation. Nature 491: 541-546.

Musat N, Halm H, Winterholler B, Hoppe P, Peduzzi S, Hillion F, et al. (2008) A single-cell view on the ecophysiology of anaerobic phototrophic bacteria. Proceedings of the National Academy of Sciences 105: 17861-17866.

Nauhaus K, Treude T, Boetius A & Krüger M. (2005) Environmental regulation of the anaerobic oxidation of methane: a comparison of ANME-I and ANME-II communities. Environmental Microbiology 7: 98-106.

Nauhaus K, Albrecht M, Elvert M, Boetius A & Widdel F. (2007) In vitro cell growth of marine archaeal-bacterial consortia during anaerobic oxidation of methane with sulfate. Environmental Microbiology 9: 187-196.

Niemann H, Lösekann T, de Beer D, Elvert M, Nadalig T, Knittel K, et al. (2006) Novel microbial communities of the Haakon Mosby mud volcano and their role as a methane sink. Nature 443: 854-858.

Orphan VJ & House CH. (2009) Geobiological investigations using secondary ion mass spectrometry (SIMS): microanalysis of extant and paleo-microbial processes. Geobiology 7: 360-372. .

Orphan VJ, House CH, Hinrichs K-U, McKeegan KD & DeLong EF. (2002) Multiple archaeal groups mediate methane oxidation in anoxic cold seep sediments. Proceedings of the National Academy of Sciences 99: 7663-7668.

Orphan VJ, House CH, Hinrichs KU, McKeegan KD & DeLong EF. (2001) Methane-consuming archaea revealed by directly coupled isotopic and phylogenetic analysis. Science 293: 484-487.

Orphan VJ, Ussler W, Naehr TH, House CH, Hinrichs KU & Paull CK. (2004) Geological, geochemical, and microbiological heterogeneity of the seafloor around methane vents in the Eel River Basin, offshore California. Chemical Geology 205: 265-289.

Ottesen EA, Hong JW, Quake SR & Leadbetter JR. (2006) Microfluidic digital PCR enables multigene analysis of individual environmental bacteria. Science 314: 1464-1467.

Pace NR, Stahl DA, Lane DJ & Olsen GJ. (1985) Analyzing natural microbial populations by rRNA sequences. ASM American Society for Microbiology News 51: 4-12.

Pernthaler A, Dekas AE, Brown CT, Goffredi SK, Embaye T & Orphan VJ. (2008) Diverse syntrophic partnerships from deep-sea methane vents revealed by direct cell capture and metagenomics. Proc Natl Acad Sci U S A 105: 7052-7057.

Preisler A, de Beer D, Lichtschlag A, Lavik G, Boetius A & Jorgensen BB. (2007) Biological and chemical sulfide oxidation in a Beggiatoa inhabited marine sediment. ISME J 1: 341-353.

Prosser JI. (2012) Ecosystem processes and interactions in a morass of diversity. Fems Microbiology Ecology.

Rabus R, Hansen T & Widdel F. (2006) Dissimilatory sulfate-and sulfur-reducing prokaryotes. The prokaryotes 2: 659-768.

Reeburgh WS. (1976) Methane consumption in Cariaco Trench waters and sediments. Earth and Planetary Science Letters 28: 337-344.

Rossel PE, Elvert M, Ramette A, Boetius A & Hinrichs K-U. (2011) Factors controlling the distribution of anaerobic methanotrophic communities in marine environments: Evidence from intact polar membrane lipids. Geochimica et Cosmochimica Acta 75: 164-184.

Sahling H, Masson DG, Ranero CR, Hühnerbach V, Weinrebe W, Klauke I, et al. (2008) Fluid seepage at the continental margin offshore Costa Rica and southern Nicaragua. Geochemistry Geophysics Geosystems 9: Q05S05.

Sahling H, Rickert D, Lee RW, Linke P & Suess E. (2002) Macrofaunal community structure and sulfide flux at gas hydrate deposits from the Cascadia convergent margin, NE Pacific. Marine Ecology Progress Series 231: 121-138.

Schramm A, Fuchs BM, Nielsen JL, Tonolla M & Stahl DA. (2002) Fluorescence *in situ* hybridization of 16S rRNA gene clones (Clone-FISH) for probe validation and screening of clone libraries. Environmental Microbiology 4: 713-720.

Schreiber L, Holler T, Knittel K, Meyerdierks A & Amann R. (2010) Identification of the dominant sulfate-reducing bacterial partner of anaerobic methanotrophs of the ANME-2 clade. Environmental Microbiology 12: 2327-2340.

Torres ME, McManus J, Hammond DE, de Angelis MA, Heeschen KU, Colbert SL, et al. (2002) Fluid and chemical fluxes in and out of sediments hosting methane hydrate deposits on Hydrate Ridge, OR, I: Hydrological provinces. Earth and Planetary Science Letters 201: 525-540.

Torsvik V, Ovreas L & Thingstad TF. (2002) Prokaryotic diversity--magnitude, dynamics, and controlling factors. Science Signalling 296: 1064.

Turley CM. (1993). Direct estimates of bacterial numbers in seawater samples without incurring cell loss due to sample storage. In Kemp, P.F., Sherr, B.F., Sherr, E.B. and Cole, J.J. (ed.). Handbook of methods in aquatic microbial ecology. Lewis Publishers, Boca Raton, Fla: pp 143-147

Valentine DL & Reeburgh WS. (2000) New perspectives on anaerobic methane oxidation. Environ Microbiol 2: 477-484.

Wagner M, Horn M & Daims H. (2003) Fluorescence *in situ* hybridisation for the identification and characterisation of prokaryotes. Current Opinion in Microbiology 6: 302-309.

FIGURES

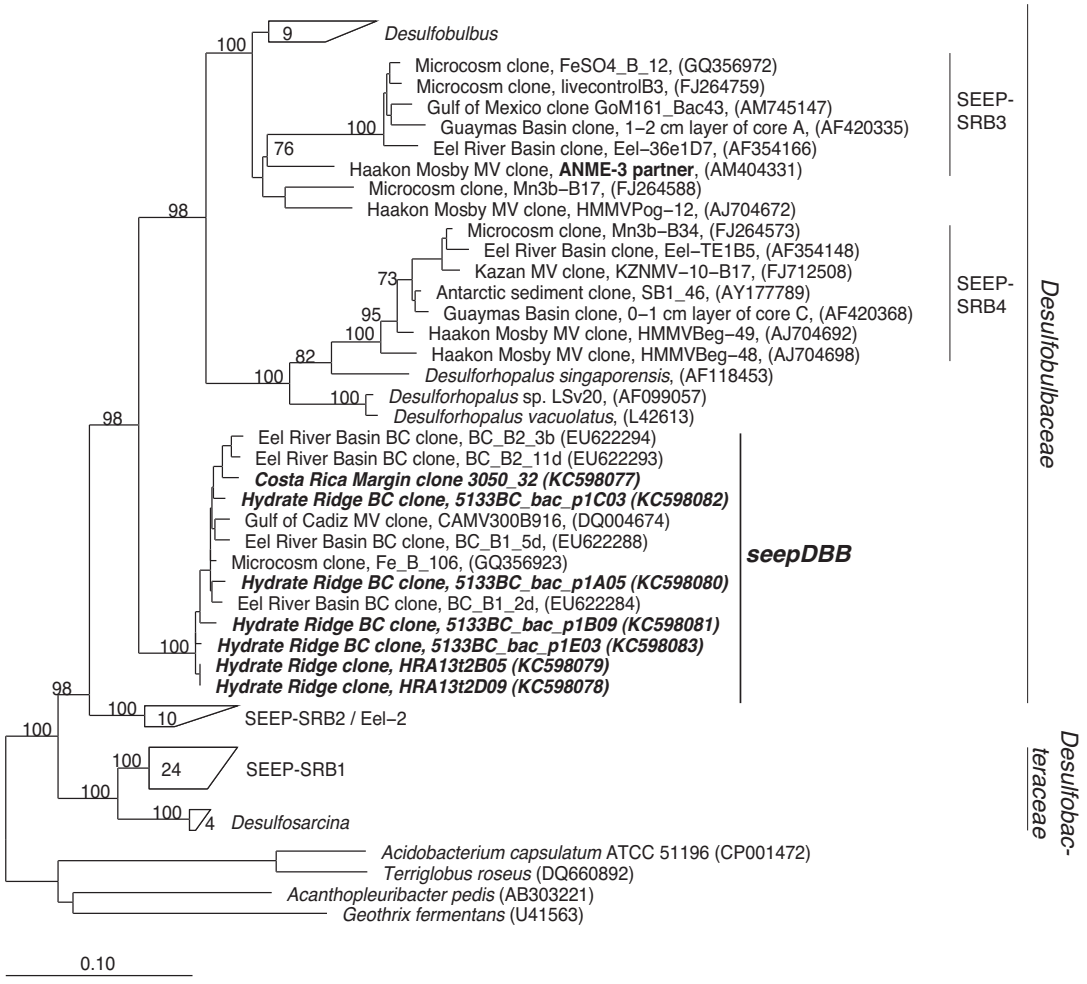

Figure 1

16S rRNA gene phylogeny of pure culture representatives and sulfate-reducing *Deltaproteobacterial* sequences retrieved from methane seeps inferred by Neighbor-joining with the Jukes and Cantor model, was used to estimate distances using the ARB database SSURef-108-SILVA-NR (www.arb-silva.de) and the provided bacterial filter. Bootstrap values were obtained in PAUP* 4.0b10 by Neighbor-joining with 1000 bootstraps. Clones from this study were added to the existing full-length 16S rRNA tree using the quick add maximum parsimony method. Scale bar represents 0.10 substitutions per site. BC = Bead-Captured (i.e., originating from magneto-FISH). Sequences from the current study are in bold italices.

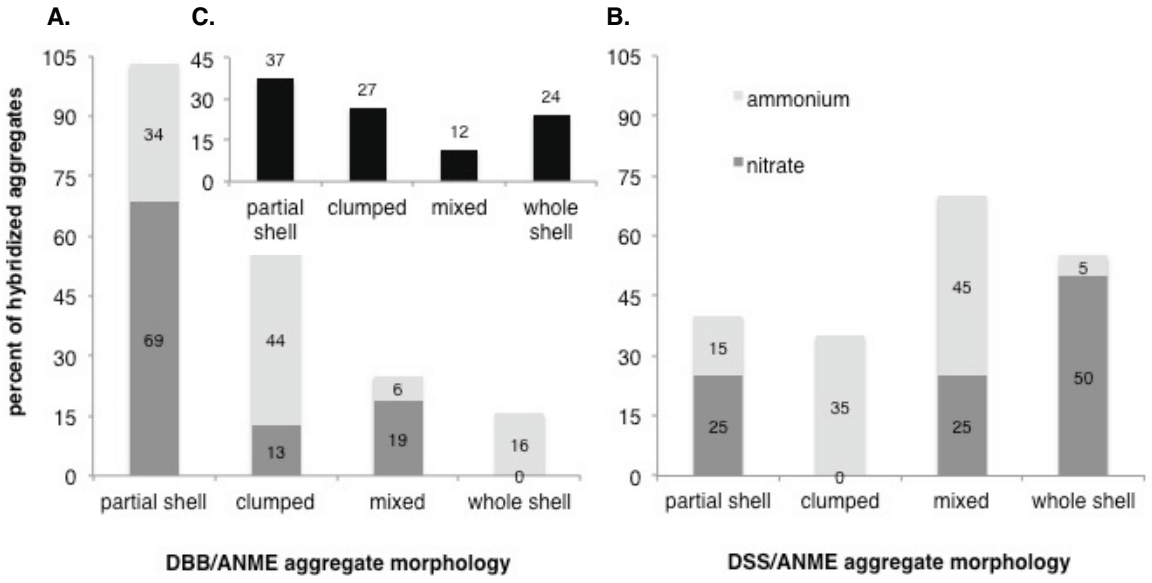

Figure 2
Relative proportions of total aggregate morphologies from (A and B) nitrogen amended incubations or (B) push core sediments collected from Eel River Basin.

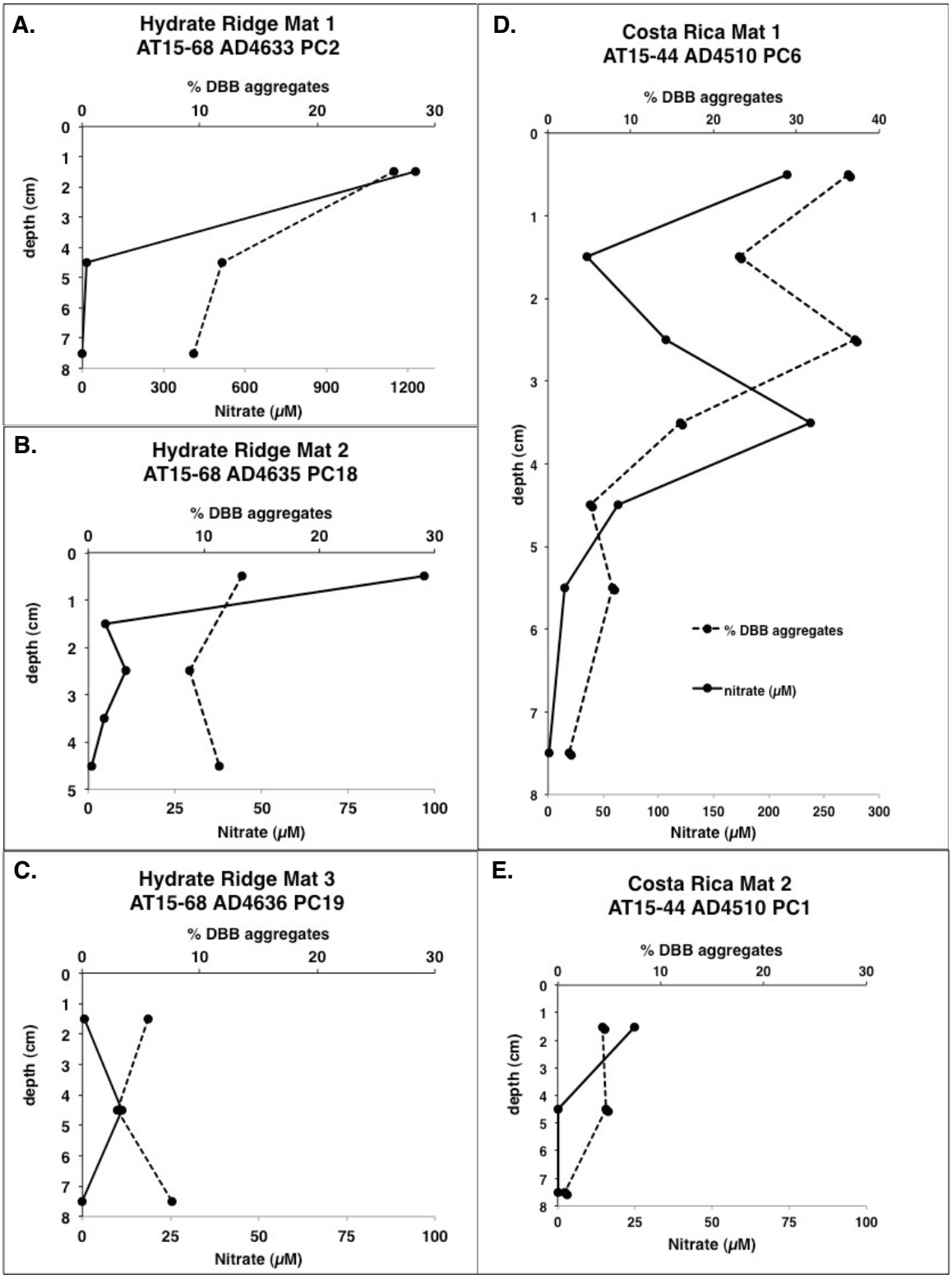
A.
Hydrate Ridge Mat 1
AT15-68 AD4633 PC2
% DBB aggregates
depth (cm)
Nitrate (μM)
B.
Hydrate Ridge Mat 2
AT15-68 AD4635 PC18
% DBB aggregates
depth (cm)
Nitrate (μM)
C.
Hydrate Ridge Mat 3
AT15-68 AD4636 PC19
% DBB aggregates
depth (cm)
Nitrate (μM)
D.
Costa Rica Mat 1
AT15-44 AD4510 PC6
% DBB aggregates
depth (cm)
% DBB aggregates
nitrate (μM)
Nitrate (μM)
E.
Costa Rica Mat 2
AT15-44 AD4510 PC1
% DBB aggregates
depth (cm)
Nitrate (μM)

Figure 3
Nitrate depth profiles and relative abundance of ANME/seepDBB (to total ANME/SRB) aggregate distribution from push cores collected from (A, B and C) Hydrate Ridge and (D and E) Costa Rica Margin methane seep.

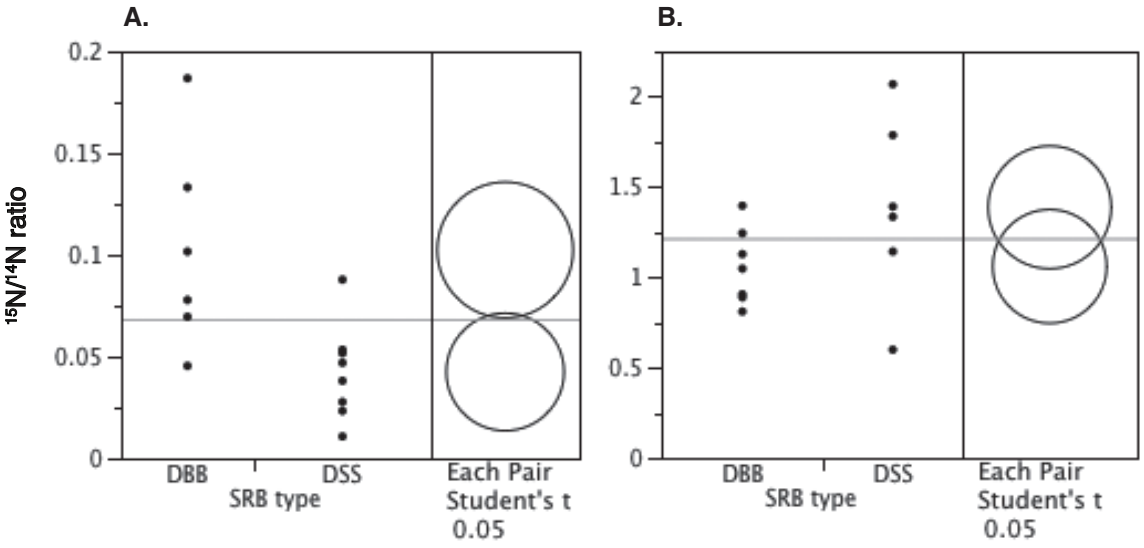

Figure 4
^{15}N enrichment measured via NanoSIMS in ANME/seepDBB and ANME/DSS aggregates from incubations of Eel River Basin methane seep sediment and amended with either (A) ^{15}N-nitrate or (B) ^{15}N-ammonium.

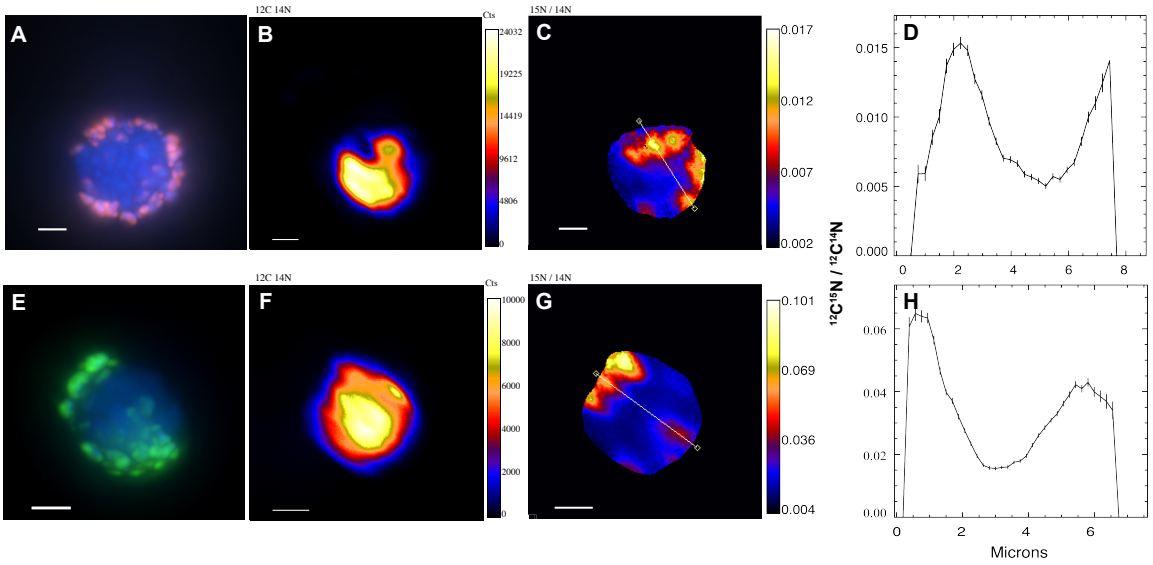

Figure 5

Examples of (A-D) ANME/DSS or (E-H) ANME/seepDBB aggregates from ^{15}N-nitrate incubations that show ^{15}N enrichment in SRB region of aggregate. (B and F) ^{12}C ^{14}N isotope images. (D and H) ^{15}N enrichment profiles of transects through adjacent (C and G) ^{15}N/^{14}N isotope images. Scale bar represents 2 µm.

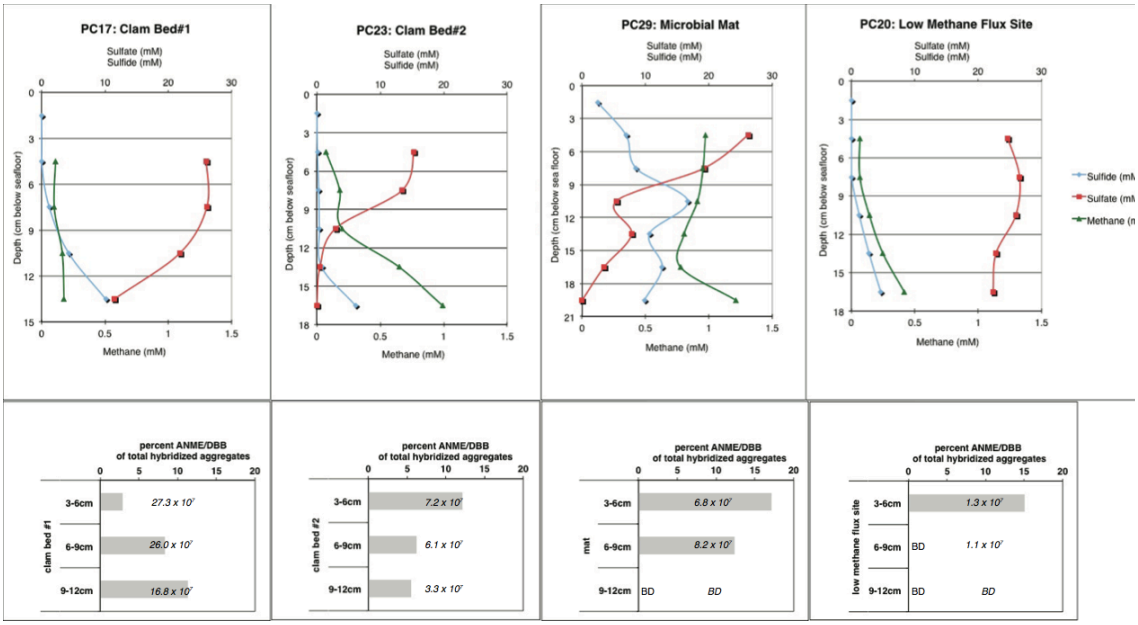

Figure S1

(top panel) Methane, sulfate and sulfide depth profiles and (lower panel) relative abundance of ANME/seepDBB (to total ANME/SRB) aggregate distribution from push cores collected from three habitats along the same transect in Eel River Basin methane seep. (lower panel) Bars represent relative abundance of ANME/seepDBB (to total ANME/SRB); numbers on bars represent total aggregates/ml (as estimated via DAPI counts). BD = below detection.

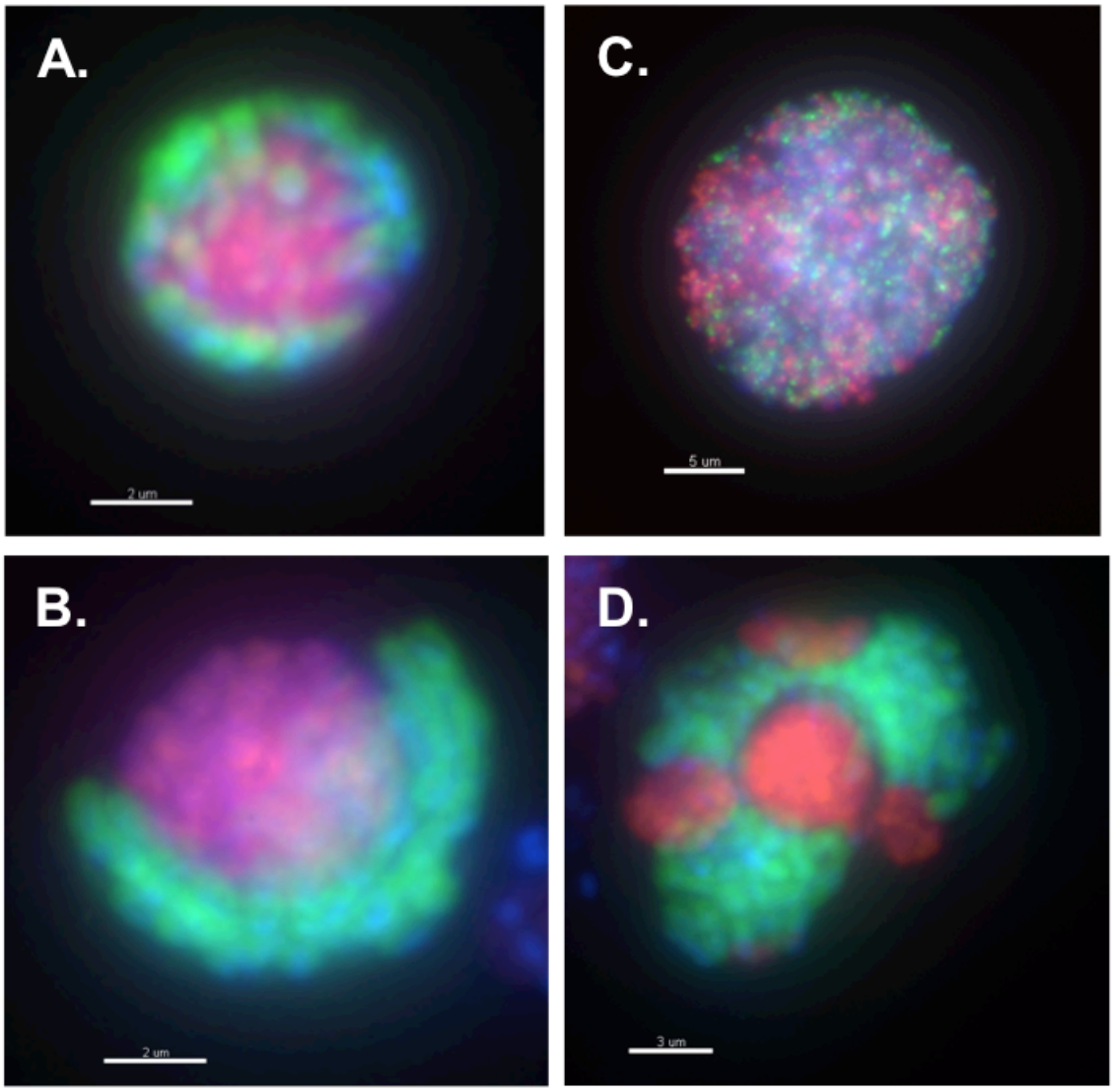

Figure S2
Examples of (A) shell, (B) partial shell, (C) mixed and (D) clumped aggregate morphology. Aggregates were hybridized with probes seepDBB653 (green; targeting methane seep Desulfobulbaceae; this study) and EelMsMX_932 (red; targeting ANME; Boetius et al., 2000). All cells were counter stained (blue) using DAPI.

sample name	location	date	cruise	dive	latitude and longitude	depth (mbsl)	push core	sediment depths (cmbsf)	habitat	sample first described	analysis
	Eel River Basin	**Oct-06**	**AT 15-11**								
clam1	Northern Ridge			AD4256	40°N 48.6 124°W 36.6	520	PC17	3 to 12	clam bed	this study	agg. counts, geochemistry
low-methane	Northern Ridge			AD4256	40°N 48.6 124°W 36.6	520	PC20	3 to 12	low methane	this study	agg. counts, geochemistry
clam2	Northern Ridge			AD4256	40°N 48.6 124°W 36.6	520	PC23	3 to 12	clam bed	this study	agg. counts, geochemistry
mat	Northern Ridge			AD4256	40°N 48.6 124°W 36.6	520	PC29	3 to 12	microbial mat	Pernthaler et al., 2008	DNA, agg. counts, geochemistry
incubation, PC11	Southern Ridge			AD4254	40°N 47.2 124°W 35.7	520	PC11	0 to 12	clam bed	Dekas et al., 2009	FISH-nanoSIMS, agg. counts
incubation, PC14	Southern Ridge			AD4254	40°N 47.2 124°W 35.7	520	PC14	0 to 15	microbial mat	Dekas et al., 2009	FISH-nanoSIMS
	Costa Rica Margin	**Feb-09**	**AT 15-44**								
Costa Rica Mat 1	Jaco Summit			AD4510	9°N 10.3 84°W 47.9	745	PC6	0 to 9	microbial mat	Dekas et al., in review	DNA, agg. counts, geochemistry
Costa Rica Mat 2	Jaco Summit			AD4510	9°N 10.3 84°W 47.9	745	PC1	0 to 9	microbial mat	Dekas et al., in review	agg. counts, geochemistry
	Hydrate Ridge	**Aug-10**	**AT 15-68**								
Hydrate Ridge Mat 1	Southeast Knoll			AD4633	44°N 27.0 125°W 1.7	625	PC2	0 to 9	microbial mat	this study	agg. counts, geochemistry
Hydrate Ridge Mat 2	Hydrate Ridge South			AD4635	44°N 34.1 125°W 9.1	775	PC18	0 to 6	microbial mat	this study	agg. counts, geochemistry
Hydrate Ridge Mat 3	Hydrate Ridge South			AD4636	44°N 34.1 125°W 9.1	772	PC19	0 to 9	microbial mat	this study	agg. counts, geochemistry
DNA sample	Hydrate Ridge South			AD4629	44°N 34.1 125°W 9.1	774	PC9	0 to 3	microbial mat	this study	DNA
	Hydrate Ridge	**Sep-11**	**AT 18-10**								
DNA sample	Hydrate Ridge North			J2 593 E3	44°N 40.0 125°W 6.0	600	PC47	0 to 9	microbial mat	this study	DNA

Table S1. Summary of samples used in this study. mbsl = meters below sea level, cmbsf = centimeters below sea floor, agg = aggregate

*Chapter 3**

***This chapter, written by Abigail Green Saxena, is being combined with another dataset to be submitted to a peer-reviewed journal.**

Effects of the sulfate reduction-inhibitor molybdate on anaerobic methane-oxidizing community metabolism, ANME/bacterial aggregate composition and cell growth

A. Green-Saxena[1] and V.J. Orphan[2]

Divisions of [1]Biology and [2]Geological and Planetary Sciences, and [3]Global Environmental Center, California Institute of Technology, 1200 East California Boulevard, Pasadena, CA 91125

ABSTRACT

Here we show a detailed study in which AOM sediment collected from Hydrate Ridge was amended with sodium molybdate and ^{15}N-labeled ammonium under a methane headspace and incubated for 13 months. Sulfide production along with sulfate depletion was monitored and supported the complete inhibition of sulfate reduction throughout the incubations. Counts of aggregates hybridized with ANME- and bacterial-specific mono-labeled oligonucleotide probes show that with time, there was a shift in the aggregate composition favoring ANME-only aggregates in inhibited incubations only, suggesting the bacterial partner may be decaying rather quickly in the absence of its primary ability to harvest energy, while ANME cells persist. In order to determine if the remaining primarily ANME-only aggregates were still growing we used fluorescence *in situ* hybridization coupled to nano-scale secondary ion mass spectrometry (FISH-NanoSIMS) to quantify ^{15}N-ammonium incorporations in the aggregates after 7 months. In non-inhibited controls ^{15}N-ammonium incorporation (avg. 5.6 atom%) was well above that of natural abundance (0.36 atom%). However, in the inhibited treatment, aggregates showed an average of 0.58 atom% ^{15}N incorporation, which is not above the background value for potential abiotic adsorption of ^{15}N-ammonium (0.60 atom%), suggesting little to no incorporation occurred. These data suggest that while the SRB decay and the ANME persist, the ANME are not able to synthesize new proteins and thus are not able to grow when sulfate reduction is inhibited.

INTRODUCTION

The anaerobic oxidation of methane (AOM) is responsible for recycling up to 80% of the oceanic methane production (Reeburgh, 2007). This crucial biogeochemical process serves as a major sink for methane, a greenhouse gas with heat trapping capabilities up to 20 times stronger than CO_2 (Schiermeier, 2006). Syntrophic aggregates of anaerobic methane-oxidizing archaea (ANME) and sulfate-reducing bacteria (SRB) appear to carry out the anaerobic oxidation of methane (Orphan et al., 2001a). In the following putative pathway, sulfate serves as the electron acceptor for methane (Boetius et al., 2000; Iverson and Jorgensen, 1985): $CH_4 + SO_4^{2-} \rightarrow HCO_3^- + HS^- + H_2O$. However, to date, neither ANME nor SRB involved in this reaction have been grown in pure culture, and thus the pathway for AOM, including the method for electron transfer, remains unclear (Knittel and Boetius, 2009). Indeed, Milucka and colleagues (2012) recently proposed a new pathway in which ANME-2 is capable of both the anaerobic oxidation of methane and reduction of sulfate to disulfide (or other S0 compounds), which is then scavenged by the SRB and disproportionated to sulfide and sulfate.

As sulfate-reducing bacteria were initially implicated as an agent responsible for AOM (Reeburgh, 1976), multiple studies have used sulfate reduction inhibitors such as molybdate or tungstate to validate and study dynamics of AOM (Alperin and Reeburgh, 1985; Hansen et al 1998; Iversen et al., 1987; Nauhaus et al., 2005; Orcutt et al., 2008). Molybdate is a commonly used sulfate reduction inhibitor as it serves as a structural

analogue to sulfate (Reuveny, 1977) and several studies have demonstrated that it successfully inhibits the SRB community in a mixed enrichment culture including non-SRB members (Lovely et al., 1982; Compeau and Bartha, 1985). While earlier studies investigating AOM found little to no inhibition of methane oxidation by sulfate-reduction inhibitors (Alperin and Reeburgh, 1985; Hansen et al 1998; Iversen et al., 1987), Hoehler et al. (1994) point out that conditions of such studies may have led to an increase in methanogenesis, confounding the results. More recent studies from different habitats report near to complete AOM inhibition (Nauhaus et al., 2005; Orcutt et al., 2008).

Due to the difficulties of getting the ANME/SRB consortia into pure culture, prior sulfate-reduction inhibition studies are based on bulk geochemical measurements in which they inhibit sulfate reduction in an entire community and measure the AOM of that community (Alperin and Reeburgh, 1985; Hansen et al 1998; Iversen et al., 1987; Nauhaus et al., 2005; Orcutt et al., 2008). This allows us to see the effect of sulfate reduction inhibition on AOM as a whole it does not show what is happening to the AOM consortia on a cellular level, knowledge which could shed light on the dynamics of this symbiosis. Whether either partner in the symbiosis is able to persist, metabolize and grow in the presence of sulfate-reducing inhibitors remains unclear.

Tracking the effects of sulfate-reducing inhibitors on aggregate abundance and composition can be accomplished via fluorescence *in situ* hybridization (FISH) which can then be coupled to nano-scale secondary ion mass spectrometry (NanoSIMS) in order to measure growth in consortia incubated with ^{15}N-labeled ammonium (Orphan et al., 2009). FISH-NanoSIMS allows the coupling of function with identity through the measurement of ^{15}N incorporation in individual cells or aggregates whose phylogenetic identity is

determined via FISH. Here we use a combination of geochemical studies, FISH, and FISH-nanoSIMS to study the effects of a sulfate reduction inhibitor on the metabolic processes and growth of the ANME and bacterial cells involved in AOM.

METHODS

Site Selection, Sampling and Processing:

Push core samples were collected in August 2010 (AT 15-68) from active methane seeps in Hydrate Ridge (Boetius and Seuss 2004) off the coast of Oregon using manned submersible Alvin. Push core PC9 was collected through a microbial mat (Hydrate Ridge South, AD4629, 44°N 34.09 125°W 9.14, 774 m water depth). Microcosm experiments from the top 0-3 cm of PC9 sediment were set up shipboard. Sediments were mixed approximately 1:3 with filtered seawater (sparged with argon) and aliquotted into 40 ml glass bottles (with butyl stoppers) with a 20 ml methane headspace (overpressured to 30 psi). The sediment slurries were amended with 0 or 2 mM ^{15}N-ammonium and 0 or 25 mM sodium molybdate and incubated anaerobically at 4-8 ºC. Killed controls were amended with 2 mM ^{15}N-ammonium and treated with formaldehyde (final concentration of 3.7%). Sediment samples were taken anaerobically via syringe at 0, 1, 3 and 7 months.

Fluorescence *in situ* Hybridization (FISH) and aggregate counts:

Sediment samples were fixed in 2% paraformaldehyde for approximately 1 hour at room temperature, washed twice with phosphate-buffered saline (PBS; Pernthaler et al., 2008), once with 1:1 PBS: ethanol, resuspended in 100% ethanol and stored at -20°C. For FISH analyses, 150 µl fixed sediment was brought to 0.9 ml in a TE (10 mM Tris-HCl and 1 mM

EDTA (pH 9.0)), 0.01 M pyrophosphate solution, heated in a histological microwave oven (Microwave Research and Applications, Carol Stream, IL) for 3 minutes at 60°C. Samples were then cooled to room temperature and sonicated on ice for 3 10 second bursts with a Vibra Cell sonicating wand (Sonics and Materials, Danbury, CT) at an amplitude setting of 3.0. Percoll (900 µl) was then added to the bottom of the 2 ml tubes, which were then centrifuged at 14000 rpm for 20 minutes at 4°C. The supernatant was filtered onto a 3.0 µm pore-sized polycarbonate filter (Millipore, Billerica, MA). A Cy3-labeled oligonucleotide probe targeting anaerobic methane-oxidizing archaeal clade ANME-2 (Eel_MS_932; Boetius et al., 2000) and a FITC-labeled general bacterial probe (EUB338 mix; Amann et al., 1995) were then used in a FISH reaction following the protocol outlined in Orphan et al (2001). Micrograph images were taken with a Deltavision RT microscope system (Applied Precision, Issaquah, WA). ANME/EUB and ANME-only aggregates were counted from a total of 50 aggregate-containing fields per sample. Relative numbers of ANME-only aggregates are expressed as percent ANME-only of total hybridized aggregates.

Fluorescence *in situ* Hybridization Nanoscale Secondary Ion Mass Spectrometry (FISH-NanoSIMS):

Five aggregates from an ammonium- and sodium molybdate-amended incubation (2 mM ^{15}N-ammonium, 25 mM sodium molybdate, sampled at 7 months), and two aggregates from an ammonium-amended (2 mM ^{15}N-ammonium, sampled at 7 months) incubation were examined; all incubations were inoculated with methane seep sediment slurries from a push core collected through a microbial mat in Hydrate Ridge (PC-9,

AD4629, AT 15-68).

Fixed and washed sediment samples (150 µl) for FISH analysis were treated as described above and applied to a Percoll density gradient as described in Orphan et al (2002). All samples were deposited onto custom cut indium tin oxide (ITO) coated glass and hybridized with Cy3- and FITC-labeled oligonucleotide probes Eel_MS_932 (Boetius et al., 2000) and EUB338 (Amann et al., 1995) and mapped for nanoSIMS analysis (Orphan et al., 2002; Dekas and Orphan, 2011). Clostridia spores (with known $\delta^{13}C$ and $\delta^{15}N$) were spotted onto a blank section of a separate ITO coated glass square and used as standards during the analysis. Samples were analyzed using a CAMECA NanoSIMS 50L housed at Caltech, using a mass resolving power approximately 5,000.

A primary Cs^+ ion beam (0.5 to 1.5 pA) was used to raster over target cells, with a raster size ranging from 10 to 30 µm. Secondary ion images were collected at 256 x 256 pixel resolution with a dwell time of 3,000 to 8,000 ct/pixel over a period of 5 to 12 hours, resulting in 54 to 129 cycles, depending on target size. Due to time constraints, aggregates were not sampled through their entire Z planes. Clostridia spores were measured in ion image mode using the same range in ion beam current as a standard to ensure there were no matrix effects in the analysis. Several masses were collected in parallel including: $^{12}C^{14}N^-$, and $^{12}C^{15}N^-$ using electron multiplier detectors. Resulting ion images were processed using the L'Image software (developed by L. Nittler, Carnegie Institution of Washington, Washington D.C.). The reported isotope ratio for each aggregate was extracted from the image by identifying a region of interest (ROI) – the aggregate – within each image. The aggregate edge was automatically defined in L'image by setting a lower threshold of 5% of the maximum value of $^{12}C^{15}N/^{12}C^{14}N$ counts within a given cycle. If this automatic ROI

definition included non-aggregate elements from the surrounding area, the portion of the ROI that only contained the aggregate was traced manually and subsequently used as the final ROI. The ratio from the cycle with the highest $^{12}C^{15}N/^{12}C^{14}N$ was then collected from each aggregate. The $^{12}C^{15}N/^{12}C^{14}N$ ratio is hereafter referred to as the $^{15}N/^{14}N$ ratio.

Geochemistry:

In order to analyze sulfide concentrations in the microcosms at each time point, subsamples of the aqueous phase of incubated sediment slurries (the initial time point was taken from an aliquot of the original un-amended sediment slurry) were filtered via a 0.2 μm filter and combined with 1 M zinc acetate at a 1:1 ratio. Sulfide concentration was then determined using a colorimetric Cline assay (Cline, 1969) measured on a 96-well format TECAN Sunrise spectrophotometer (TECAN, Männedorf, Switzerland).

In order to determine sulfate concentrations, subsamples of the aqueous phase of incubated sediment slurries were filtered via a 0.2 μm filter and frozen at -20˚C until analysis. Parallel ion chromatography systems operated simultaneously (Dionex DX-500, Environmental Analysis Center, Caltech) were used to measure ammonium, nitrate, nitrite and sulfate in the porewater samples. A single autosampler loaded both systems' sample loops serially. The 10 μl sample loop on the anion IC system was loaded first, followed by a 5 μl sample loop on the cation IC system. Temperatures of the columns and detectors were not controlled.

Nitrite, nitrate and sulfate were resolved from other anionic components in the sample using a Dionex AS-19 separator (4x250 mm) column protected by an AG-19 guard (*4x50 mm). A hydroxide gradient was produced using a potassium hydroxide eluent

generator cartridge and pumped at 1 mL per minute. The gradient began with a 10 mM hold for 5 minutes, increased linearly to 48.5 mM at 27 minutes and finally to 50 mM at 41 minutes. 10 minutes were allowed between analyses to return the column to initial conditions. Nitrite and nitrate were determined for UV absorption at 214 nm using a Dionex AD25 Absorbance detector downstream from the conductivity detection system. Suppressed conductivity detection using a Dionex ASRS-300 4 mm suppressor operated in eluent recycle mode with an applied current of 100 mA was applied to detect all other anions, including redundant measurement of nitrite and nitrate. A carbonate removal device (Dionex CRD 200 4 mm) was installed between the suppressor eluent out and the conductivity detector eluent in ports.

Ammonium was resolved from other cationic components using a Dionex CS-16 separator column (5x250 mm) protected by a CG-16 guard column (5x50). A methylsulfonate gradient was produced using a methylsulfonic acid based eluent generated cartridge and pumped at 1 mL per minute. The gradient began with a 10 mM methylsulfonate hold for 5 minutes, then increased to 20 mM at 20 minutes following a non-linear curve (Chromeleon curve 7, concave up), increased further to 40 mM at 41 minutes following a non-linear curve (Chromeleon curve 1, concave down). 10 minutes were allowed between analyses to return the column to initial conditions. Suppressed conductivity detection using a Dionex CSRS-300 4 mm suppressor operated in eluent recycle mode with an applied current of 100 mA.

Standard curves were generated for each species. For nitrate, nitrite, and sulfate, standard measurements were fitted to a linear curve; for ammonium, standard measurements were fitted to a quadratic curve. Standard ranges were 10 μM to 2 mM

(nitrate, nitrite) and 500 μM to 32 mM (sulfate). Standard deviation of repeated injections of a standard (250 μM nitrate and nitrite, 8000 μM sulfate) throughout the analysis were 4.2 μM (nitrate), 5.8 μM (nitrate) and 113 μM (sulfate).

RESULTS AND DISCUSSION

Geochemistry

Sulfide production was measured as a proxy for sulfate reduction in four sets of duplicate incubations: Blank (no amendments), non-inhibited control (2 mM ^{15}N-ammonium added), a killed control (2 mM ^{15}N-ammonium; treated with formaldehyde at initial time point) and an incubation in which sulfate reduction was inhibited (25 mM sodium molybdate, 2 mM ^{15}N-ammonium). The killed control and inhibited incubations exhibited little to no sulfide production over the course of 13 months, suggesting no sulfate reduction occurred in these samples (Figure 1). The small increase in sulfide between the 0 and 1 month time points (< 1 mM increase) may be an artifact of sampling; the initial time point was taken from an aliquot of the original un-amended sediment slurry and may thus vary slightly from the sulfide levels in the respective incubation bottles listed above. The blank and non-inhibited control incubations showed a large increase in sulfide (> 14 mM) from the 0 to 1 month time point. Interestingly, all of these high sulfide accumulation incubations had instances of sulfide loss at various point between the 1 and 13 month time points. These data suggest that either 1. sampling error occurred and sulfide was lost due to abiotic oxidation or 2. some component of the incubation was able to oxidize sulfide *in situ*. The latter may result from the likely presence of sulfur-oxidizing bacteria in the incubations, the sediment for which was collected from the top 3 cm horizons of a push core collected through a sulfur-

oxidizing microbial mat. Several species of sulfur-oxidizers can store nitrate intracellularly for use as a terminal electron acceptor in the sulfide oxidation reaction and thus would be viable in these anaerobic incubations (Preisler et al., 2007). This metabolic reaction produces ammonium, which was seen to accumulate in the amendment-free "blank" incubations (the addition of 2 mM ammonium results in concentrations above the detection limit in other incubations) in which ammonium levels increase from 559 and 755 μM ammonium at 1 month to 1463 and 1580 μM at 13 months in incubations Blank A and Blank B, respectively.

Sulfate depletion was also measured in three sets of the same duplicate incubations: Blank (no amendments), non-inhibited control (2 mM ^{15}N-ammonium added) and an incubation in which sulfate reduction was inhibited (25 mM sodium molybdate, 2 mM ^{15}N-ammonium). The inhibited incubations show a near constant concentration of approximately 24 mM sulfate from the 1 to 13 month time points, suggesting no sulfate reduction occurred. Blank and non-inhibited control incubations however show a depletion of sulfate below that of 0.8 mM after 13 months, suggesting the majority of the sulfate had been reduced.

Change in aggregate abundance and composition over time

As prior studies have estimated a doubling time of 3 to 7 months for ANME SRB aggregates (Orphan et al., 2009; Nauhaus et al., 2007), we conducted aggregate counts over a period of 7 months (sampling at 0, 1, 3 and 7 months) in the control and inhibited incubations. Total aggregates counted (from 50 aggregate-containing fields per time point) in the control incubation increased with time from 438 at the initial time point to 705 after 7 months,

suggesting growth. However, total aggregates counted in the inhibited incubation were much lower at 7 months (150) than at the initial time point (396). The percent of ANME-only aggregates (out of total ANME-containing aggregates) was initially low in both incubations (10% and 11% in control and inhibited incubations, respectively). Aggregate composition in the control sample showed a relatively slight shift towards ANME-only aggregates at 1 month (23%), which decreased at 3 (18%) and 7 (16%) months (Figure 2). The inhibited incubation revealed a more dramatic and continual shift towards ANME-only aggregates over time, with ANME-only aggregates comprising 83% of total hybridized aggregates at the 7 month time point. Whether the ANME-only aggregates were comprised of new growth or the previously existing ANME/bacterial aggregates in which the SRB cells decayed was unclear based on these data alone. If the ANME-only aggregates observed in the later time points were once ANME/bacterial aggregates it is interesting that the bacterial and not the ANME cells decayed. This would suggest that the bacterial cells do not survive when sulfate-reduction is inhibited whereas the ANME cells are at least able to persist under these conditions. NanoSIMS studies were subsequently done in order to determine if cells in the ANME-only aggregates were actively growing.

FISH-NanoSIMS

Incorporation of ^{15}N-labeled ammonium has been previously used as a proxy for protein synthesis in microbial populations at the community and cell-specific levels (Kruger et al., 2008; Orphan et al., 2009). In order to determine if aggregates that persisted in the presence of a sulfate reduction inhibitor were growing, we performed FISH-NanoSIMS analyses on five such aggregates incubated with 25 mM sodium molybdate and 2 mM ^{15}N-labeled

ammonium for 7 months. Three of the aggregates from the inhibited incubation were ANME-only and had similar ^{15}N incorporation values (0.56, 0.49 and 0.45 atom %; Table 1). We also examined, from the same incubation, two ANME/bacteria aggregates, one with approximately 1.3 ANME cells for every bacterial cell (0.43 ^{15}N atom %) and another with approximately 20 ANME cells for each bacterial cell (0.96. ^{15}N atom %). While these incorporation values are above that of natural abundance (0.36 atom %), all but one are below the background value determined for potential abiotic adsorption of ^{15}N-ammonium (0.60 atom %; Orphan et al., 2009), suggesting no growth had occurred. These data do not rule out the possibility that the aggregates are still carrying out unknown dissimilatory reactions.

Interestingly, the one aggregate that did show significant levels of ^{15}N incorporation had a unique pattern of incorporation consisting of small hot spots of ^{15}N (Figure 3). While ANME/SRB aggregates typically have an ANME:SRB cell ratio of 1:2 or 1:3 (Orphan et al., 2009; Nauhaus et al., 2007), this aggregate had a much higher ANME:bacteria ratio of 20:1. Non-SRB bacteria have been reported previously in association with ANME (Pernthaler et al., 2008) and as the bacterial probe used in our study was a general one, it is possible the bacteria in this unusual configuration were not SRB, explaining the potential growth under sulfate reduction-inhibiting conditions.

A baseline level of ^{15}N incorporation was also determined via measurement of aggregates incubated with 2 mM ^{15}N-labeled ammonium in the absence of any inhibitors. The ANME/bacteria and ANME-only aggregates showed very similar ^{15}N incorporation levels after 7 months (5.4 and 5.9 atom %, respectively; Table 1). While these levels are lower (about an order of magnitude) than what has been previously published from studies of

similar AOM microcosms (Dekas et al., 2009; Orphan et al., 2009), they are still much higher than natural abundance (0.36 atom %) as well as the background value for potential abiotic adsorption of ^{15}N-ammonium (0.60 atom %; Orphan et al., 2009), confirming growth in the control incubation. Between the 1 and 7 month time points we observed a decrease in sulfide production which could indicate sulfate reduction was not occurring and therefor growth (and ^{15}N incorporation) would be limited. This decrease in sulfide could also be explained by the likely presence of sulfide-oxidizing bacteria in the incubations (as discussed above). If sulfide-oxidizing bacteria were active, this could lead to the production of ammonium (seen to accumulate in Blank incubations), which would dilute the ^{15}N-ammonium incorporation signal.

CONCLUSIONS

Anaerobic methane oxidation, serving as a sink for this potent greenhouse gas, is a crucial biogeochemical process and yet little is known about the dynamics that exist between the two partners which effect this process. Numerous studies have focused on the effects of sulfate reduction inhibitors on the AOM process as a whole (Alperin and Reeburgh, 1985; Hansen et al., 1998; Iversen et al., 1987; Nauhaus et al., 2005; Orcutt et al., 2008), but the effect of these inhibitors on the cells comprising the ANME/SRB consortia remained unknown. In order to study dynamics of AOM we inhibited sulfate reduction and followed the metabolic processes of the microcosm community as well as the effect of aggregate composition and growth on a cellular level. Here we show that while bacterial cells appear to decay, ANME-2 cells persist in the form of ANME-only aggregates, which are capable of little to no growth when sulfate reduction is inhibited.

ANME-1, -2 and -3 cells have been found without a bacterial partner (Knittel and Boetius, 2009; Orphan et al., 2002; Omoregie et al., 2008), suggesting an alternative metabolism may be possible for these archaea. Our data suggest the growth and metabolism of ANME-2 is tightly linked to the bacterial partner. A study by Nauhaus et al., (2005), showed the addition of molybdate completely inhibited AOM in ANME-2 but not ANME-1 dominated communities, suggesting growth independent of sulfate reduction may have occurred. Further studies on the effects sulfate reduction-inhibition on the growth ANME-1 may reveal alternative growth requirements for ANME-1 and -2.

ACKNOWLEDGEMENTS

We would like to acknowledge Ankur Saxena for figure design, Yunbin Guan for his assistance with NanoSIMS, and the science party of cruise AT 15-68 and pilots of the D.S.R.V. Alvin for their assistance with various aspects of this work. Funding for this work was provided by the Department of Energy Division of Biological Research (DE-SC0004949; to V.J.O.), and a National Science Foundation Graduate Research Fellowship (to A.G.-S.). Samples were collected with funding from the National Science Foundation (BIO-OCE #0825791; to V.J.O.).

REFERENCES

Alperin MJ & Reeburgh WS (1985) Inhibition experiments on anaerobic methane oxidation. Applied and Environmental Microbiology 50: 940-945.

Amann RI, Ludwig W & Schleifer K-H (1995) Phylogenetic identification and *in situ* detection of individual microbial cells without cultivation. Microbiological reviews 59: 143-169.

Boetius A, Ravenschlag K, Schubert CJ, et al. (2000) A marine microbial consortium apparently mediating anaerobic oxidation of methane. Nature 407: 623-626.

Boetius A, Ravenschlag K, Schubert CJ, et al. (2000) A marine microbial consortium apparently mediating anaerobic oxidation of methane. Nature 407: 623-626.

Boetius A & Suess E (2004) Hydrate Ridge: a natural laboratory for the study of microbial life fueled by methane from near-surface gas hydrates. Chemical Geology 205: 291-310.

Cline JD (1969) Spectrophotometric determination of hydrogen sulfide in natural waters. Limnology and Oceanography 454-458.

Compeau G & Bartha R (1985) Sulfate-reducing bacteria: principal methylators of mercury in anoxic estuarine sediment. Applied and Environmental Microbiology 50: 498-502.

Dekas AD, Poretsky RS & Orphan VJ (2009) Deep-sea archaea fix and share nitrogen in methane-consuming microbial consortia. Science 326: 422-426.

Dekas AE & Orphan VJ (2011) Identification of diazotrophic microorganisms in marine sediment via fluorescence *in situ* hybridization coupled to nanoscale secondary ion mass spectrometry (FISH-NanoSIMS). Methods Enzymol 486: 281-305.

Hansen LB, Finster K, Fossing H & Iversen N (1998) Anaerobic methane oxidation in sulfate depleted sediments: effects of sulfate and molybdate additions. Aquatic Microbial Ecology 14: 195-204.

Hoehler TM, Alperin MJ, Albert DB & Martens CS (1994) Field and laboratory studies of methane oxidation in an anoxic marine sediment: Evidence for a methanogen, sulfate reducer consortium. Global Biogeochemical Cycles 8: 451-463.

Iversen N & Jörgensen B (1985) Anaerobic methane oxidation rates at the sulfate-methane transition in marine sediments from Kattegat and Skagerrak (Denmark). Limnol. Oceanogr 30: 944-955.

Iversen N, Oremland RS & Klug MJ (1987) Big Soda Lake (Nevada). 3. Pelagic methanogenesis and anaerobic methane oxidation. Limnol. Oceanogr 32: 804-808.

Knittel K & Boetius A (2009) Anaerobic Oxidation of Methane: Progress with an unknown process. Annu. Rev. Microbiol. 63: 311-334.

Krüger M, Wolters H, Gehre M, Joye SB & Richnow HÄ (2008) Tracing the slow growth of anaerobic methane-oxidizing communities by 15N,Äêlabelling techniques. FEMS microbiology ecology 63: 401-411.

Lovley DR, Dwyer DF & Klug MJ (1982) Kinetic analysis of competition between sulfate reducers and methanogens for hydrogen in sediments. Applied and Environmental Microbiology 43: 1373-1379.

Milucka J, Ferdelman TG, Polerecky L, et al. (2012) Zero-valent sulphur is a key intermediate in marine methane oxidation. Nature 491: 541-546.

Nauhaus K, Albrecht M, Elvert M, Boetius A & Widdel F (2007) In vitro cell growth of marine archaeal-bacterial consortia during anaerobic oxidation of methane with sulfate. Environmental Microbiology 9: 187-196.

Nauhaus K, Albrecht M, Elvert M, Boetius A & Widdel F (2007) In vitro cell growth of marine archaeal-bacterial consortia during anaerobic oxidation of methane with sulfate. Environmental Microbiology 9: 187-196.

Nauhaus K, Treude T, Boetius A & Krüger M (2005) Environmental regulation of the anaerobic oxidation of methane: a comparison of ANME-I and ANME-II communities. Environmental Microbiology 7: 98-106.

Omoregie EO, Mastalerz V, de Lange G, et al. (2008) Biogeochemistry and community composition of iron-and sulfur-precipitating microbial mats at the Chefren Mud Volcano (Nile Deep Sea Fan, Eastern Mediterranean). Applied and Environmental Microbiology 74: 3198-3215.

Orcutt B, Samarkin V, Boetius A & Joye S (2008) On the relationship between methane production and oxidation by anaerobic methanotrophic communities from cold seeps of the Gulf of Mexico. Environmental Microbiology 10: 1108-1117.

Orphan VJ, House CH, Hinrichs K-U, McKeegan KD & DeLong EF (2002) Multiple archaeal groups mediate methane oxidation in anoxic cold seep sediments. Proceedings of the National Academy of Sciences 99: 7663-7668.

Orphan VJ, House CH, Hinrichs KU, McKeegan KD & DeLong EF (2001) Methane-consuming archaea revealed by directly coupled isotopic and phylogenetic analysis. Science 293: 484-487.

Orphan VJ, Turk KA, Green AM & House CH (2009) Patterns of 15N assimilation and growth of methanotrophic ANME-2 archaea and sulfate-reducing bacteria within structured syntrophic consortia revealed by FISH-SIMS. Environ Microbiol doi:10.1111/ j.1462-2920.2009.01903.x.

Pernthaler A, Dekas AE, Brown CT, Goffredi SK, Embaye T & Orphan VJ (2008) Diverse syntrophic partnerships from deep-sea methane vents revealed by direct cell capture and metagenomics. Proc Natl Acad Sci U S A 105: 7052-7057.

Preisler A, de Beer D, Lichtschlag A, Lavik G, Boetius A & Jorgensen BB (2007) Biological and chemical sulfide oxidation in a Beggiatoa inhabited marine sediment. ISME J 1: 341-353.

Reeburgh WS (1976) Methane consumption in Cariaco Trench waters and sediments. Earth and Planetary Science Letters 28: 337-344.

Reeburgh WS (2007) Oceanic methane biogeochemistry. Chemical Reviews 107: 486-513.

Reuveny Z (1977) Derepression of ATP sulfurylase by the sulfate analogs molybdate and selenate in cultured tobacco cells. Proceedings of the National Academy of Sciences 74: 619-622.

Schiermeier Q (2006) Methane finding baffles scientists. Nature 439: 128-128.

FIGURES and TABLES

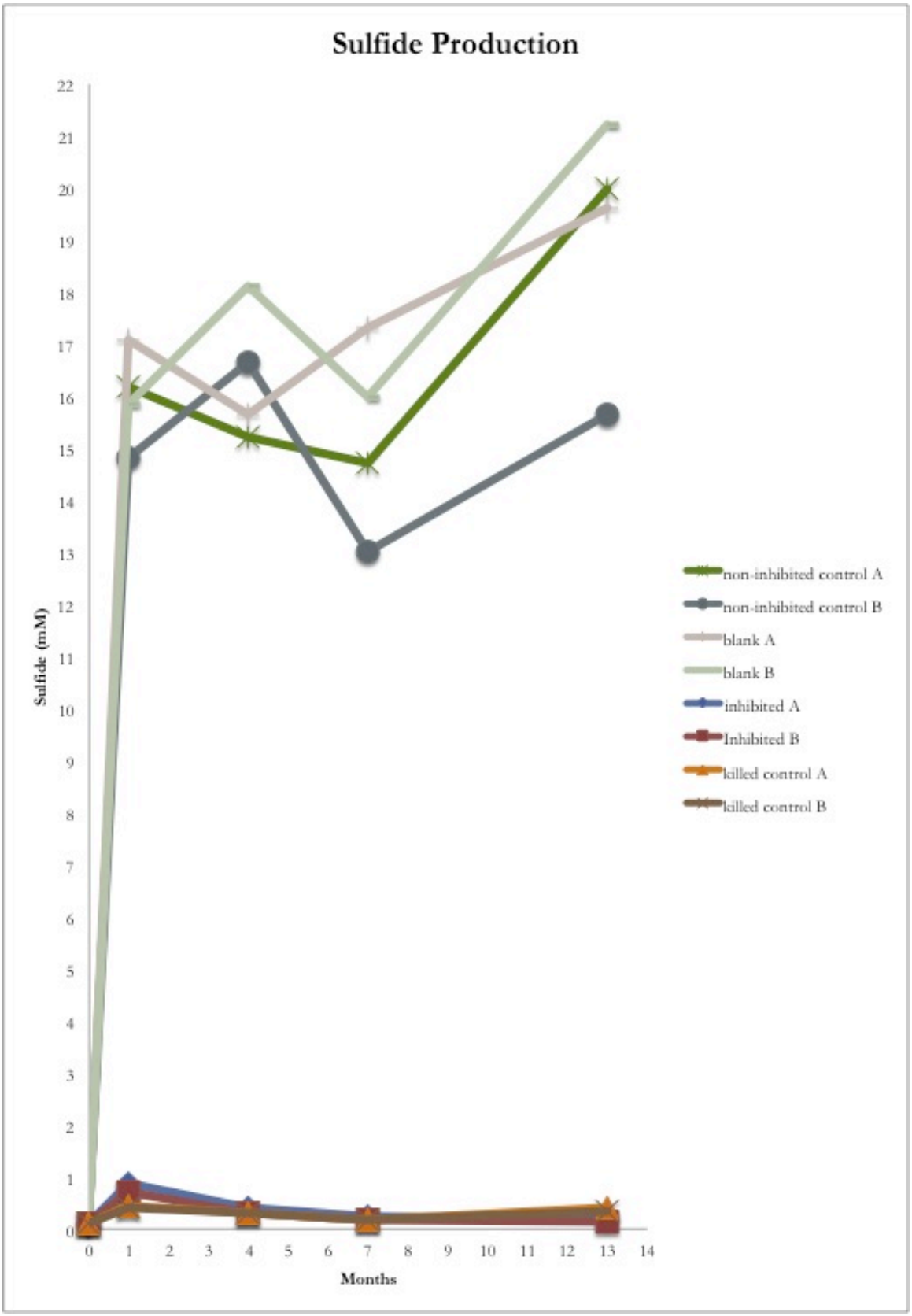
Sulfide Production
Sulfide (mM)
Months
non-inhibited control A
non-inhibited control B
blank A
blank B
inhibited A
Inhibited B
killed control A
killed control B

Figure 1a.

Sulfide production measured in 4 duplicate sets of incubations over 13 months. Control incubations were amended with 2 mM ^{15}N-ammonium; blank incubations had no amendments; inhibited incubations were amended with 2 mM ^{15}N-ammonium and 25 mM sodium molybdate; killed controls were amended with 2 mM ^{15}N-ammonium and treated with 3.7 % formaldehyde at the initial time point.

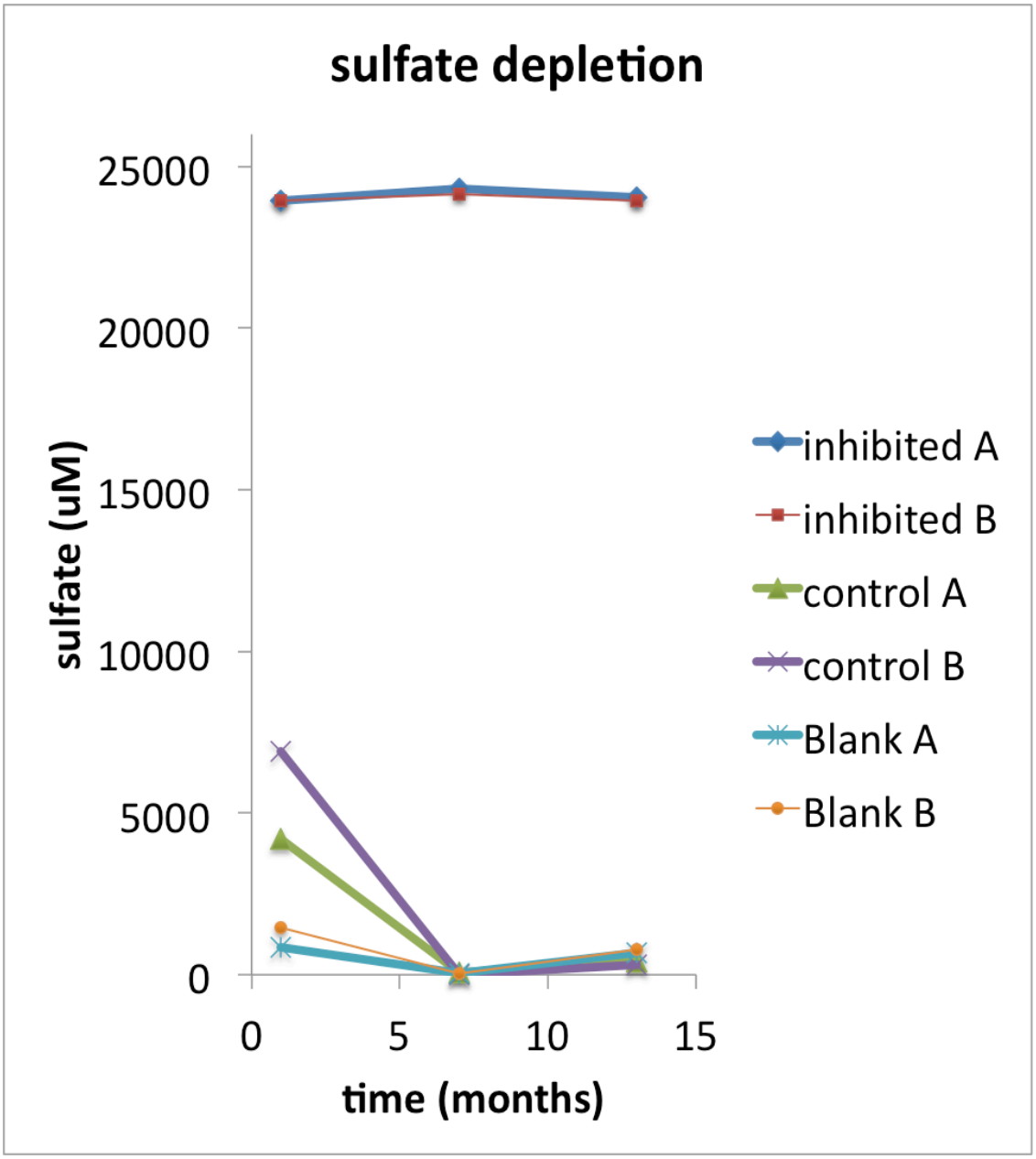

Figure 1b.

Sulfate depletion measured in 3 duplicate sets of incubations over 13 months. Control incubations were amended with 2 mM ^{15}N-ammonium; blank incubations had no amendments; inhibited incubations were amended with 2 mM ^{15}N-ammonium and 25 mM sodium molybdate.

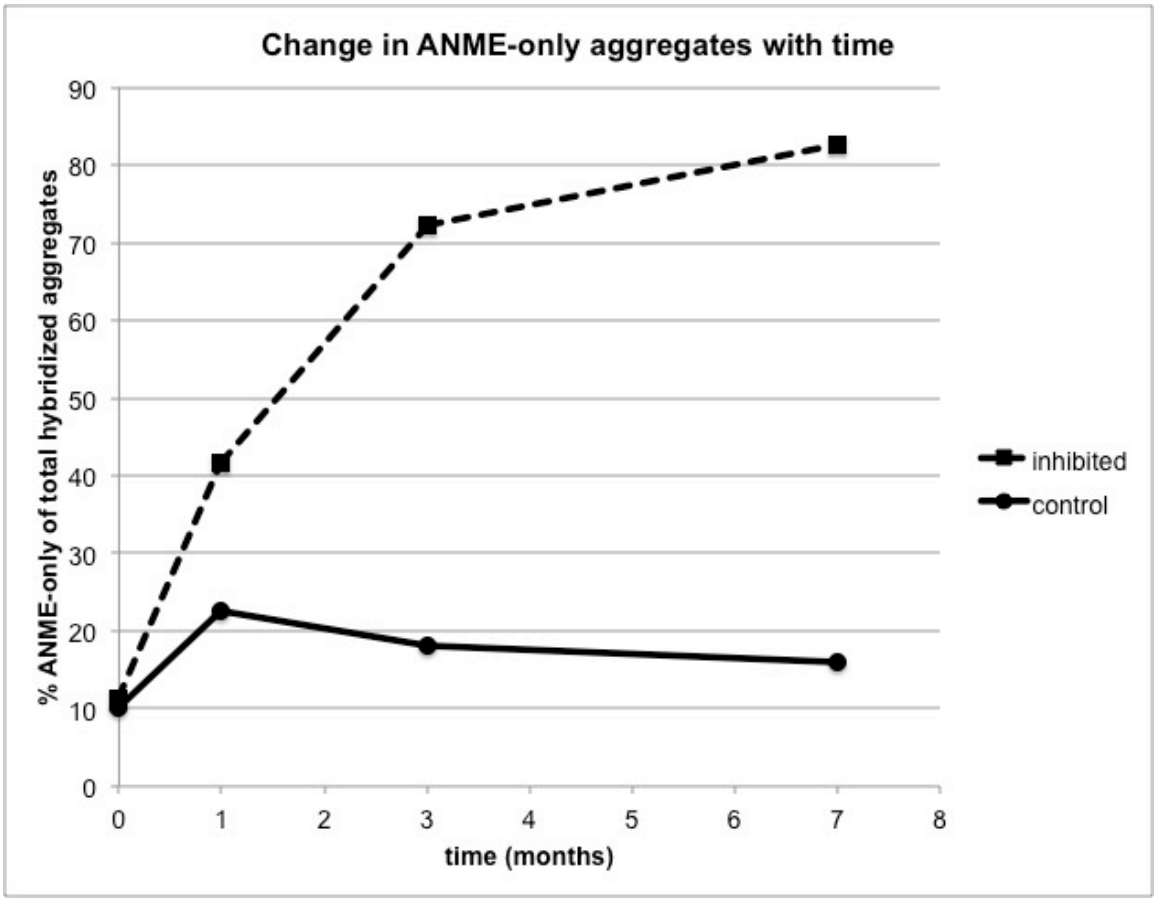

Figure 2.

Change in aggregate composition over time. ANME/bacteria and ANME-only aggregates were counted from samples taken at 0, 1, 4 and 7 months. Cy3- and FITC-labeled oligonucleotide probes Eel_MS_932 (ANME-2; Boetius et al., 2000) and EUB338 (general bacteria; Amann et al., 1995), respectively, were used in FISH reactions. Aggregates counts are expressed as the percent of ANME-only aggregates out of all ANME-only and ANME/bacteria aggregates counted (each point represents 50 aggregates-containing fields counted).

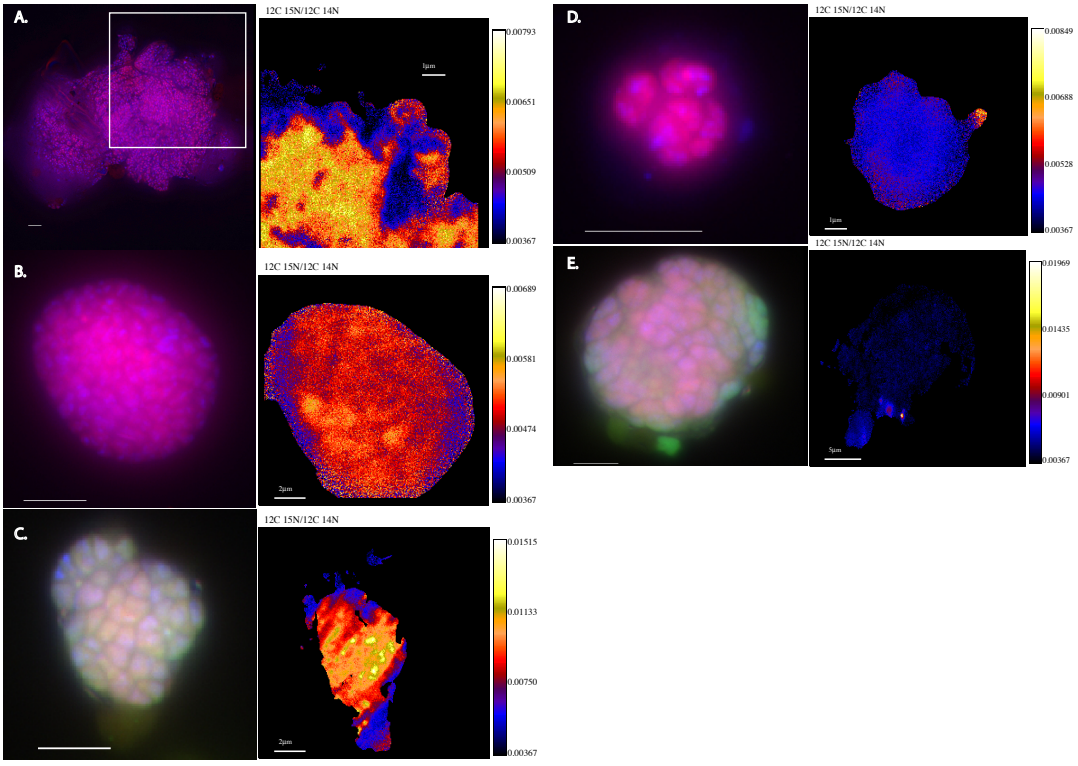

Figure 3.

Corresponding FISH and ion micrographs of aggregates examined via FISH-NanoSIMS from the inhibited incubation, amended with 2 mM ^{15}N-ammonium and 25 mM sodium molybdate and sampled at 7 months. Cy3- and FITC-labeled oligonucleotide probes Eel_MS_932 (ANME-2; Boetius et al., 2000) and EUB338 (general bacteria; Amann et al., 1995), respectively, were used in FISH reactions. FISH micrograph lettering corresponds to aggregate name in Table 1. Scale bars in FISH micrographs represent 5 μm.

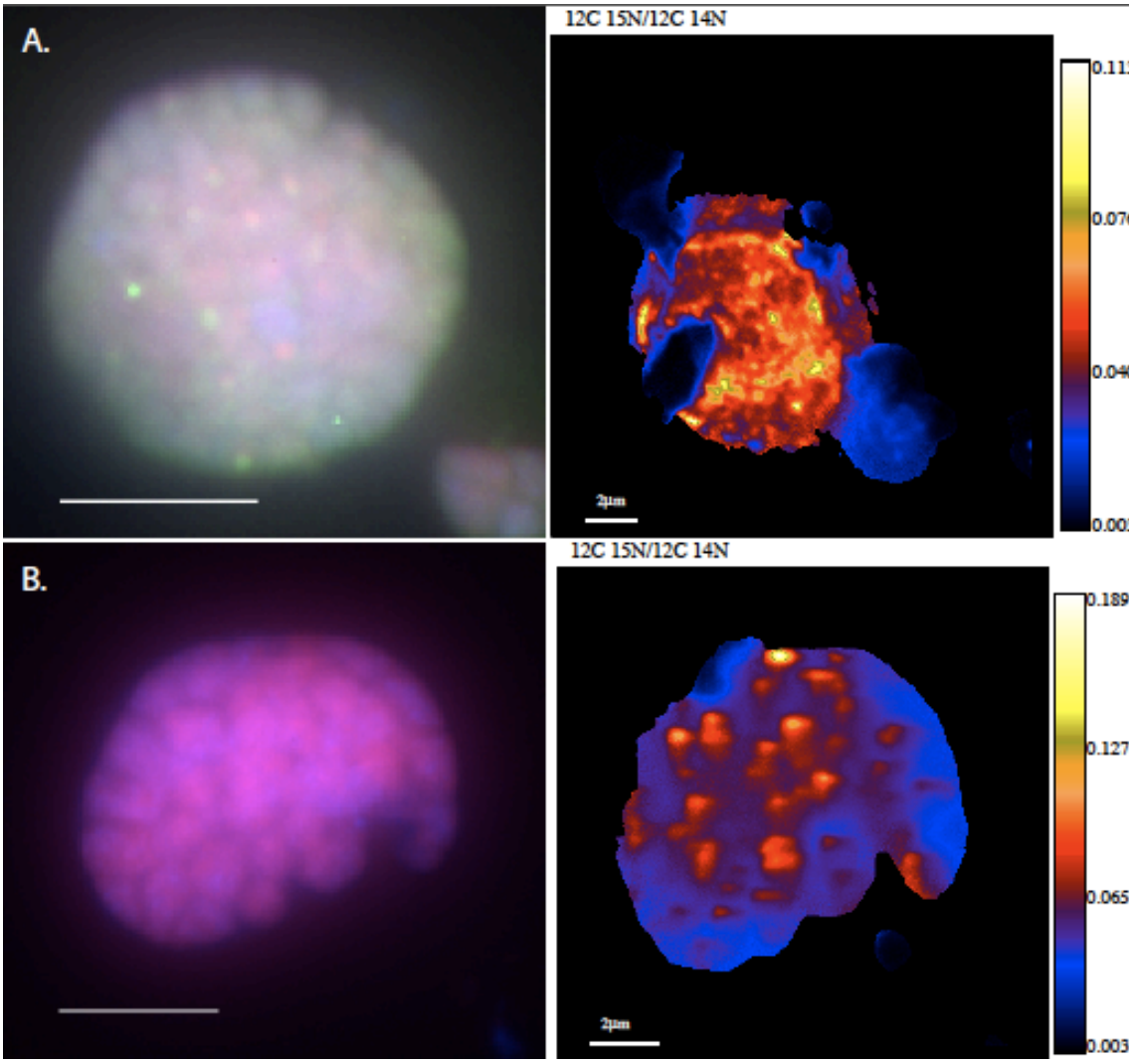

Figure 4.

Corresponding FISH and ion micrographs of aggregates examined via FISH-NanoSIMS from the control incubation (no inhibitor), amended with 2 mM ^{15}N-ammonium and sampled at 7 months. Cy3- and FITC-labeled oligonucleotide probes Eel_MS_932 (ANME-2; Boetius et al., 2000) and EUB338 (general bacteria; Amann et al., 1995), respectively, were used in FISH reactions. FISH micrograph lettering corresponds to aggregate name in Table 1. Scale bars in FISH micrographs represent 5 µm.

Table 1. ^{15}N atom % (highest cycle avg.) of each aggregate investigated via NanoSIMS.

incubation	aggregate	^{15}N atom % (highest cycle avg.)
inhibited	A (ANME only)	0.5570
inhibited	B (ANME only)	0.4940
inhibited	C (ANME/bacteria)	0.9560
inhibited	D (ANME only)	0.4540
inhibited	E (ANME/bacteria)	0.4290
control	A (ANME/bacteria)	5.3720
control	B (ANME only)	5.9140

Conclusions

The work presented in my thesis encompasses two unique ecosystems, terrestrial mud volcanoes and marine methane seeps. The uniting factor leading to their investigation is that both ecosystems are rich in methane, a potent greenhouse gas. Understanding the *in situ* microbial communities and processes can help us to understand what keeps these critical ecosystems in balance. I therefore chose to focus on the sulfur-cycling microorganisms, a prominent and diverse assemblage of microorganisms, in an attempt to uncover novel niches and processes, which would likely be crucial to the functioning of these ecosystems.

Sulfur cycling in terrestrial mud volcanoes has been largely unexplored and here we provided a comparative view of the microbial communities and processes involved in sulfur cycling in multiple terrestrial mud volcanoes of Azerbaijan. Further, mud volcanism in Azerbaijan is one of the controlling factors for the vast oil and gas fields in this area; thus elucidating microbial processes in this region is important as these processes can play an important role in the degradation of hydrocarbon inside the reservoirs. Functional gene phylotypes affiliated with sulfur-oxidizing bacteria (SOB) revealed putative chemosynthetic metabolisms including sequences clustering with obligate aerobes and facultative anaerobes collectively capable of respiring a variety of sulfur species to the with oxygen or nitrate. In addition to finding strong evidence for viable thermophilic sulfate-reducing bacteria (SRB) in this non-thermic mud, we also found that SRB may potentially (based on related cultured phylotypes) be divided into niches based on their carbon

oxidation pathways, with incomplete carbon oxidizers potentially preferring gryphon features and the shallow waters of salse lake features. Together these data represent a diverse array of previously unexplored microbial metabolisms in these mud volcanoes. We also found FISH and rate measurement evidence for the anaerobic oxidation of methane coupled to sulfate reduction, a process which we explored further in the more tractable marine methane seeps.

The anaerobic oxidation of methane, serving as a sink for this potent greenhouse gas, is a crucial biogeochemical process and yet little is known about the dynamics that exist between the two partners which effect this process: SRB and anaerobic methane-oxidizing archaea (ANME). In order to study these dynamics we inhibited sulfate reduction and followed the metabolic processes of the microcosm community as well as the effect of aggregate composition and growth on a cellular level using FISH coupled to nanoscale secondary ion mass spectrometry (FISH-NanoSIMS). We revealed that while bacterial cells appear to decay, ANME cells persist in the form of ANME-only aggregates, which are capable of little to no growth when sulfate reduction is inhibited. These data are the first to show what happens to the ANME/SRB consortia growth on a cellular level when sulfate-reduction is inhibited. We also explored factors influencing the diversity of SRB in association with ANME.

Very little is known about factors influencing the distribution and fitness of distinct sulfate-reducing bacteria partnered with anaerobic methane-oxidizing archaea (ANME). Poorly constrained ecological and physico-chemical factors are almost certainly important to this symbiosis as a whole, and present a unique opportunity to uncover additional environmental regulators of sulfate-dependent methane oxidation. We applied a

combination of molecular, geochemical and FISH-NanoSIMS analyses of *in situ* seep sediments and methane-amended sediment incubations from diverse locations (Eel River Basin, Hydrate Ridge and Costa Rican Margin seeps) to investigate the distribution and physiology of a newly identified subgroup of the Desulfobulbaceae (seepDBB) found in consortia with ANME-2c archaea, and compared these to the more commonly observed associations between the same ANME partner and the Desulfobacteraceae (DSS). By first investigating the geochemical parameters that co-occur with higher abundances of ANME/seepDBB we uncovered a novel positive correlation between these aggregates and nitrate concentrations. This relationship with nitrate was experimentally confirmed using sediment microcosms, in which the abundance of ANME/seepDBB was greater with the addition of nitrate relative to the unamended control. Additionally, FISH-NanoSIMS revealed significantly higher ^{15}N-nitrate incorporation levels in individual aggregates of ANME/seepDBB relative to ANME/DSS aggregates from the same incubation. These combined results suggest that nitrate is a geochemical effector of ANME/seepDBB aggregate distribution, and may provide a unique niche for these consortia through the utilization of a greater range of nitrogen substrates than the ANME/DSS.

In sum these data uncover novel aspects of the sulfur-cycling microbial communities in two crucial ecosystems rich in natural methane stores. We demonstrated that sulfur oxidation has the potential to proceed both aerobically and anaerobically in terrestrial mud volcanoes. This knowledge helps us understand under what conditions sulfate may be formed to support the active SRB community, some members of which we revealed are likely capable of anaerobic methane oxidation (AOM). We further explored the symbiosis responsible for AOM in marine methane seeps and were able to show just how crucial

sulfate reduction is to this symbiosis by inhibiting sulfate reduction and recording a lack of growth in the ANME cells. We then revealed that the unexplained diversity in SRB associated with ANME cells can be at least partially explained by preferential nitrate utilization by one particular partner, the seepDBB. This discovery reveals that nitrate is likely an important factor in marine methane seep ecosystem functioning.

The combination of geochemical and FISH-NanoSIMS work presented here has not only uncovered novel microbial niches, it has also honed these methods for future work in the field. Our combination of fieldwork, *in situ* geochemical measurements, and FISH-NanoSIMS investigations of microcosm incubations allows for a comprehensive view of the microorganisms both in their native environment and in experimental settings. The detailed study of these microorganisms in their native ecosystem allows for a deep understanding of the factors which affect them and their ecosystem and also can generate hypotheses which are testable not only by bulk rate measurements of microbial processes but also at a cellular resolution via manipulated microcosms. Studies such as these allow for a more complete understanding of not only *in situ* communities and processes but also novel factors that may be central to the ecosystem and yet were heretofore unknown.

On a more personal level these studies have led to my development as a scientist and microbial ecologist. I chose to come to graduate school at the California Institute of Technology because I firmly believe that with the right technology and understanding we can begin to restore balance to ecosystems that have been nearly destroyed by global change. With an enlivened mind and a full toolbox I now plan to continue on that journey.

Author Publications (during PhD)

1. Dekas, A.E., Chadwick, G., Connon, S.A., Fike, D., McCay, D., **Green-Saxena, A**., Dalleska, N., and Orphan, V.J. (in prep) Investigating the Biogeochemical Controls on Deep-Sea Diazotrophy and Its Significance to Local and Global Ecosystems

2. **Green-Saxena, A.,** Dekas, A.E., and Orphan, V.J. (in prep) Effects of the sulfate reduction-inhibitor molybdate on anaerobic methane oxidizing community metabolism, ANME/bacterial aggregate composition and cell growth

3. Trembath-Reichert, E., **Green-Saxena, A**., Poretsky, R., Orphan, V.J. (in review) Whole cell magnetic enrichment of environmental microbial consortia using rRNA targeted Magneto-FISH

4. **Green-Saxena, A.,** Dekas, A.E., Dalleska, N., Orphan, V.J. (in review) Nitrate-based niche differentiation by distinct sulfate-reducing bacteria involved in the anaerobic oxidation of methane.

5. Yang, S., Matsen, J.B., Kanopka, M., **Green-Saxena, A.**, Clubb, J., Sadilek, M., Orphan, V.J., Beck, D., and Kalyuzhnaya, M.G. (2013) Global molecular analyses of methane metabolism in methanotrophic Alphaproteobacterium, *Methylosinus trichosporium* OB3b. Part II. metabolomics and 13C-labeling study. *Frontiers in Microbiology* **4**.

6. **Green-Saxena, A.,** Feyzullayev, A., Hubert, C.R.J., Kallmeyer, J., Krueger, M., Sauer, P., Schulz, H.-M. and Orphan, V.J. (2012, Journal Cover) Active sulfur cycling by diverse mesophilic and thermophilic microorganisms in terrestrial mud volcanoes of Azerbaijan. Environmental Microbiology 14(12): 3271-3288

7. Bailey, J.V., Raub, T.D., Meckler, A.N., Harrison, B.K., Raub, T.M.D., **Green, A.M.,** Orphan, V.J. (2010) Pseudofossils in relict methane seep carbonates resemble endemic microbial consortia. Palaeogeography, Palaeoclimatology, Palaeoecology 285 131-142

8. Orphan, V.J., Turk, K.A., **Green, A.M**., House, C.H. (2009) Patterns of 15N assimilation and growth of methanotrophic ANME-2 archaea and sulfate-reducing bacteria within structured syntrophic consortia revealed by FISH-SIMS. Environmental Microbiology 11:1777-1791